ASSESSMENT OF CARBON DIOXIDE TRANSMISSION THROUGH
POROUS BUILDING MATERIALS IN RELATION TO INDOOR AIR QUALITY

A THESIS SUBMITTED TO
THE GRADUATE SCHOOL OF NATURAL AND APPLIED SCIENCES
OF
MIDDLE EAST TECHNICAL UNIVERSITY

BY

BAŞAK YÜNCÜ

IN PARTIAL FULFILLMENT OF THE REQUIREMENTS
FOR
THE DEGREE OF MASTER OF SCIENCE
IN
BUILDING SCIENCE
IN
ARCHITECTURE

APRIL 2016

Approval of the thesis:

ASSESSMENT OF CARBON DIOXIDE TRANSMISSION THROUGH POROUS BUILDING MATERIALS IN RELATION TO INDOOR AIR QUALITY

submitted by **BAŞAK YÜNCÜ** in partial fulfillment of the requirements for the degree of **Master of Science in Building Science in Architecture Department, Middle East Technical University** by,

Prof. Dr. Gülbin Dural Ünver   _____
Dean, **Graduate School of Natural and Applied Sciences**

Prof. Dr. T. Elvan Altan   _____
Head of Department, **Architecture**

Assoc. Prof. Dr. Ayşe Tavukçuoğlu   _____
Supervisor, **Architecture Dept., METU**

Prof. Dr. Emine N. Caner-Saltık   _____
Co-Supervisor, **Architecture Dept., METU**

Examining Committee Members:

Assoc. Prof. Dr. Ali Murat Tanyer   _____
Architecture Dept., METU

Assoc. Prof. Dr. Ayşe Tavukçuoğlu   _____
Architecture Dept., METU

Prof. Dr. Figen Beyhan   _____
Architecture Dept., Gazi University

Prof. Dr. Mustafa Tokyay   _____
Civil Engineering Dept., METU

Assoc. Prof. Dr. Halis Günel   _____
Architecture Dept., METU

Date: 15 April 2016

I hereby declare that all information in this document has been obtained and presented in accordance with academic rules and ethical conduct. I also declare that, as required by these rules and conduct, I have fully cited and referenced all material and results that are not original to this work.

Name, Last name : Başak Yüncü

Signature   :

ABSTRACT

ASSESSMENT OF CARBON DIOXIDE TRANSMISSION THROUGH POROUS BUILDING MATERIALS IN RELATION TO INDOOR AIR QUALITY

Yüncü, Başak

M.S. in Building Science, Department of Architecture

Supervisor : Assoc. Prof. Dr. Ayşe Tavukçuoğlu

Co-supervisor : Prof. Dr. Emine N. Caner-Saltık

April 2016; 112 pages

There is lack of knowledge on breathing features adequacy of porous building materials for sustaining indoor air quality. There is necessity to examine gas diffusion characteristics of breathing porous building materials and the relation of those characteristics with IAQ.

A comprehensive study, therefore, was conducted on mud brick as a traditional building material and AAC as a contemporary building material which are well-known by their high breathable characteristics. Their air permeability features were examined in terms of water vapor and carbon dioxide diffusion characteristics. A practical experimental method composed of single and double chamber diffusion tests was developed representing the gas diffusion from inside to outside through a porous wall. CO_2 was used as a tracer gas since its presence at certain level adversely-effect the indoor air quality.

The results have shown that single chamber setup is useful for assessing CO_2 diffusion rate, while double chamber setup is obligatory to identify whether the material is

attracted to the tracer gas or not. That knowledge is crucial to clarify how much tracer gas is actually permeated through or retained in the material. If a porous material is attracted to CO_2, the data on diffusion rate obtained from single chamber setup is misleading.

Both mud brick and AAC are highly-porous, -water vapor permeable and lightweight materials while differing in their CO_2 permeability characteristic. Mudbrick is more CO_2 transmissive than AAC, while AAC absorbs/adsorbs CO_2 more than it transmits. However, no evident correlation between water vapor permeability and CO_2 diffusion characteristics was identified.

Key words: CO_2 diffusion rate, water vapor permeability, mud brick, autoclaved aerated concrete, indoor air quality.

ÖZ

İÇ ORTAM HAVA KALİTESİ İLE İLİŞKİLİ OLARAK GÖZENEKLİ YAPI MALZEMELERİNİN İÇİNDEN KARBONDİOKSİT GEÇİŞİNİN İNCELENMESİ

Yüncü, Başak

Yüksek Lisans, Yapı Bilimleri, Mimarlık Bölümü

Tez Yöneticisi: Doç. Dr. Ayşe Tavukçuoğlu

Ortak Tez Yöneticisi: Prof. Dr. Emine N. Caner-Saltık

Nisan 2016; 112 sayfa

Gözenekli yapı malzemelerinin, iç ortam hava kalitesini iyileştirmek üzere nefes alma özelliklerinin yeterliliği hakkında yeterli bilgi bulunmamaktadır. Dolayısıyla, nefes alan gözenekli yapı malzemelerinin gaz difüzyon özellikleri ve bu özelliklerin iç ortam hava kalitesiyle olan ilişkisinin araştırılması gerekmektedir.

Bu bağlamda, yüksek nefes alırlıklarıyla bilinen geleneksel yapı malzemesi olan kerpiç ve günümüz yapı malzemesi olan gaz beton üzerinde kapsamlı bir inceleme yapılmıştır. Bu malzemelerin hava geçirimlilik özellikleri, su buharı ve CO_2 difüzyon karakteristikleri bakımından incelenmiştir. İç ortamdan dış ortama gözenekli malzeme içinden gaz difüzyonunu/iletimini gösteren, tek odacıklı ve çift odacıklı deney düzeneklerinden oluşan pratik bir test metodu geliştirilmiştir. CO_2 yoğunluğunun belirli seviyelerin üzerine çıkması, iç ortam hava kalitesini olumsuz yönde etkilediği bilindiğinden, izleme gazı olarak CO_2 kullanılmıştır.

Sonuçlar göstermiştir ki, tek odacıklı test düzeneğinin, CO_2 difüzyon hızını tespit etmek için kullanılabilirken, çift odacıklı test düzeneği, malzemenin izleme gazıyla etkileşime

girip girmediğini belirlemek üzere kullanılması şarttır. Bu bilgiler izleme gazının ne kadar miktarda malzeme içinde tutulduğunu açıklığa kavuşturmak üzere çok önemlidir. Test edilen malzemenin CO_2 ile etkileşime girdiği durumlarda, tek odacıklı deneyden elde edilen verilerle hesaplanan CO_2 difüzyon hızı yanıltıcıdır.

Yüksek oranda gözenekliliğe ve su buharı geçirimliliğine sahip, hafif malzemeler olan kerpiç ve gaz betonun, CO_2 geçirimlilik özellikleri bakımından birbirinden oldukça farklı oldukları gözlenmiştir. Taşıyıcı kerpiç bloklar, kendi içinden geçişine izin verdiğinden daha fazla CO_2'i içinde tutan taşıyıcı ve dolgu amaçlı kullanılan gaz beton çeşitlerinden daha fazla CO_2 geçirimlidir. Bununla birlikte, malzemelerin su buharı ve CO_2 geçirimlilikleri arasında tutarlı bir korelasyona rastlanmamıştır.

Anahtar kelimeler: CO_2 difüzyon hızı, su buharı geçirimliliği, kerpiç, gaz beton, iç ortam hava kalitesi

ACKNOWLEDGEMENTS

TABLE OF CONTENTS

LIST OF TABLES

LIST OF FIGURES

LIST OF SYMBOLS AND ABBREVIATIONS

AAC	Autoclaved aerated concrete
IAQ	Indoor air quality
VOC	Volatile organic compound
SBS	Sick building syndrome
G2	G2 type autoclaved aerated concrete (infill)
G4	G4 type autoclaved aerated concrete (load bearing)
UPV	Ultrasonic pulse velocity
MoE	Modulus of elasticity
I_s	Point load stress index
Met	Metabolismic equivalent
RD_{SINGLE}	CO_2 concentration decay rate in a single-chamber diffusion test
RD_{DOUBLE}	CO_2 concentration decay rate in a double-chamber diffusion test
RD_{SINGLE}	CO_2 concentration increase rate in a double-chamber diffusion test
RT	Rate of transmission
$RT_{(CO2)}$	Rate of CO_2 transmission
$RT_{(H2O)}$	Rate of water vapor transmission
SD	Equivalent air thickness of water vapor permeability
1/SD	Water vapor permeance
T_{DECAY}	Decay time
$T_{CRITICAL}$	Time critical
M_{CH-1}	CO_2 amount in Chamber-1
M_{CH-2}	CO_2 amount in Chamber-2
$M_{RETAINED}$	CO_2 amount retained by the material
E	CO_2 diffusion rate

D_{EFF}	Effective diffusion coefficient
D_i	Diffusion index
C_{MAX}	CO_2 concentration peak level
μ	Water vapor transmission coefficient
ϕ	Porosity
ρ	Density

CHAPTER 1

INTRODUCTION

With the industrial revolution, energy consumption of the world accelerated. In the 20th century, meeting the energy demand of the developing world became a problem. Moreover, excessive carbon emissions due to energy generation by using fossil fuels have been disturbing the natural balance of the atmosphere. This situation created serious problems, such as global warming and climate change, which are some of the key concerns for the whole world. Considering that there is an increase in demand for the built environment and indoor comfort conditions required from that built environment, the environmental impact of building constructions and their maintenance became inevitably great and reached to critical ranges threatening the natural balance of earth. To overcome the problems of energy shortage, global warming and climate change, the emphasis is given to the research fields of renewable energy, energy efficiency, sustainability and green building design.

Functional systems, such as heating, cooling, air conditioning and ventilation are considered as the most energy demanding systems in buildings. In order to provide energy efficiency, thermal insulation and natural ventilation became important issues. In this context, there are many studies, applications and regulations to increase energy efficient of built environment, therefore to decrease environmental impact of built environment. For that purpose the tendency is to define thermal performance of buildings and building materials in use. There are studies on establishing natural ventilation strategies for built environment as well to define the indoor air quality in terms of moisture in the air and contamination of air. Ideal indoor conditions can only be provided by sustaining both thermal comfort conditions and good indoor air quality. Besides thermal comfort conditions, adequate ventilation is surely necessary for maintaining healthier indoor air, which is crucial for well-being of occupants. However, thermal performance of buildings seems to be a primary concern, while ventilation is considered as comparatively-less

important. The tendency to provide indoor ventilation is the establishment of fully-airtight building enclosures which do not permit natural ventilation through the openings and building skin resulting in the integration of additional and mechanical features into today's buildings. In this context, the adequate and natural ventilation by the building envelope seems to be neglected by the designers and the occupants for the sake of energy efficiency. As a result, a serious problem of bad indoor air quality which appeared in contemporary airtight buildings came into existence as one of the most common reasons of "sick building syndrome (SBS)".

Therefore, a conscious approach is needed to design energy efficient buildings providing comfortable and healthy indoor conditions at the same time. Here, one of the main problems causing bad indoor air quality is the fully-airtight building skin. The airtightness between the edges/joints where the openings and the building skin comes together should be provided with an elaborate architectural detailing and workmanship. However the building skin should still contribute to the indoor air quality by allowing air diffusion between inside and outside at certain levels. The study concerns such an approach, briefly considers the self-breathing capability of building skins which are composed of porous and breathable building materials.

1.1. Argument

In the literature, breathing properties of building materials are investigated mostly in terms of water vapor permeability and air flow resistivity. However, those properties of building materials have not been interpreted together to assess their air diffusion properties. In addition there is lack of knowledge in literature on adequacy of air diffusion characteristics for providing better indoor air quality. Therefore, the relationships between air diffusion features of porous building materials and indoor air quality have not been correlated or examined yet. The breathing performance of traditional buildings, such as mudbrick houses, and the contribution of that performance to healthy indoor conditions, especially to indoor air quality is an inspiring research topic and needs comprehensive studies. For that purpose, some test methods must be developed in order to practically-

determine gas diffusion characteristics of porous materials for comparisons and to reveal the relationships between those characteristics and their contribution to indoor air quality.

According to the studies in related literature, water vapor permeability characteristics of building materials are investigated in order to determine the compatibility of neighboring wall layers with a concern of long term durability of buildings and materials (Kömürcüoğlu, 1962; Collepardi, 1990; Houben and Guillaud, 1994; Akkuzugil, 1997; Caner, 2003; Esen *et al*., 2004; Kefee, 2005; Örs, 2006; Morton, 2008; Šadauskiene, 2009; Tavukçuoğlu et al., 2012). Although, there is limited information on how water vapor permeability of wall units can be useful for maintaining ideal indoor relative humidity levels.

Airflow resistivity is another parameter indicating the breathing properties of a material. This parameter is commonly used for determination of the acoustic properties of porous building materials (Martens *et al.*, 1985; ASTM, 2009; Crispin *et al*., 2014; Tao *et al.*, 2015). However, none of those studies mention the airflow resistivity parameter as a medium for predicting the ability of a breathing material to adjust gas concentration levels between two environments separated by that material.

Several studies are conducted on indoor air quality and its assessment (EPA, 1991; Persily, 1997; Wolkoff, 1998; Phillips *et al.*, 1999; Swift, 2010; Wang and Zhang, 2010; Hess-Kosa, 2011; Shin, 2013). Moreover, indoor air quality standards are defined by authorities (ASHREA, 2006; WHO, 2006). An existing standard defines the method for determining air change in a single zone by means of a tracer gas dilution. This standard test method examines tracer gas dilution in a space with an induced airflow through inlets and outlets (ASTM, 2015). None of these studies and standards mention a correlation between indoor air quality and breathing features of a building material.

There is no existing standard test method developed in order to better understand how fast CO_2 diffuses through a material from one environment to another without induced airflow. Therefore, this study focuses on developing a practical test method to investigate the carbon dioxide diffusion characteristics of porous wall units. The potentials and

restrictions of mud brick and autoclaved aerated concrete are examined and compared in terms of their breathing characteristics and their contribution to good indoor air quality by allowing a decrease of indoor air pollutant concentration levels by diffusion through their body.

The results support the idea of maintaining healthy indoor air by the help of breathing walls. In other words, breathing walls can minimize the mechanical ventilation needs for fresh air intake by benefitting from indoor gas concentration adjustment abilities of air permeable skin. Therefore, the results are also useful to discuss the airtightness aspect of passive house technology.

1.2. Objectives

The basic aim of this study is to develop a practical test method and investigate the relationship between breathing features of porous wall units and their contribution to indoor air quality by means of laboratory analyses.

This study aims:

- To determine the breathing features of traditional and contemporary porous wall units in terms of water vapor and CO_2 permeability;
- To investigate and compare the potentials of highly breathing materials, mud brick and AAC, to enhance the indoor air quality;
- To develop a practical laboratory test method in reference to "concentration decay method" defined in a standard (ASTM, 2015), representing diffusion of CO_2 from high-concentrated indoor to low-concentrated outdoor without any induced airflow;
- To develop another practical test method which enables determination of attraction between a tracer gas and a building material;
- To determine CO_2 diffusion characteristics of breathing materials by using the data achieved by the practical CO_2 diffusion test methods developed in the study;
- To define the mud brick from Hamzalı Village and AAC masonry wall units in terms of their basic physical, physicomechanical and mechanical characteristics;

4

- To identify raw material characteristics of mud based materials of Hamzalı Village;
- To discuss the impact of "breathable building skins" versus "fully-airtight building envelope" on maintaining good indoor air quality in a more sustainable manner, which has not been considered in Passive House approach.

1.3. Disposition

This study is presented in 6 chapters, of which this introduction is the first.

In the second chapter, the literature review composed of present studies and data on "indoor air quality", "diffusion and effusion of gasses", "parameters to define breathing features of materials", "parameters to define indoor air change", "indoor air quality assessment" and "highly breathing porous materials" are presented briefly.

The third chapter, material and method, clearly explains the procedures of the experimental laboratory tests and describes the materials used for this study.

The fourth chapter, results, includes tables, graphics and figures presenting the experimental test results.

The fifth chapter, discussion, is where the results are discussed.

Finally, the last chapter is composed of the conclusion part which summarizes the concluded remarks of the study and also the recommendations for further research.

CHAPTER 2

LITERATURE REVIEW

In this chapter, the related studies on indoor air quality, diffusion and effusion of gasses, parameters to define breathing features of materials, parameters to define indoor air change, indoor air quality assessment and breathing features of porous materials in the literature are summarized.

2.1 Indoor Air Quality (IAQ)

There are multiple criteria to be satisfied in order to design ideal indoor environments. "Indoor air quality and ventilation", "thermal comfort", "acoustics and noise", "lighting levels" and "visual perception" are the five key concerns in terms of providing good indoor environmental quality. Swift et al. also state that good indoor air quality can be maintained by decent ventilation and distribution throughout the building, assuming that the outdoor environment is not contaminated (Swift, *et.al.*, 2010)

This part of the literature review will be focusing on approaches on airtight and breathing building envelopes, sick building syndrome, indoor air pollutants and criteria on indoor air quality assessment.

2.1.1. Approaches on Airtight and Breathing Building Envelopes

Fennell and Haehnel (2005) defines airtightness as the quantity of air leakage in a building related to its size. They also noted that air leakage is unintended air movement throughout the building envelope which is considered separately from fresh air intake issue. Therefore, the article suggests airtightness standards achieved by means of air barriers. Although they add to the cost of the building, air barriers reduce fossil-fuel emissions, operating costs and building failures, according to the authors.

Also Katunsky *et al.* (2013) cover airtightness as essential to energy efficiency in buildings, in a study that investigates the airtightness of buildings in Slovakia and compares the results to other countries. The study concludes that 43% of the investigated buildings do not comply with minimum required airtightness levels. A maximum required airtightness level is not mentioned in the study.

On the other hand, Sherman and Chan (2004) claim that airtightness of buildings is a state of art which should be considered thoroughly. Because, over-leakage or over-tightness is likely to weaken the efficiency of designed ventilation systems of buildings. Achieving high airtightness may seem to be desirable from the energy efficiency point of view. However, air infiltration may enable indoor air pollutants to dilute by providing fresh air and improve the IAQ. Therefore, high airtightness would worsen IAQ and thus create a need of an additional mechanical ventilation system, which increases energy consumption. In conclusion, maintaining ideal IAQ by consuming less energy can be possible by a conscientiously-thought-out design approach which includes airtightness at not more than a certain degree.

The term "breathing wall" presents a wall which is composed of similarly water vapor permeable layers and which continuously allows water vapor back and forth through the wall section. Breathing features of a wall contributes to it long term durability by keeping condensation and entrapped moisture problems away from the building (Tavukçuoğlu *et al.*, 2012).

Entrapped moisture is one of the main deterioration factors, thus impervious and dense layers in a wall system would make it less durable compared to a breathing wall. Most of the historical and traditional renders and mortars enable losing excess moisture due to their absorbent and permeable properties. Therefore, renders and mortars are supposed to be water impermeable but water vapor permeable at the same time (Collepardi, 1990; Houben and Guillaud, 1994; Akkuzugil, 1997; Morton, 2008). Also the studies of Esen *et al.* (2004) and Caner (2003) approve the compatibility and continuity of water vapor permeability within the wall systems of the investigated historical structures.

As one of the conclusions of the study on the impact of the exterior painted thin-layer render's water vapor and liquid water permeability on the moisture state of the wall insulating system, Šadauskiene (2009) indicated that water vapor permeable paints are preferable in order to meet the requirement of a stabilized moisture state of a wall, by allowing the penetrated moisture to leave.

Yoon and Hoyano (1998) propose a passive ventilation system in a building with air tight walls benefitting from a pitch roof composed of breathing walls. The roof is configured as in **Figure 2.01** (Yoon and Hoyano, 1998).
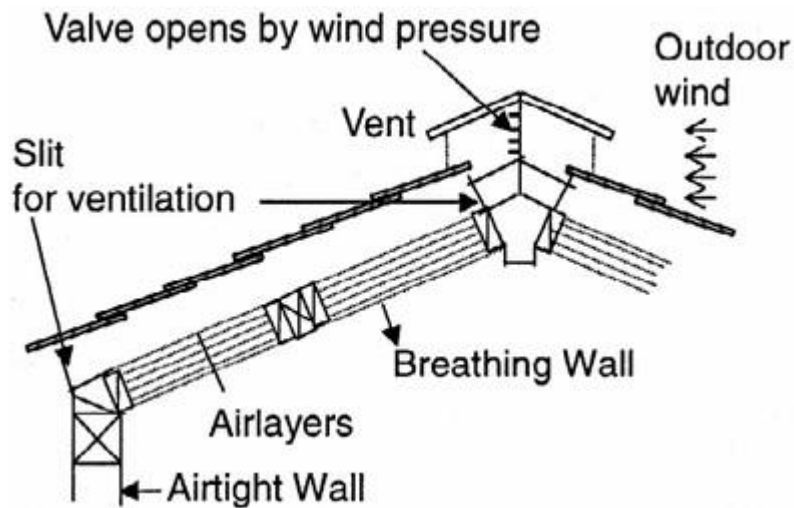
Figure 2.01. Proposed indoor natural ventilation system (Yoon and Hoyano, 1998).

Breathing wall concept proposed by Yoon and Hoyano is different from breathing walls composed of water vapor permeable building materials in the literature. Here, the roof components named as "breathing walls" are composed of exterior finishing material, a number of perforated aluminum foil sheets and interior finishing material as presented in **Figure 2.02** (Yoon and Hoyano, 1998). Aluminum foil is chosen for the system considering its low emittance and high reflective features in order to hinder energy loss while creating air layers. The study concludes that a pitch roof composed of "breathing

walls" is effective on heat recovery and preventing internal condensation.
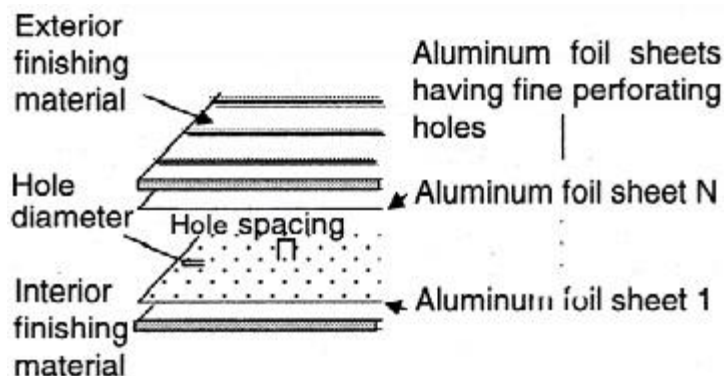
Figure 2.02 Conceptional diagram of the "breathing wall" (Yoon and Hoyano, 1998).

2.1.2. Sick Building Syndrome (SBS)

In the Encyclopedia of Public Health, sick-building syndrome (SBS) is referred as phenomena in buildings where occupants have symptoms such as headaches, sensory organ irritations, cough; dry or itchy skin; dizziness and nausea; difficulties in concentration; fatigue and sensitivity of odors; associated with acute discomfort. In SBS, these symptoms and discomfort are seemed to be related with spending time in the building, but identifying a specific cause or illness is not possible. Causes of SBS are listed as "inadequate ventilation, poor heating, bad acoustics, chemical contaminants from outdoor sources, and biological contaminants" (Kirch, 2008a). Conforming the symptoms is difficult by the help of available laboratory tests and medical examination, since they are reversible and fade away when the occupant leaves the building (Kirch, 2008b).

Gochfeld (2007) states that as a consequence of the fuel crisis in 1970s, energy efficient buildings constructed at the time were airtight and, compared to before, less fresh air was added to the air conditioning due to fuel conservation programs. He claims that this change of conditions led to SBS.

SBS and its effects were underestimated at first. Murphy (2006) narrates the history of SBS; how it is gradually taken into consideration by authorities from 1970's to the recent years in United States and how it has been related to social issues such as politics, racism

10

and feminism. According to Murphy, in 1980's, even the headquarters of United States Environmental Protection Agency (EPA) in Washington was identified as a sick building.

Indoor air pollution is ranked among the top four environmental risks in the US. People spend their %90 of their lives indoors where pollution is continuously two to five times more than it is outdoors. Moreover, concentration levels of pollutants are reported up to a hundred times more indoors when compared to outdoors. EPA published an online fact sheet on sick building syndrome where (i) pollutant source removal or modification, (ii) increasing ventilation rates, (iii) air cleaning, (iv) and education and communication are presented as solutions to sick building syndrome (EPA, 1991).

2.1.3. Indoor Air Pollutants

Other than outdoor-related pollutants, there are three kinds of indoor air pollution sources: occupant-related sources, activity-related sources and building-related sources.

Occupant related indoor air pollution sources originate from human breath and skin metabolism. They are mostly composed of carbon dioxide and human VOCs (volatile organic compounds) as shown in **Table 2.01** (Phillips *et.al*., 1999)

Table 2.01 Inorganic and organic chemical pollutants of occupant-related pollution sources (Phillips *et.al*., 1999).

Sources	Inorganic component	Organic component
Human breath	carbon dioxide moisture ammonia sulfured hydrogen carbon monoxide	isoprene, acetone, ethanol, acetaldehyde, acetic acid allyl alcohol, amyl alcohol methyl alcohol, phenol, toluene
Skin metabolism	carbon monoxide carbon dioxide ammonia	Acetone toluene methane

There is a correlation between occupant activity and indoor carbon dioxide and oxygen levels. Oxygen consumption and carbon dioxide production of a person is higher during

high energy demanding physical activity while it is the lowest when the person is resting (**Figure 2.03** and **Table 2.02**). This correlation is useful in understanding indoor air quality by carbon dioxide monitoring. On the other hand, this method indicates only the occupant related indoor air pollution, since it is not correlative to other indoor air pollutants (Persily, 1997).
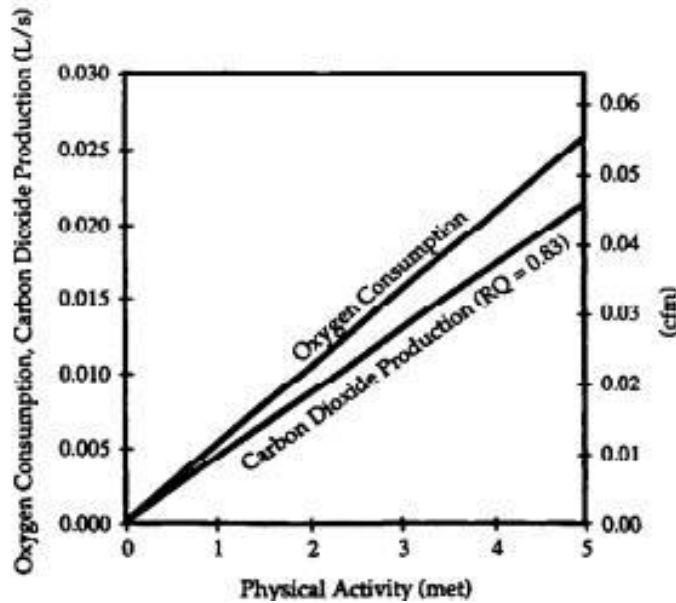
Figure 2.03 Carbon dioxide generation and oxygen consumption according to physical activity (Persily, 1997).

Table 2.02. Typical met (metabolic equivalent) levels for various activities (Persily, 1997)

Activity	Met (metabolic equivalent)
Seated, quiet	1.0
Reading and writing, seated	1.0
Typing	1.1
Filing, seated	1.2
Filing, standing	1.4
Walking at 9 m/s (2 mph)	2.0
House cleaning	2.0-3.4
Exercise	3.0-4.0

Secondly, activity-related sources can be listed as chemical products used for cleaning and maintaining, personal hygiene products, emissions from office equipment and commercial activities, pesticides, insecticides, construction, demolition, and renovation activities. Some common indoor VOCs are formaldehyde, benzene, carbon tetrachloride, trichloroethylene, tetrachloroethylene, chloroform, there different types of dichlorobenzene, ethylbenzene, toluene, and xylene. (Hess-Kosa, 2011).

Third and the last, building-related sources such as building materials, finishing materials and furnishing and their potential pollutants are given in **Table 2.03**. (Wolkoff, 1998). Poorly contained sewage gases as in a case of leaking sewer vents and contaminated HVAC system can also be added to building-related indoor pollution sources (Hess-Kosa, 2011).

Wolkoff (1998) studied five different building products from the chemical emission point of view. His work describes qualitative observations on the impact of air velocity, temperature, humidity, and air on long term VOC emissions from building products.

Table 2.03. Chemical pollutants of building related pollution sources (Wolkoff, 1998).

Sources	Pollutants
Shell and façade construction, Concrete	asbestos, phenol, phenoxyethanol, odors, added pesticides
Wallboard or drywall	aldehydes (formaldehyde etc.), odors
Insulation	Formaldehyde, asbestos
PVC materials	polyvinyl chloride
Paneling	aldehydes (formaldehyde etc.) heptachlor (a pesticide against mold)
Wood Paintings, coatings, sealants, adhesives Roofing	Formaldehyde and other VOCs, ammonia, amines, odors

According to Wolkoff (1999), emission testing of primary emissions of building products is insufficient to understand the secondary emissions which are likely to dominate the entire lifespan of the building after the initial decay period. Therefore, also the potential secondary emissions from the product surface or from the chemicals used for cleaning and maintenance should be considered during the process of new product development and material selection strategies for new buildings.

Shin *et al.* (2013) conducted an experiment in order to determine the VOC emission factors of carpet and, detected six VOCs: toluene, tetrachloroethene, chlorobenzene, ethylbenzene, styrene, and dichlorotoluene. In order to determinate the VOCs emission factors in dry building materials, the study suggested an integrated modelling study.

2.1.4. Criteria on Indoor Air Quality Assessment

Defining and controlling indoor air quality, setting measurable parameters, and developing methods of analysis and evaluation has been challenging for researchers. Professional experts developed, revised and updated guidelines to consider indoor air quality. American Society of Heating, Refrigerating and Air-conditioning Engineers (ASHRAE) has defined acceptable indoor air quality by using measurable parameters such as humidity, ventilation and exhaust rates, concentration limits of selected contaminants in the standard ANSI/ASHRAE Standard 62.1-2004, 2006 supplement (ASHRAE, 2006).

Based on criteria such as existence of indoor sources, availability of toxicological and epidemiological data, and indoor levels exceeding the levels of health concern, the pollutants are divided into two groups, by World Health Organization (**Table 2.04**). The first group implies the pollutants that are considered to be included in the WHO indoor air quality guidelines. Whereas, the second group includes the pollutants of potential interest with insufficient evidence to take place in the present guidelines (WHO, 2006).

In one of the studies of Wang and Zhang (2010), human psychological sensations related to indoor air quality is been investigated by a research on occupant based and building

based indoor air pollutants, and their joint effect. Carbon dioxide was selected as an indicator of the occupant based indoor air pollution, while formaldehyde was selected for the building based one. Using logarithmic index evaluation method, recommended concentration limits of these indicators are evaluated, in comparison to human psychological sensations. The study concluded that personal dissatisfaction is high, even though the concentrations of the two indicators are under the standard recommended limits. Which means, when the standard recommended concentration limits of indicators are set by the authorities, the joint effect of their superposition must be considered as well.

Table 2.04. Indoor air pollutants considered by World Health Organization (WHO, 2006).

Group 1. Development of guidelines recommended	Group 2. Current evidence uncertain or not sufficient for guidelines
Benzene Carbon monoxide Formaldehyde Naphthalene Nitrogen dioxide Particulate matter (PM2.5 and PM10) Polycyclic aromatic hydrocarbons, (especially benzo-[a]-pyrene) Radon Trichloroethylene Tetrachloroethylene	Acetaldehyde Asbestos Biocides, pesticides Flame retardants Glycol ethers Hexane Nitric oxide Ozone Phthalates Styrene Toluene Xylenes

2.2. Diffusion and Effusion of Gasses

Diffusion and effusion are the spontaneous processes of molecular motion. In the kinetic-molecular theory developed by Maxwell and Boltzmann, it is assumed that the gas particles are continuously in an arbitrary and linear motion until they collide with each other or with the walls of the container where the particles change directions and keep moving linearly until the next collision.

Diffusion is the motion of molecules from high concentration to low concentration and the substance moves down concentration gradient. Effusion is the escape of molecules from one closed space to another through a small orifice on the barrier between those two spaces.

Particles of a specific gas substance have different molecular speeds which is mostly close to the most probable speed. This speed increases with temperature increase. An increase of 300°K triples the diffusion coefficients. (Cussler, 1997). Under the same conditions of temperature and pressure, the rates of diffusion or effusion of gasses are inversely proportional to the square root of their molar masses. In other words, lighter molecules diffuse or effuse faster than the heavier ones. Diffusion and effusion characteristics of gasses depend on not only their molar mass, but also their molecular weight. For example, O_2 molecules diffuse in air slower than H_2O molecules but faster than CO_2 molecules. Because, their molecular weight and volume are greater than those of H_2O but less than O_2 (Liley and Gambill, 1973, Cussler, 1997; Yates and Johnson, 2007; Silberberg, 2013; Tro, 2013, Chang and Thoman, 2014).

Diffusion rate of a gas or vapor under constant conditions can be calculated using **Equation 1**, according to Fick's law (Jacobs, 1967; Cussler, 1997; Wilson *et. al*. 2009).

$$E = A\ (\ C_{source} - C_0\ )\ D_{eff}\ /\ L \dots\dots\dots\dots\dots\dots\dots\dots\dots\dots\dots\dots\dots\dots\dots\dots\dots\dots\dots\dots\mathbf{(1)}$$

Where;

E: Diffusion rate, $mg.s^{-1}$

A: Area of the plane perpendicular to the direction of diffusion, cm^2

C_{source}: Concentration at the source, mg/cm^3

C_0: Concentration at the destination, mg/cm^3

D_{eff}: Effective diffusion coefficient of the gas in the porous medium considered, cm^2/s

L: Thickness of the porous material which diffusion occurs through, cm

Diffusion coefficients in air, molecular volume and molar mass of some common gasses in the air under 1 atmosphere pressure from the literature are given on the **Table 2.05.** (Cussler, 1997).

Table 2.05. Diffusion coefficient (cm^2/s) in air, molecular volume and molar mass of water vapor, carbon dioxide and oxygen in gas form, under 1 atm. pressure (Cussler, 1997).

Substance	Diffusion coefficient in air (cm^2/s)	Temperature (˚C)	Molecular Volume ($cm^3.mol^{-1}$)	Molar Mass (g)
H_2O	0.282	16	18.9	18
CO_2	0.148	9	34.0	44
O_2	0.176	0	25.6	32

2.3. Parameters to Define Breathing Features of Materials

Several studies by other researchers produced data on breathing features of building materials by using two parameters: water vapor permeability properties and air flow resistivity. Literature review related to these parameters are summarized under related sub-headings.

2.3.1. Water Vapor Permeability

Turkish Standards Institution (TSE) defined standard testing methods for determining water vapor transmission properties of different building materials. As reported in the Turkish Standards, TS 7847, the water vapor permeability properties of specimens are determined by the water vapor permeability resistance coefficient (μ) and the equivalent air thickness of water vapor permeability (SD) values (TSE, 2001; TSE 2012).

In ASTM E 96-93 standard, the rate of vapor transmission when there is pressure difference of 1 Pa between two sides of the material. The calculation does not include the thickness of the material. The permeance of a unit material can be calculated, if the material is homogeneous (ASTM, 1993). Water vapor transmission rates below

0.6g.h^{-1}.m^{-2} indicate low, values between 0.6 g.h^{-1}.m^{-2} and 6.0g.h^{-1}.m^{-2} indicate medium and values higher than 6.0 g.h^{-1}.m^{-2} indicate high permeability for building materials (**Table 2.06**). Equivalent air layer thickness of water vapor diffusion (SD, m) above 1.4m indicate low, values between 1.4m and 0.14m indicate medium and values below 0.14m indicate high permeability for building materials as presented in **Table 2.06** (TSE, 1999).

Table 2.06. Water vapor permeability classification according to equivalent air layer thickness of water vapor diffusion (SD, m) and water vapor transmission rates (RT, g.h^{-1}.m^{-2}) of building materials (TSE, 2012).

Parameter	Low permeability	Medium permeability	High permeability
SD	>1.4 m	0.14m - 1.4m	<0.14m
RT	< 0.6 g.h^{-1}.m^{-2}	0.6 g.h^{-1}.m^{-2}- 6.0 g.h^{-1}.m^{-2}	> 6.0 g.h^{-1}.m^{-2}

Water vapor permeability is considered as one of the compatibility indicators. As Kömürcüoğlu (1962) states, in order to acquire a homogeneous structure, adjacent building materials should be compatible with each other. For example, in the case of mud brick structures, other building materials of the structure must be as elastic, flexible, organic and breathing as mud.

Permeability of applied finishes on mud brick walls play an important role on the performance and durability of them. Supporting studies show that renderings and mortars resistant to water vapor transmission fail in evacuating the moisture that is likely to penetrate into the wall system, especially when the internal water vapor pressure is higher than the external one (Kefee, 2005).

Historical and traditional structures of Anatolia show that the buildings are constructed by breathing materials which enable continuous water vapor permeance throughout the wall section. In addition, building materials with similar SD values are used adjacently. Thus, possible moisture accumulation in the wall system is prevented by the continuous water vapor permeability of breathing walls. (Akkuzugil, 1997).

Total equivalent air thickness of water vapor permeability (SD_{total}) of a wall section which consists of multiple layers is calculated by using **Equation 2** (TSE, 2012).

$$SD_{total} = (\mu_1 \ x \ S_{01}) + (\mu_2 \ x \ S_{02}) + (\mu_3 \ x \ S_{03}) + \ldots + (\mu_n \ x \ S_{0n}) \ldots\ldots\ldots\ldots\ldots..\ldots \textbf{(2)}$$

A graphic with SD values and thicknesses of different layers can be used for analyzing the wall system to detect the interfaces that hinder the continuity of water vapor permeability in the system (Örs, 2006).

An assessment on breathing characteristics of building materials in terms of their water vapor permeability and air permeability was conducted in the scope an existing study in the literature. Many types of building materials such as insulation materials, strand board, plywood, brick, wood, concrete, mortar, cement board, gypsum board and stone were assessed. The study reveals that there is no evident correlation between water vapor permeability and air permeability parameters (Mukhopadhyaya *et al.*, 2011).

2.3.2. Airflow Resistivity

Airflow resistivity is the quotient of the specific airflow resistance of a material divided by its thickness. Airflow resistance is the quotient of the air pressure difference across a material divided by the volume velocity of airflow through the specimen.

Fibrous and porous sound absorbent materials can be characterized by their airflow resistivity values. This physical parameter is used for evaluating the acoustic behavior and dynamic stiffness of sound absorbent materials for acoustical design purposes (Schiavi *et al.*, 2011).

ASTM C522-03, the standard test method for air flow resistance of acoustical materials serves the purpose of measuring airflow resistivity of materials which absorb or attenuate sound (ASTM, 2009). ISO 9053(2011) and TS EN 29053 (1996) are other similar standards on airflow resistivity measurement method. In all these standards, airflow resistivity is characterized as a parameter which indicates the acoustical properties of a

material. No relation between this parameter and indoor air quality is mentioned in these standards.

2.4. Parameters to Define Indoor Air Change

Airflow rate and air change rate are commonly used important parameters for HVAC systems design and for determining airtightness properties of indoor spaces. These parameters are calculated for an envelope consisting of barriers between a conditioned space and the outdoors. Airflow through the envelope occurs by means of doors, windows, roofs, walls, floors and ductwork according to the standards (ASHRAE, 2007; ASTM, 2011).

2.4.1. Airflow Rate

Air flow rate is the volume of air passing through a space from and to outdoors by time. Supply and exhaust air flow rates are calculated and HVAC systems are designed accordingly, in order to comply with the indoor air quality standards. Air change rate of a space can by calculated by using the airflow rate data.   (ASHRAE, 2007).

2.4.2. Air Change Rate

Air change rate is the change of air in a closed space per hour. It is calculated by using **Equation 3**. It is a parameter commonly used for determining the airtightness and the ventilation needs of a space according to occupancy (ASHRAE, 2007).

According to ASHRAE (2007), air change rate of a room can be expressed as:

ACR= 60 x CFM/V…………………………………………………………….…(**3**)

Where;

ACR: air change rate (1/h)

CFM: air flow rate (m^3/s)

V: volume of the room (m^3)

2.4.3. Airtightness Properties

Airtightness is the degree of resistance to airflow of a tested envelope. Blower door test is a method for determining airtightness of buildings as defined in the standard ASTM E1827-11 (ASTM, 2011).

Under the conditions determined by the standard, the higher air change rates indicate less airtightness in the building. Less than 5 air changes per hour (ACH, h^{-1}) at 50 Pascal pressure is recommended to be achieved for energy efficient buildings (Miller et al., 2010).

2.5. Indoor Air Quality Assessment

Several sampling and analytical methods has been developed and standardized in the past years, in order to measure presence and levels of contaminants such as pollens and spore allergens, microbic vital allergens, pathogenic microbes, toxigenic microbes, volatile organic compounds, molds, carbon dioxide, carbon monoxide and formaldehyde (Hess-Kosa, 2011).

Hodgson (2006), instead of using long term surveys and long term sampling in determining sick building syndrome, offers an alternative approach which is based on short term quantification of symptoms, and short term sampling techniques or direct reading, in his research supported by Health Services Research Foundation, Pittsburgh, Pennsylvania. So that, the existence of dose-response relationships within sick building syndrome is put emphasis on.

A case study, conducted in the University of Chieti, Italy, evaluated the airborne micro flora of the research laboratories in the campus. The study suggests that the indoor environments of the laboratories should be examined and monitored periodically in terms of microbial pollution by using settle plate method which is an appropriate and low-price technique of examining the indoor air quality (Di Giulio *et al.*, 2009).

The survey data on temperature, relative humidity, air exchange rate, concentration of NO2, formaldehyde and total volatile organic compounds (TVOCs) in order to determine the status of dwellings and indoor air quality in Sweden is provided by the Swedish National Housing, Building and Planning. Parallel to previous Scandinavian studies, most of the housing stock did not satisfy the ventilation guidelines set by the Swedish building code. In conclusion, indoor air of dwellings with higher air exchange rate tend to have higher NO2 (outdoor related pollutant) levels, whereas it has less formaldehyde and TVOC levels compared to dwellings with lower air exchange rate (Langer and Bekö, 2013).

In a research study on assessment of indoor air quality in crowded educational spaces, a classroom and a design studio are investigated by collecting numerical data of temperature, relative humidity, carbon dioxide and airspeed for about five months period of time. The study concluded that carbon dioxide and heat accumulation, low relative humidity and low air change rate are the main reasons of the discomfort. Efficient use of the existing air inlets connected to the fan coils is suggested as a solution to the existing problem. It is also emphasized that human comfort and indoor air quality should be considered at the design stage (Beruz, 2012).

EnergyPlus and CONTAM models of the sixteen selected reference buildings from a former study would serve as baseline studies to be useful in prospective analyses to support the design alternative indoor air quality control and ventilation strategies which can be not only energy efficient but also beneficial for maintaining good IAQ (Ng *et al.,* 2012).

2.5.1. Commonly Used Standard Test Methods

ASTM issued a standard test method for determining air change in a single zone by means of a tracer gas dilution, under the fixed designation E741. Concentration decay method, constant injection method and constant concentration method are the three techniques presented within the scope of this standard test method (ASTM, 2013).

A recent study addresses CO emission from gasoline-powered electric generators and its dilution in single or multiple zone closed chambers. Firstly, in order to come up with a correlation between CO generation and oxygen consumption, eight experiments on a single shed was conducted. Then the shed was modelled on CONTAM, the computer program. Finally, the model is demonstrated in a simulated single family house using the weather data of New Orleans in summer of 2005. In conclusion, the CO levels of the house could reach and remain beyond the threshold limit value for an 8-hour-period (Wang et al., 2012).

2.5.2. Carbon Dioxide as a Commonly Used Indicator for Testing IAQ

According to ASHRAE 62.1 standard, indoor CO_2 levels below 5000 ppm would not pose a health risk. However, it is also mentioned that when CO_2 concentration is 700 ppm above outdoor levels, which is usually between 300 ppm and 500 ppm, occupants experience discomfort due to bio-effluents (ASHREA, 2007). In short the 1000ppm-1200ppm is the range above which people feel discomfort in indoor conditions.

A recent study shows significant and meaningful reduction on decision making performance of occupants when the CO_2 concentrations increased from 600 ppm to 1000 ppm and 2500 ppm (Satish *et al*., 2014). Also other earlier studies support that people perform poorly when CO_2 concentrations are above certain limits (Kajtar, 2003; Kajtar, 2006).

CO_2 concentration levels can reach up to 1900 ppm in meeting rooms after a 30-90 minute meeting (Fisk *et al*. 2010). Some other studies reveal that average CO_2 concentration levels can be above 2000 ppm and peak levels may exceed 3000 pm in classrooms (Corsi *et al.*, 2002; Whitmore *et al*., 2003)

For a local study, residences, classrooms and offices in different neighborhoods in Turkey investigated in terms of indoor air quality by measuring carbon dioxide concentration levels. The study introduced a correlation between the carbon dioxide levels and the number of occupants, the relative humidity (RH) and the concentration level of respirable

23

particles. As a result, CO_2 concentration and RH levels increase by occupancy. It is concluded that ventilation performed according to constant carbon dioxide monitoring would help sustaining indoor air quality in a more energy efficient manner (Bulut, 2012).

2.6. Highly Breathing Porous Materials

Mud brick (traditional) and autoclaved aerated concrete (contemporary) are commonly used porous building materials which are known to be highly breathing. This part of the study consists of reviews on mud brick and AAC.

2.6.1. Review on Mud Brick

Morton (2008) defines mud brick buildings (earth masonry) as built out of unfired earth bricks, which contains clay as the binding material, brought together mostly by the help of earth based mortar.

Torraca (2009) states that earth -as a building material- is composed of fragmented minerals from the original volcanic or sedimentary rock, minerals as the product of chemical decay process, new minerals produced by water contact and dissolved substances in it, and organic products of biological process. He also mentions that amount of clay in mud as a building material is important, since it provides plasticity when it is wet and hardness when it is dry, whereas excess of clay causes shrinkage and cracking when the material dehydrates. Earth for construction contains 20-30 % clay and silt, and 70-80 % sand. Vegetal fibers, dung, lime or cement may be added to the earth in order to form hardened mud brick in quality construction. Another source supports the data of Torraca. Kömürcüoğlu (1962) implies that it is imperative to acknowledge the composition and characteristics of mud which is a natural building material emerging from decomposition of miscellaneous stones and from their fragmentation and disintegration. Clay, the binding element in mud brick, swells in case of water intake and shrinks when the water content evaporates. Non-binding materials such as minerals, sand, stone types, natural fibers, and timber type of additives are to be added to mud in order to prevent excessive volume change and cracking.

Güdücü (2003) examined some burnt mud brick walls of Shapinuwa, the Hittite city for a study on the Hittitian mud brick and mud plaster technology. She found that the mud brick samples have water vapor permeability resistance coefficient (μ) values between 0.57 and 0.99. Another study obtained data of μ values of historical and traditional mud bricks of Anatolia between 2.75 and 3.23 (Akkuzugil, 1997)

2.6.2. Review on Autoclaved Aerated Concrete

According to Turkish Standard TS EN 12602, AAC is specified as the lightweight concrete product which is obtained from a process of adding a pore-forming agent to a mixture of fine grained siliceous aggregate and lime or cement as the inorganic binder and a consecutive steam curing process for strengthening the product mechanically (TSE, 2011)

Due to its high porosity, heat transmission and fire resistance, lightweightness and unique breathing properties, autoclaved aerated concrete (AAC) is one of the most commonly used building materials in today's buildings (Narayanan and Ramamurthy, 2000; Taşdemir and Ertokat, 2002; Andolsun, Tavukçuoğlu, Caner- Saltık, 2005).

There are several AAC block types with different porosity characteristics. For example, higher number of larger pores are observed in G2 type AAC in comparison with G4, a denser and less porous type (**Figure 2.04**). Water and gas permeability of AAC with different densities are quite similar and the artificial air pores do not have a significant effect on these properties (Andolsun, 2006; Jacobs and Mayer, 1992).
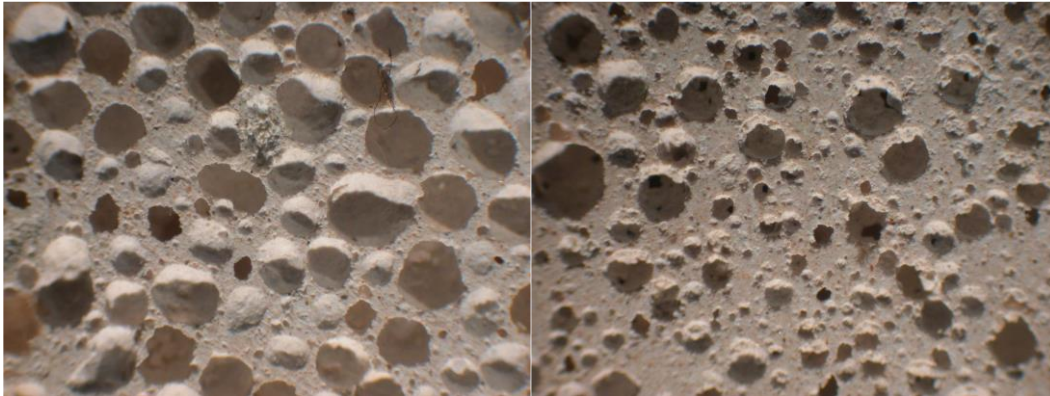
(a) G2   **(b)** G4

Figure 2.04. The microscopic images of G2 (a) and G4 (b) type autoclaved aerated concrete. The longer side of the micrograph: 1cm (Andolsun, 2006).

Andolsun also compares the study of Jacobs and Mayer to result found by RILEM. According to RILEM, μ values of AAC materials are between 4 and 10 depending on its dry density, which is higher than the values found by Jacobs and Mayer (Andolsun, 2006).

A Turkish AAC manufacturer company states that the μ values of their AAC products change in a range of 5-10 μ (AKG Gazbeton, 2013).

One of the basic degradation mechanisms of concrete materials is carbonatation which has a possible effect on their durability. CO_2 reacts with $Ca(OH)_2$ (portlandite) and other C-S-H phases (tobermorite in this case) and forms $CaCO_3$ during the carbonatation process. The reactions process as in **Equation 4**, **Equation 5** and **Equation 6**.

$$5CaO \cdot 6SiO_2 \cdot 5H_2O + 5CO_2 \rightarrow 5CaCO_3 + 6SiO_2 + 5H_2O \dots\dots\dots\dots\dots\dots\dots\text{(4)}$$

$$5CaO \cdot 6SiO_2 \cdot 5H_2O \leftrightarrow 5Ca(OH)_2 + 6SiO_2 \dots\dots\dots\dots\dots\dots\dots\dots\dots\dots\dots\text{(5)}$$

$$Ca(OH)_2 + CO_2 \rightarrow CaCO_3 + H_2O \dots\dots\dots\dots\dots\dots\dots\dots\dots\dots\dots\dots\text{(6)}$$
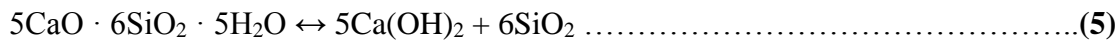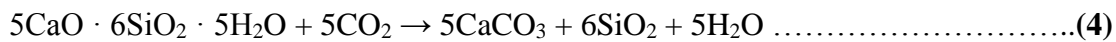
When moisture meets CO_2, carbonic acid is formed and $CaCO_3$ reacts with carbonic acid. These reactions are presented in **Equation 7** and **Equation 8**.

$$CO_2 + H_2O \rightarrow H_2CO_3 \dots\dots\dots\dots\dots\dots\dots\dots\dots\dots\dots\dots\dots\dots\dots\text{(7)}$$

$$H_2CO_3 + CaCO_3 \rightarrow Ca(HCO_3)_2 \dots\dots\dots\dots\dots\dots\dots\dots\dots\dots\dots\dots\dots\text{(8)}$$

These reactions result in degradation of autoclaved aerated concrete by means of shrinkage, cracks and fractions (Matsushita et al., 2000; Matsushita et al. 2004; Kus and Carlsson, 2003).

CHAPTER 3

MATERIAL AND METHOD

In this chapter, the methods used for the sampling and laboratory analyses conducted on the samples were explained in detail. The sampling of porous materials, namely mudbrick and autoclaved aerated concrete and the laboratory tests used for their material characterization were explained. The focus was given on the analyses of breathing features of mudbrick and AAC materials in terms of water vapor permeability and carbon dioxide diffusion characteristics. The analytical methods defined in standards for water vapor permeability characterization and the methods adapted and developed from the standard methods for measuring CO_2 diffusion characteristics were described here under respective subheadings. The relevant tests to monitor the interaction between CO_2 and AAC were also explained in this chapter.

3.1. Sampling

In the study, mud brick as a traditional building material and autoclaved aerated concrete (AAC) as a contemporary building material were examined in terms of their air permeability characteristics and their contribution to indoor air quality. Both materials are well-known by their high breathable characteristics. Although, the adequacy of their breathing features for sustaining acceptable indoor air quality have not been identified yet by means of comprehensive studies.

Such a study was configured to examine breathing features of:
- The traditional/original mud brick block units which were obtained from approximately 70 year-old traditional buildings **(Figure 3.01)** in Hamzalı Village (Sulakyurt, Kırıkkale).
  - The commonly-used types of AAC blocks, type G2 (infill unit) and type G4 (load-bearing unit) for construction of contemporary building walls (**Figure 3.02**).

Figure 3.01. The building and the walls where the samples of mud brick block, mud mortar and mud plaster, Hamzalı Village, Kırıkkale.

Figure 3.02. The G2 and G4 type AAC samples provided from a local producer and cut to the same size as mud brick from Hamzalı Village.

The mud brick from Hamzalı Village is still well-performing in existing traditional mud brick houses as a load bearing wall unit. Some samples of neighboring mud mortar and plasters which complement the mudbrick wall section were also collected for some supportive laboratory tests. The autoclaved aerated concrete (AAC) material studied in

this research is produced according to the standard TS EN 771-4 by a local manufacturer. The AAC samples are subjected to investigations after being stored in the laboratory for two years. Whereas, mud brick is a material which has a wide range of variety in terms of characteristics depending on the raw material, manufacturing method, its purpose and the region where it is from. In order to define the material properly and compare it to the other studied mud brick types from the literature, the mud brick samples from Hamzalı Village are studied in terms of their physical, physicomechanical, mechanical, compositional and raw material characteristics. The sample types for each analysis are specified on the **Table 3.01** and **Table 3.02**.

During the CO_2 diffusion experiments it is determined that AAC samples retain an inevitable amount of CO_2. Therefore additional water vapor permeability tests with G2 and G4 type AAC prisms are performed after they were exposed to 20% CO_2 and 100 relative humidity for a week. Also single and double-chamber CO_2 diffusion tests are performed with G2 and G4 type AAC blocks exposed to 20% CO_2 and 100 relative humidity for three weeks.

In short, the CO_2 diffusion tests are applied for:

- Mud brick block from Hamzalı Village
- Unexposed G2 and G4 blocks (stored in the laboratory for 2 years after production)
- Exposed G2 and G4 blocks (exposed to 20% CO_2, 100% RH, for 3 weeks)

In order to better understand the breathing properties of AAC after it completes its carbonation process, the tests are conducted on both unexposed and exposed AAC blocks.

Table 3.01. The sample types used for the analysis of the physical and physicomechanical characteristics

Related Analysis	Method of Analysis	Type of the Material
Physical, Physicomechanical and Mechanical Characteristics		
Bulk density (g.m^{-3})	RILEM, 1980; Teutonico, 1988	Mud brick prisms G2 type AAC prisms G4 type AAC prisms
Effective porosity (%, volume)	RILEM, 1980; Teutonico, 1988	Mud brick prisms G2 type AAC prisms G4 type AAC prisms
Equivalent air thickness of water vapor permeability (SD, m)	TS EN ISO 7783, 2012 ASTM E96/E96M-15	Mud brick prisms Mud plaster fragment Mud mortar fragment G2 type AAC block G4 type AAC block
Water vapor diffusion resistance index (μ, unitless)		
Water vapor diffusion rate (RT, g.h^{-1}.m^{-2})		
Water vapor permeability (1/SD, m^{-1})		
Critical time (T$_{CRITICAL}$, s) Decay time (T$_{DECAY}$, h)	Single-chamber and double-chamber CO_2 diffusion tests (method developed in this study, adopted from ASTM E 741-11:2011)	Mud brick block G2 type AAC block G4 type AAC block
CO_2 Concentration decay/increase curves (CO_2 concentration versus time)		
Rates of CO_2 Concentration decay (RD) and increase (RI) (mg.m^{-3}.s^{-1})	ASTM 741-11, 2011 Jacobs, 1967 Cussler, 1997 Wilson et al., 1999	
CO_2 diffusion rate (E, mg.s-1)	Jacobs, 1967 Cussler, 1997 Wilson et al,1999	
Effective CO_2 diffusion coefficient (D$_{EFF}$, cm^2.s^{-1})		
Diffusion index (D$_i$, 1/d)		
Ultrasonic pulse velocity (m.s^{-1})	ASTM D 2845-08:2008; RILEM, 1980	Mud brick prisms G2 type AAC prisms G4 type AAC prisms
Modulus of elasticity (GPa)	ASTM D 2845-08:2008; RILEM, 1980	Mud brick prisms G2 type AAC prisms G4 type AAC prisms
Point load stress index (I$_s$, MPa) & Uniaxial compressive strength (UCS, MPa)	Indirect calculation of the compressive strength by using the point load test data – ISRM Point Load Test 1985; Winkler, 1986.	Mud brick cubes G2 type AAC G4 type AAC

Table 3.02. The codes of the samples used for the analysis of the compositional and raw material characteristics

Related Analysis	Method of Analysis	Type of the Material
Compositional and Raw Material Characteristics		
Binder/aggregate ratio (%, weight)	Sieve analysis – Teutonico, 1988	Mud brick Mud mortar Mud plaster
Particle size distribution (%, weight)	Sieve analysis – Teutonico, 1988	Mud brick fragment Mud plaster fragment Mud mortar fragment
Binder (clay) type	Determination of the mineral struction by using X-Ray Diffractometer	< 0,063mm particles extracted from the mud brick samples
Chemical reaction between AAC & CO_2	Weight increase in AAC samples after being exposed to high CO_2 and RH levels for a week	G2 and G4 type AAC prisms
	Compositional molecular change of AAC after being exposed to high CO_2 and RH levels	Grinded G2 and G4 type AAC

3.2. Material Characterization

Sieve analysis is performed to determine the binder/aggregate, silt/clay and fiber ratio of the mud brick, the mud plaster and the mud mortar samples. First, the samples are left in distilled water and the fibers floating on water are extracted. Then, the samples are mixed with water and the particles which do not sink, but stay suspended on the water one minute after being mixed, are taken into another beaker by using a syringe. The amount of the clay and silt content which sinks to the bottom of the beaker after 24 hours is dried in an incubator (60 C°) after the limped water above it is taken out by a syringe. This procedure is repeated three times for each sample to wash the clay and silt off the samples decently. By this method, the clay and silt content in the samples are extracted from the other parts of the samples (**Figure 3.03**).

XRD analysis is performed on the extracted clay in order to determine the clay type in the samples (**Figure 3.04**). The rest of the samples are dried in an incubator and sift through

4 mm, 2 mm, 1 mm, 0.500 mm, 0.250 mm, 0.125 mm and 0.063 mm sieves (**Figure 3.03**). Particles which are collected in each sieve are weighed and the percentage of each particle size is calculated by weight.

During the carbon dioxide permeability tests where AAC blocks are involved, it is observed that the increase in CO_2 concentration in Chamber 2 is not as much as the concentration decay in Chamber 1. A preliminary experiment is performed on the AAC samples to determine if the AAC samples retain CO_2 or react with it. First, G2 and G4 type AAC prisms with known dry weight are exposed to 20% CO_2 and %100 relative humidity for a week. Then the weight increase is detected in each dried sample after the preliminary experiment. Therefore additional XRD analyses are performed on unexposed and exposed AAC samples in order to determine any molecular difference between those two.

Figure 3.03. The sieves used for the sieve analysis in order to determine the particle size distribution of the mud brick, mud plaster and mud mortar samples.
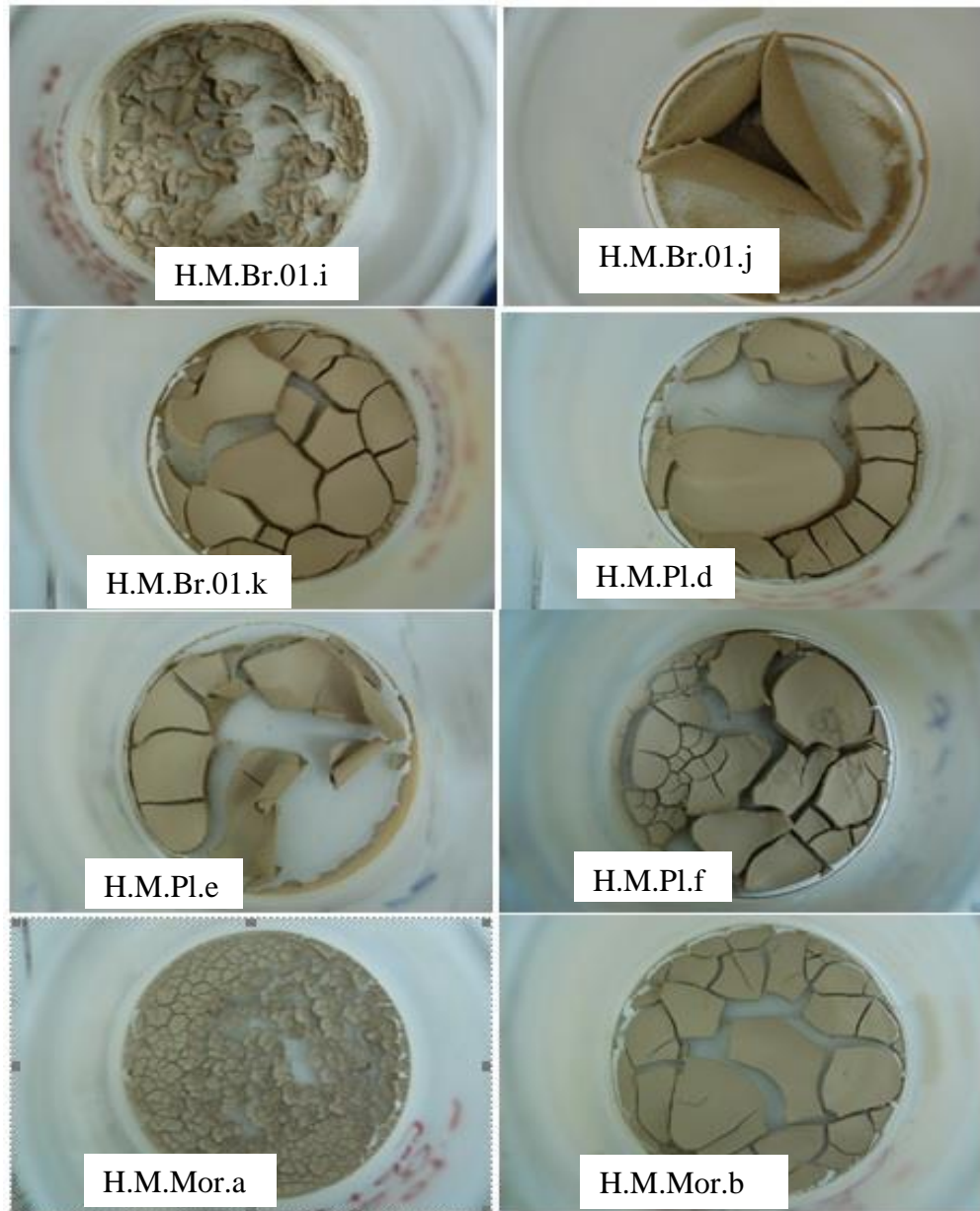
Figure 3.04. The clay and silt content extracted from the mud brick (H.M.Br.01.i, H.M.Br.01.j and H.M.Br.01.k), mud plaster (H.M.Pl.d, H.M.Pl.e and H.M.Pl.f) and mud mortar (H.M.Mor.a and H.M.Mor.b) samples.

3.3. Determination of Water Vapor Permeability Characteristics

Water vapor permeability characteristics of building materials are evaluated by measurable parameters defined in standards: water vapor permeability (1/SD, m^{-1}), water vapor permeance (SD, m), water vapor transmission rate (RT, $g.h^{-1}.m^{-2}$) and water vapor

diffusion resistance index (μ, uniteless) (RILEM, 1980; Teutonico, 1986; TS EN ISO 7783, 2012; TS EN 1015-19:2000; ASTM E96-92, 1992; DIN 52615, 1987).

Water vapor permeance (SD, m) is the time rate of water vapor transmission through unit area of flat material or a wall section induced by unit vapor pressure difference between two specific surfaces, under specified temperature and humidity conditions. It is calculated using **Equation 9** (ASTM, 1992).

$$SD = \mu \times S_O = (\delta_L \times A \times \frac{P_1 - P_2}{I}) - S_L \dots\dots\dots\dots\dots\dots\dots\dots\dots\dots\dots\dots\dots\dots\dots\dots\dots \textbf{(9)}$$

Where;

SD: Equivalent air thickness of water vapor permeability (m)

μ: Water vapor permeability resistance coefficient $= SD/S_O$

S_O: Thickness of the sample (m)

δ_L: (Constant) 6.89×10^{-6} (kg/mh (kg/m²))

A: Area of the sample through which water vapor is transmitted (m²)

P_1: P_O multiplied by % relative humidity in the container (kg/m²)

P_2: P_O multiplied by % relative humidity in the medium (kg/m²)

P_O: Pressure at measured temperature (kg/m²) (18.6466 mm Hg $=$ 253.5016 kg/m² at 21ºC) (Lange and Forker, 1967).

I: Weight change in unit time (kg/h)

S_L: Air thickness beneath the sample (m)

Water vapor permeability (1/SD, m^{-1}) is the time rate of water vapor transmission through the unit area of flat material of the unit thickness induced by the unit vapor pressure difference between two specific surfaces, under specified humidity and temperature conditions (ASTM, 1992).

Water vapor transmission rate (RT, g.h^{-1}.m^{-2}) is the steady water vapor flow in unit time through unit area of a body, normal to specific parallel surfaces, under specific conditions of temperature and humidity at each surface (ASTM, 1992). Water vapor transmission rate is calculated by using **Equation 10** (ASTM, 1992).

$$RT = (\text{Weight change}) / (\text{Time} \times \text{Area}) \dots\dots\dots\dots\dots\dots\dots\dots\dots\dots\dots\dots.\textbf{(10)}$$

For determination of the water vapor characteristics of mud brick and AAC samples, experimental set up is arranged according to related standards as shown in **Figure 3.05** and **Figure 3.06** (RILEM, 1980; Teutonico, 1986; TS prEN 7783-2:1999; TS EN 1015-19:2000; ASTM E96-92, 1992; DIN 52615, 1987).
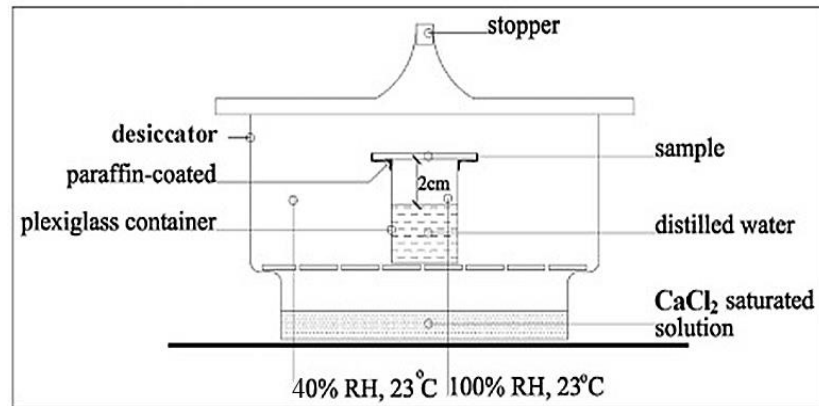
Figure 3.05. The experimental set up for the water vapor permeability tests in accordance with the related standards

Figure 3.06. The experimental set up for the water vapor permeability tests in accordance with the related standards

3.4. Determination of Carbon Dioxide Diffusion Characteristics

The aim of investigating the CO_2 diffusion characteristics of porous materials is to better understand how fast CO_2 diffuses from one environment to another through these materials without an induced air flow. In this study, two experimental set ups are developed for the suggested single and double chamber CO_2 diffusion tests. These test methods are developed in order to generate data which enables calculation of measurable parameters presented specific to this study. The related parameters suggested to determine CO_2 diffusion characteristics are listed as follows:

- **Concentration decay rate for single chamber** (RD_{SINGLE}, $mg.m^{-3}.s^{-1}$): It is the rate presenting the fastest reduction in CO_2 concentration in a certain period of time till the fastest decay starts to slow down. The RD_{SINGLE} specific to each material is obtained by the regression analysis of the CO_2 concentration decay curve which is acquired by single-chamber diffusion test with high CO_2 concentration.

- **Concentration decay rate for double chamber** (RD_{DOUBLE}, $mg.m^{-3}.s^{-1}$): It is the rate presenting the fastest reduction in CO_2 concentration in a certain period of time till the fastest decay starts to slow down. The RD_{DOUBLE} specific to each material is obtained by the regression analysis of the CO_2 concentration decay curve which is acquired by double-chamber diffusion test with high CO_2 concentration.

- **Concentration increase rate** (RI_{SINGLE}, $mg.m^{-3}.s^{-1}$): It is the rate presenting the fastest increase in CO_2 concentration in a certain period of time till the fastest increase starts to slow down. The RD_{SINGLE} specific to each material is obtained by the regression analysis of the CO_2 concentration decay curve which is acquired by double-chamber diffusion test with high CO_2 concentration.

- **Decay time** (T_{DECAY}, h): The period of time passes until the CO_2 concentration decays to 1000ppm in a single-chamber test with low concentration.

- **Critical time** ($T_{CRITICAL}$, s): The period of time passes until the fastest concentration decay rate starts to slow down.

- **Diffusion rate** (E, $mg.s^{-1}$): The amount of CO_2 diffuses through a porous material by time (Jacobs, 1967; Wilson *et. al*, 2009). It can be calculated by using RD values obtained from the single chamber tests using **Equation 11**.

$E = RD_{SINGLE} \times V$……………………………………………………….……….**(11)**

Where,

E: Diffusion rate, $mg.s^{-1}$

RD_{SINGLE}: Concentration decay rate from the single-chamber test, $mg.m^{-3}.s^{-1}$

V: Volume of the chamber, m^3 ($0.016m^3$ for this case)

- **Effective diffusion coefficient** (D_{EFF}, $cm^2.s^{-1}$): The amount of CO_2 which crosses through the unit section area of a porous material perpendicular to the diffusion direction in unit time and with unit concentration gradient. It can be calculated by the **Equation 12** which was derived from formulas in the Fick's law (Jacobs, 1967; Wilson *et. al*, 2009

$$D_{EFF} = \frac{E \times L}{A \, (C_{SOURCE} - C_0)}$$ …………………………………………………**(12)**

Where,

D_{eff}: Effective diffusion coefficient, $cm^2.s^{-1}$

E: Diffusion rate, $mg.s^{-1}$

L: Thickness of the porous wall unit which diffusion occurs through, cm

A: Area of the plane perpendicular to the direction of diffusion, cm^2

C_{SOURCE}: The initial CO_2 concentration in the chamber during a single-chamber test, $mg.cm^{-3}$

C_0: CO_2 concentration in the outer environment during the single-chamber test, $mg.cm^{-3}$

- **Diffusion index** (D_i, $1.d^{-1}$): The constant parameter about CO_2 diffusion characteristics specific to a porous material independent from its sizes. It is a parameter suggested in this study and calculated by using **Equation 13**.

$D_i = D_{EFF} \times A \times 3600 \times 24$……………………………………………...**(13)**

Where,

D_i: Diffusion index, $1/d^{-1}$

D_{EFF}: Effective diffusion coefficient, $cm^2.s^{-1}$

A: Area of the plane perpendicular to the direction of diffusion, cm^2

– **Amount of retained CO_2** ($M_{RETAINED}$, mg,%): The CO_2 amount retained by the porous material during the double-chamber tests by the end of 24h. It is also possible to calculate the percentage of the retained amount proportioned to the total CO_2 amount in the system using this parameter.

– **Amount of remained CO_2 in Chamber-1** (M_{CH-1}, mg, %): The CO_2 amount remained in Chamber-1 during the double-chamber tests by the end of 24h.

– **Amount of transmitted CO_2 to Chamber-2** (M_{CH-2}, mg, %): The CO_2 amount transmitted through the porous material during the double-chamber tests by the end of 24h.

– **Concentration peak level** (C_{MAX}, $mg.m^{-3}$): The maximum level of CO_2 concentration achieved in the chamber during the single-chamber CO_2 diffusion tests.

Double-chamber and single-chamber set-ups are developed in order to understand the air exchange between two adjacent environments through the porous wall section in between. The experiments are performed on mud brick, G2 type and G4 type autoclaved aerated concrete blocks. The experimental set-ups are based on the tracer gas (CO_2 in this case) concentration decay method from the ASTM E 741-11 (2011) standard, adopted and developed to be able to collect standard quantitative data.

The double-chamber experimental set-up is composed of two chambers which are airtight acrylic glass prisms (130mm x 390mm x 310mm, 0.016 m^3) and a sample block of examined material (180mm x 125mm x 310mm) in between these two chambers. The single-chamber set-up is composed of an airtight acrylic glass prism (130mm x 390mm x 310mm, 0.016 m^3) and a sample block sealed to it and open to air exchange with the outer environment (laboratory). To avoid any air leakage, set-ups are sealed by sealants (**Figure 3.06** and **Figure 3.07**). CO_2, which is chosen as the tracer gas, is generated by mixing

acetic acid and sodium bicarbonate ($NaHCO_3$) in a beaker put in the Chamber 1 (**Equation 14**).

$$C_2H_4O_2 + NaHCO_3 \rightarrow NaC_2H_3O_2 + H_2O + CO_2 \dots\dots\dots\dots\dots\dots\dots\dots\dots\dots\dots \textbf{(14)}$$

A CO_2 concentration of 2000 ppm in the chamber was provided by mixing 10ml acetic acid, 0.2 g sodium bicarbonate and 20 ml distilled water and this mixture generated 50mg CO_2 source in the chamber measured by the CO_2 measuring probe. A CO_2 concentration of 18000ppm in the chamber was provided by 50ml acetic acid and 2 g sodium bicarbonate without distilled water and that mixture generated 500mg CO_2 in the chamber measured by the CO_2 measuring probe.

Two different CO_2 concentration levels were set as initial levels in the chambers with CO_2 source. 2000 ppm is chosen as the realistic indoor concentration and 18000 ppm is chosen as an exaggeratedly high concentration in order to obtain a more detectable CO_2 flow rate in a shorter duration. Second approach serves the experimental set up to be a practical method.

In case of double-chamber experiments, the chemical reaction generates a CO_2 concentration level of around 18000 ppm in an airtight chamber, which is assumed to simulate occupied indoors with exaggeratedly high concentration levels and 2000 ppm which simulates realistic concentrations in occupied indoors in Chamber-1. On the other hand, Chamber-2 is filled with fresh air with CO_2 concentration levels around 500 ppm. The change of CO_2 concentration levels in 24 hours is constantly measured and recorded by Testo 480 indoor air quality measuring device and its two CO_2 monitoring probes placed into Chamber-1 and Chamber-2. The accuracy of the measuring device and its probes are taken into account, which is $\pm$ 75ppm + 3% of the measured value for 0-5000ppm and $\pm$150 ppm + 5% of the measured value for above 5000ppm.
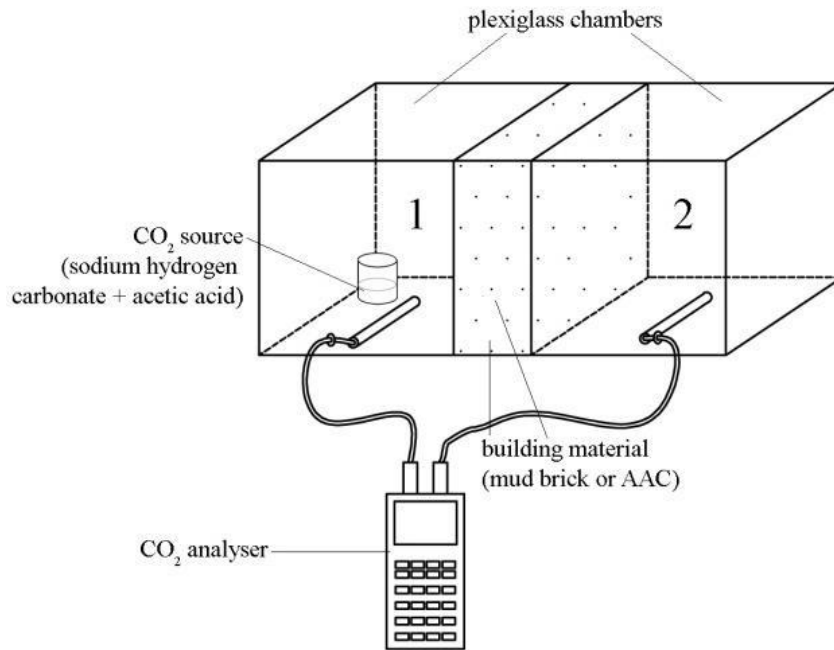
Figure 3.07. The double-chamber experimental set-up.
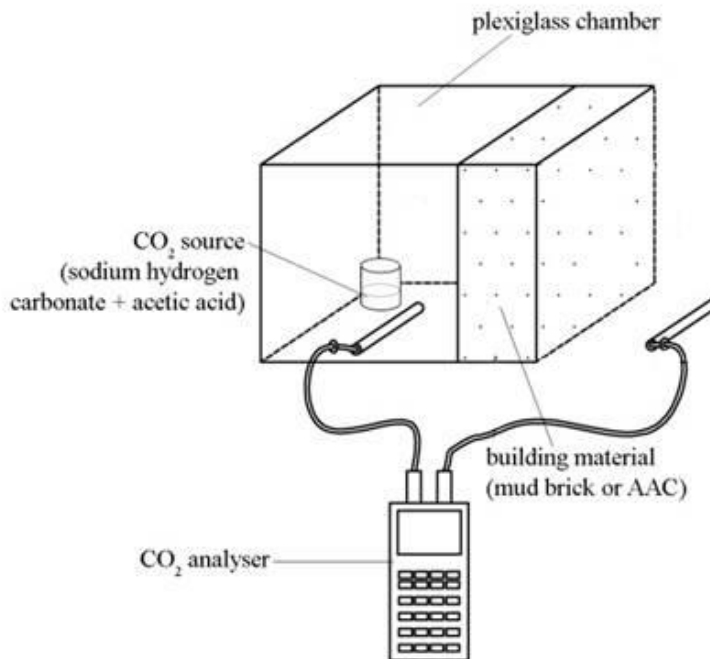
Figure 3.08. The single-chamber experimental set-up.

Figure 3.09. The double-chamber experimental set-up.

Figure 3.10. The single-chamber experimental set-up.

The methods used for the determination of CO_2 diffusion characteristics were explained in steps mainly in terms of "calibration of CO_2 measuring probes", "determination of CO_2 amount released by the source", "single-chamber diffusion tests with low and high CO_2 concentrations" and "double chamber diffusion test" under respective subheadings.

3.4.1. Calibration of the CO_2 Measuring Probes

For the calibration of the CO_2 measuring probes, they are set in airtight acrylic glass chambers together with CO_2 sources for both high and low ppm concentrations. Their reading ranges under the same indoor conditions are determine by this method.

The calibration tests are conducted by measuring different CO_2 concentrations in an airtight chamber with the two CO_2 monitoring probes which are used for the single and double-chamber CO_2 diffusion tests. It is observed that values concurrently measured by Probe-1 (Testo indoor air quality monitoring probe-371) are higher than the values measured by Probe-2 (Testo indoor air quality monitoring probe-336) and the difference increases linearly by the concentration level as shown in **Figure 3.11**.

The values measured by Probe-1 are assumed as the reference and the values from Probe-2 are calibrated accordingly by using **Equation 15**.

$y = x + 0.0831x + 116.02$ …………………………………….…………..………..…..**(15)**

Where;

y: Calibrated value read by Probe-2 (ppm)

x: Actual measured value by Probe-2 (ppm)
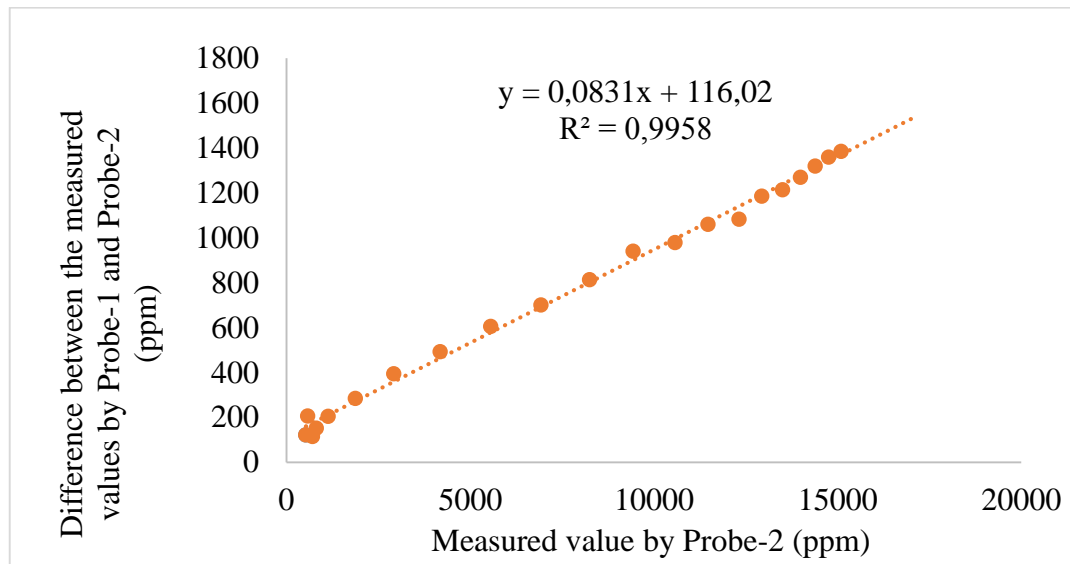
Figure 3.11. Correlation between CO_2 centration increase and concurrently measured value differences between Probe-1 and Probe-2.

The data obtained from calibration of the probes in airtight acrylic glass chambers with CO_2 source also gives information on the total CO_2 amount released by the source and the maximum CO_2 concentrations reached in the chamber. The concentration data in ppm is converted into $mg.m^{-3}$ by using **Equation 16** and the CO_2 amounts in the chambers are calculated by using **Equation 17**.

3.4.2. Production of CO_2 for Diffusion Tests

CO_2, which is chosen as the tracer gas for diffusion tests, is generated by mixing acetic acid and sodium bicarbonate ($NaHCO_3$) in a beaker (**Equation 16**). That mixture was used as the source of CO_2 and put in the relevant chamber.

$$C_2H_4O_2 + NaHCO_3 \rightarrow NaC_2H_3O_2 + H_2O + CO_2 \dots\dots\dots\dots\dots\dots\dots\dots\dots\dots\dots \textbf{(16)}$$

For single-chamber diffusion test with low concentration, the CO_2 concentration of 1500ppm was provided by mixing 10ml acetic acid, 0.2g sodium bicarbonate and 20ml distilled water. This mixture generated 50mg CO_2 source in the chamber measured by the CO_2 Measuring Probe. Together with the existing CO_2 amount in the fresh air, the highest

45

concentration of CO_2 in the chamber is expected to be 2000ppm for the single-chamber diffusion test with low CO_2 concentration.

For single and double-chamber diffusion test with high concentration, the CO_2 concentration of 17500ppm was provided by 50ml acetic acid and 2g sodium bicarbonate without distilled water. That mixture generated 500mg CO_2 in the chamber measured by the CO_2 Measuring Probe. Together with the existing CO_2 amount in the fresh air, the highest concentration of CO_2 in the chamber is expected to be 18000ppm for the single- and double-chamber diffusion tests with high CO_2 concentration.

The two different CO_2 concentration levels were needed:
−   The 2000ppm is the level corresponding to poor indoor air quality generated by crowded people during 30-60 minutes meeting. The CO_2 concentration of 1000ppm is the acceptable comfort level above which air conditioning systems function stronger in order to keep the concentration below that threshold (Fisk *et al*. 2010; ASHREA, 2007). Therefore, the preliminary tests were performed with 2000ppm as the highest amount of CO_2 concentration which represent common polluted indoor conditions.
−   The 18000ppm is an exaggeratedly-high CO_2 concentration which enables monitoring CO_2 diffusion through a material in more detectable ranges and in shorter duration. Therefore, high concentration of CO_2 was easy to generate and its use is more preferable to establish the experimental set up for practical purposes.

The maximum concentration levels in ppm are converted into mg.m^{-3} by using **Equation 17** (Yates, 2015).

$$(C \text{ in mg.m}^{-3}) = (C \text{ in ppm}) \times MW / 24.45 \dots\dots\dots\dots\dots\dots\dots\dots\dots\dots\dots\dots\dots\dots\text{(17)}$$

Where,

C in mg.m^{-3}: CO_2 concentration in mg.m^{-3}

C in ppm: CO_2 concentration in parts per million

MW: molecular weight (44.01g/mole for CO_2)

With the concentration data in $mg.m^{-3}$, the CO_2 amount in the chamber is calculated using **Equation 18**.

$$M = C \times V \dots\dots\dots\dots\dots\dots\dots\dots\dots\dots\dots\dots\dots\dots\dots\dots\dots\dots\dots\dots\dots\dots\dots\dots\dots\dots\dots\dots\dots\dots\dots.\textbf{(18)}$$

Where,
M: CO_2 amount in the chamber (mg)
C: CO_2 concentration ($mg.m^{-3}$)
V: Volume of the chamber (m^3)

3.4.3. Single-Chamber CO_2 diffusion test with low concentration of CO_2

In the experiment, 50mg CO_2 is used as the source of tracer gas resulting in the initial level of 2000ppm CO_2 concentration. Under the same relative humidity and temperature conditions provided indoor and outdoor, the CO_2 concentration in the chamber was monitored till the concentration reduced to 1000ppm while almost a constant CO_2 concentration of 500ppm were recorded outside the chamber (in the laboratory). That level is critical since fresh air supply of HVAC systems must be designed to keep the indoor concentrations at 1000ppm or below according to ASHRAE (2007). Two measuring probes were used for recording CO_2 concentration in the chamber and outside the chamber with 30s intervals. The outer environment has a concentration of approximately 500ppm. At the end of the diffusion test, the peak level of CO_2 concentration achieved in the chamber (C_{MAX}, $mg.m^{-3}$) and the time (T_{DECAY}, h) needed for the concentration decay to the level of 1000ppm were determined.

3.4.4. Single-Chamber CO_2 Diffusion Tests with high concentration of CO_2

In the experiment, 500mg CO_2 is used as the source of tracer gas resulting in an initial level of 18000ppm CO_2 concentration. Under the same relative humidity and temperature conditions provided indoor and outdoor, the CO_2 concentration in the chamber was monitored for 24 hours while almost a constant CO_2 concentration of 500ppm were recorded outside the chamber (in the laboratory). Two measuring probes were used for recording CO_2 concentration in the chamber and outside the chamber with 60s intervals.

The outer environment has a concentration of approximately 500ppm. At the end of the diffusion test, it is expected to determine:

- Concentration decay rate (RD_{SINGLE}, $mg.m^{-3}.s^{-1}$),
- CO_2 diffusion rate (E, $mg.s^{-1}$),
- Effective CO_2 diffusion coefficient (D_{EFF}, $cm^2.s^{-1}$),
- Diffusion index (D_i, d^{-1}),
- The peak level of CO_2 concentration (C_{MAX}, $mg.m^{-3}$)
- Critical time ($T_{CRITICAL}$, h).

The data obtained is presented in a graph showing the reduction in CO_2 concentration ($mg.m^{-3}$) as a function of time (s) (**Figure 3.12**). Concentration decay rate (RD, $mg.m^{-3}.s^{-1}$), the peak level of CO_2 concentration (C_{MAX}, $mg.m^{-3}$) and critical time ($T_{CRITICAL}$, s) are the data extracted from that graph while diffusion rate (E, $mg.s^{-1}$), effective diffusion coefficient (D_{EFF}, $cm^2.s^{-1}$) and diffusion index (D_i, d^{-1}) are calculated by using **Equation 11**, **Equation 12** and **Equation 13** respectively.

RD is the sharpest slope obtained by the linear regression representing the fastest CO_2 concentration decay in the chamber when the concentration difference between the chamber and outside is the highest (**Figure 3.12**). The correctness of the slope is controlled with the coefficient of determination (R-squared value) being above 0.99. Critical time ($T_{CRITICAL}$, s) is the time period passed until the fastest concentration decay starts to slow down. It was determined by the data extracted from the graph (**Figure 3.12**).
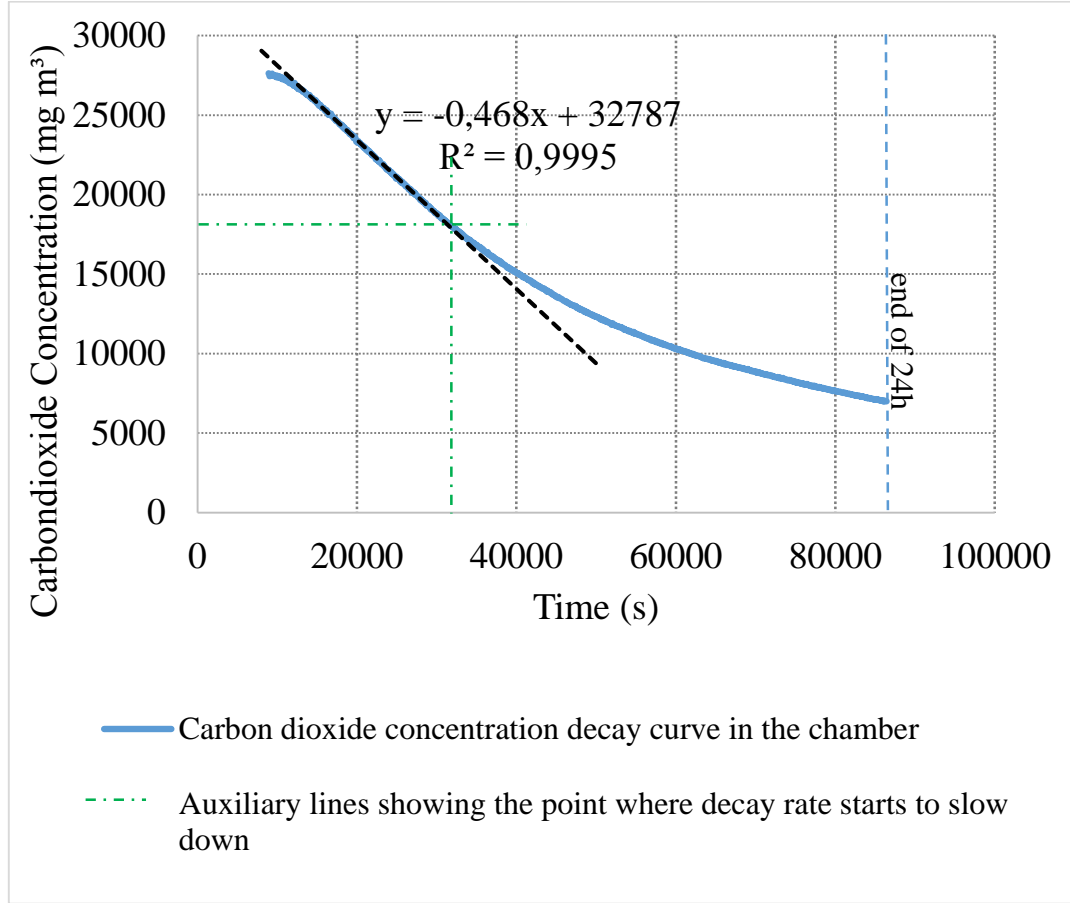
Figure 3.12. The CO_2 concentration decay curve versus time obtained by the single-chamber diffusion test at high CO_2 concentration during the 24h of experiment period, showing the slope of the fastest CO_2 concentration decay and critical time when that sharpest decline starts to slows down ($C_{MAX} = 15349$ppm, 27629mg.m^{-3}, $T_{CRITICAL} = 30000$s)

3.4.5. Double-Chamber CO_2 Diffusion Tests with high concentration of CO_2

The experimental set-up consists of two airtight acrylic glass (plexiglas) chambers and a porous material block separating them. In double-chamber CO_2 diffusion tests, 500mg CO_2 is used as the source of tracer gas resulting in an initial level of 18000ppm CO_2 concentration in Chamber 1. Under the same relative humidity and temperature conditions provided in both chambers, the CO_2 concentrations in Chamber-1 and Chamber-2 were recorded by using two measuring probes with 60s intervals during 24 hours of experiment period. At the end of the test, it is expected to determine:

- Concentration decay rate (RD_{DOUBLE}, $mg.m^{-3}.s^{-1}$)
- Concentration increase rate (RI_{DOUBLE}, $mg.m^{-3}.s^{-1}$)
- The amount of CO_2 in Chamber-1 (M_{CH-1}, in mg and %) by the end of the experiment
- The amount of CO_2 in Chamber-2 (M_{CH-2}, mg and %) by the end of the experiment
- The amount of CO_2 retained by the material ($M_{RETAINED}$, in mg and %) by the end of the experiment

The data obtained is presented in a graph showing the CO_2 concentration decay ($mg.m^{-3}$) in Chamber-1 and concentration increase ($mg.m^{-3}$) in Chamber-2 as a function of time (s) (**Figure 3.13**). Concentration decay rate (RD, $mg.m^{-3}.s^{-1}$) and concentration increase rate (RI, $mg.m^{-3}.s^{-1}$) are the data extracted from that graph.

RD_{DOUBLE} is the sharpest slope obtained by the linear regression representing the fastest CO_2 concentration decay in Chamber-1 when the concentration difference between the chambers is the highest (**Figure 3.13**). RI_{DOUBLE} is the sharpest slope obtained by the linear regression representing the fastest CO_2 concentration increase in Chamber-2 when the concentration difference between the chambers is the highest (**Figure 3.13**). The correctness of the slopes is controlled with the coefficient of determination (R-squared value) being above 0.99.
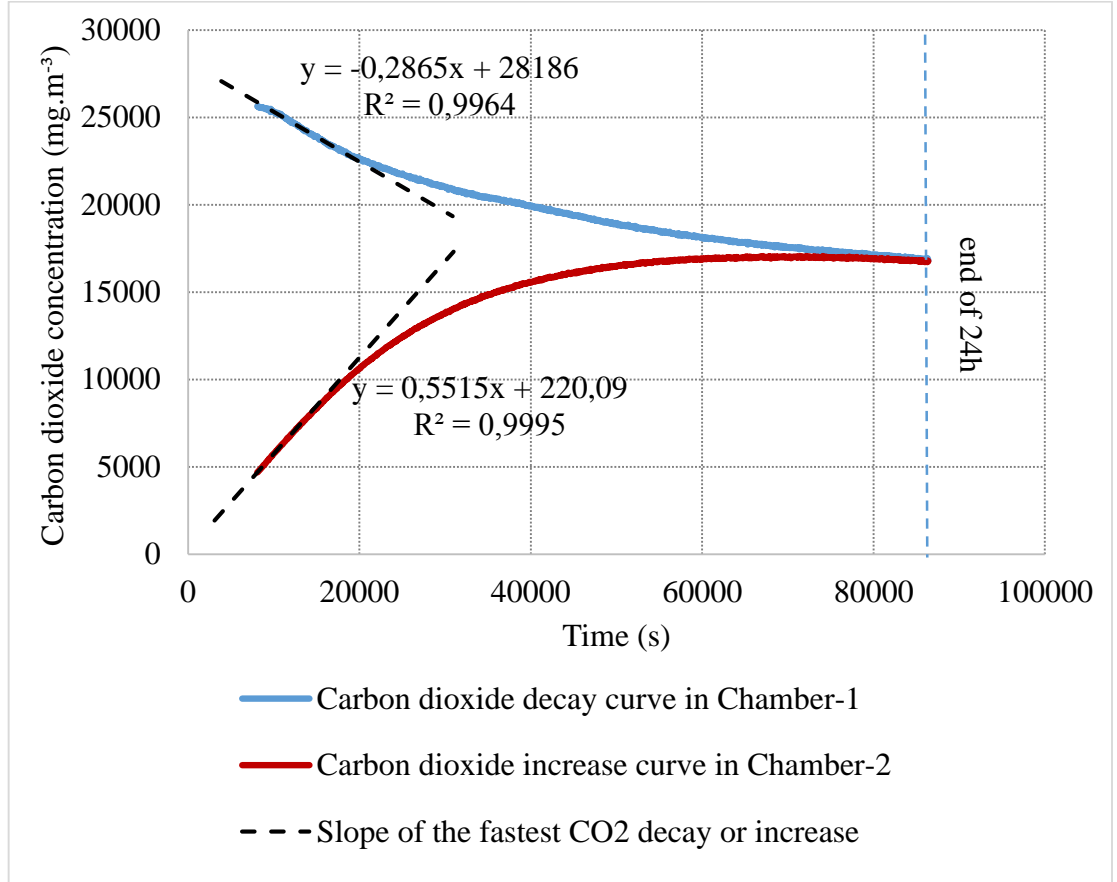
Figure 3.13. The CO_2 concentration decay curve versus time obtained by the double-chamber diffusion test at high CO_2 concentration during the 24h of experiment period, showing the slopes of the fastest CO_2 concentration decay in Chamber-1 and concentration increase in Chamber-2.

The amounts of CO_2 remained in Chamber-1 and Chamber-2 as well as the retained by the mudbrick and AAC samples are calculated by the end of 24 hours of experiment period. The **Equation 16** and **Equation 17** were used for the calculation of CO_2 amount in the chambers while **Equation 18** was used to calculate the retained amount in the material.

3.5 Identification of CO_2-philic Characteristics

In order to identify whether a materials is CO_2-philic or not, the amount of CO_2 in both chambers were measured by double-chamber experimental set up. In case that there is a certain amount of CO_2 retained in the material, the relevant laboratory tests were conducted on CO_2-exposed and –unexposed samples for monitoring the changes in

51

density, water vapor permeability, ultrasonic velocity, modulus of elasticity. The resultant products occurred after CO_2-exposure were identified by XRD analyses. The presence of any visual defect, such as cracks were visually-examined in macro scale.

Depending on the results obtained from double-chamber experiment, the material selected was exposed to 20% CO_2 concentration and 100% relative humidity for a week in CO_2 desiccator (**Figure 3.14**). The dry weight of the samples before and after exposure was measured to confirm the data obtained from double-chamber test whether CO_2 retained in the material or not.

Figure 3.14. The CO_2 desiccator in which the AAC samples were exposed to 20% CO_2 concentration and 100% relative humidity.

Since temperature fluctuations may influence the amount of CO_2 retained in the material and effect the data acquired from double-chamber tests, the CO_2 absorption/adsorption properties of materials were examined by double-chamber diffusion tests. That examination was done in double-chamber experimental set-up following the 24 hours (one day) of CO_2 diffusion through one chamber to the other, which was accepted as the standard duration for CO_2 diffusion tests. The amount of CO_2 absorbed/adsorbed by the material was determined for the case where temperature fluctuations were provided between 20°C and 40°C cyclically during double-chamber experiments.

CHAPTER 4

RESULTS

The results of laboratory analyses on "raw materials and compositional properties of Hamzalı Village traditional mudbrick", "basic materials characteristics and breathing features of that mudbrick and AAC units" with a focus on their water vapor and CO_2 diffusion characteristics are given in this section under respective subheadings.

4.1. Compositional and Raw Material Characteristics of Mud Brick

The data on compositional and raw material characteristics of the Hamzalı Village traditional mud brick, plaster and mortar samples are presented in **Table 4.01, Figure 4.01, Figure 4.02** and **Figure 4.03**. These characteristics are summarized below:

- The percentage of the silt and clay content of the mud samples is between 43% and 49% by weight (**Table 4.01, Figure 4.01** and **Figure 4.02**). This range is within the recommended silt and clay content percentage range for mud bricks, although it is close to the highest limits of it (Jimenez Delgado and Guerrero, 2007). The amount of silt and clay content in mud brick samples is 5% more, compared to the mud plaster and the mud mortar samples.
- The percentage of the aggregate content of the mud samples changes between 52% and 57% (**Figure 4.01** and **Figure 4.02**).
- The percentage of the very fine sand (0.063 mm < particle size < 0.125 mm) content of the samples changes between 23% and 28%, while that of the fine sand (0.125 mm < particle size < 0.250 mm) changes between 13.5% and 14.7% (**Figure 4.01** and **Figure 4.02**). It is observed that the aggregate types with smaller particle sizes are dominant in particle size distribution.
- It is determined that the middle size sand (0.250 < particle size < 0.500mm) and coarse sand (0.500mm < particle size< 1mm) content of the samples are in the range of 6.6-11.4 % and 3.1-4.7%. (**Figure 4.01** and **Figure 4.02**).

- Maximum 1.4 % of samples consist of very coarse sand (1 mm <particle size< 2mm) and maximum 0.7 % of samples consist of gravel (2 mm< particle size< 4 mm). These data shows that larger aggregate types such as very coarse sand and fine gravel exists in very small amounts in total mud brick, mud plaster and mud mortar compositions (**Figure 4.01** and **Figure 4.02**).
- Mud brick, mud plaster and mud mortar, the adjacently used materials, are similar in terms of their silt-clay/aggregate ratios (**Table 4.01**, **Figure 4.01** and **Figure 4.02**).
- The vegetal fiber percentage of the samples changes between 0.2% and 1.6 % by weight (**Table 4.01**).
- Quartz, calcite, kaolin, illite, albite, and cristobalite are the detected minerals in the oriented silt-clay sample extracted from the mud brick samples by the XRD analysis (**Figure 4.03**). The fingerprints of kaolin and illite in the XRD peaks indicate the binder (clay) types present in the mud brick samples.

Table 4.01. The silt-clay, aggregate and fiber ratios of the mud brick, mud plaster and mud mortar samples from Hamzalı Village, Kırıkkale (by weight).

Sample Code - Definition	Silt-Clay Ratio (%)	Aggregate Ratio (%)	Fiber Ratio (%)
H.M.Br.01 – Mud brick	48.86 ± 4.40	52.75 ± 5.53	0.15 ± 0.12
H.M.Pl.01 – Mud plaster	$43.03 + 6.14$	56.97 ± 6.14	0.89 ± 0.06
H.M.Mor.01 – Mud mortar	43.27 ± 0.87	56.73 ± 0.87	1.57 ± 0.21

The chart includes a data table:

	H.M.Br.01	H.M.Pl.01	H.M.Mor.01
■ fiber	0,16	0,85	1,19
■ x<0,063mm	47,15	42,66	42,76
■ 0,063mm<x<0,125mm	28,04	23,07	27,69
■ 0,125mm<x<0,250mm	13,74	14,68	13,49
■ 0,250mm<x<0,500mm	6,64	11,39	8,88
■ 0,500mm<x<1mm	3,13	4,73	4,26
■ 1 mm<x<2mm	1,12	1,35	1,24
■ 2mm<x<4mm	0,04	0,77	0,50
■ x>4mm	0,00	0,50	0,00
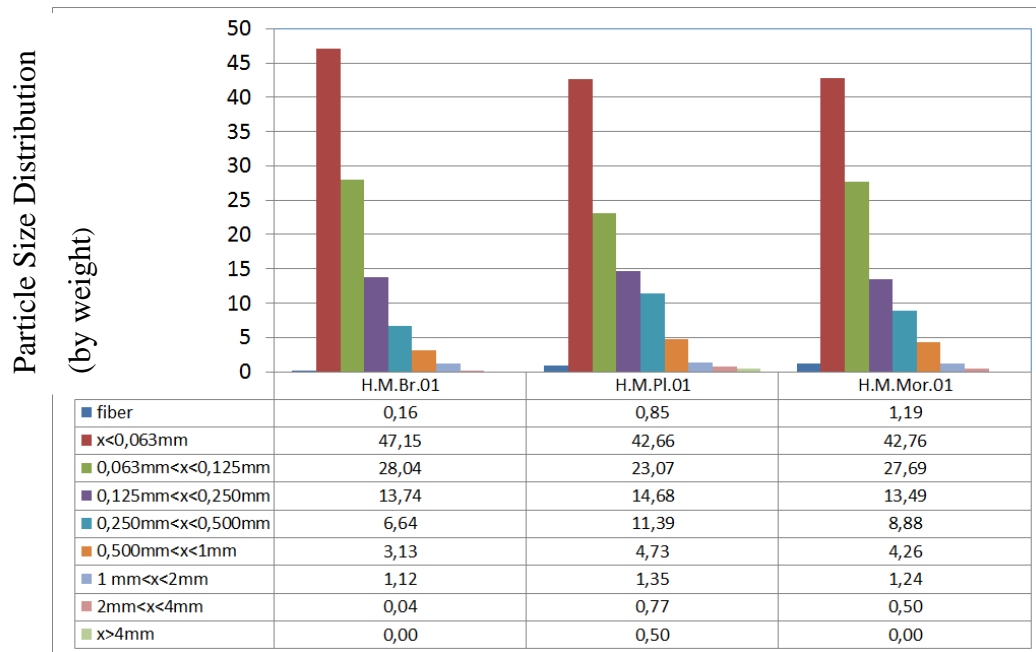
Figure 4.01. The graphics presenting the particle size distribution of mud brick, mud plaster and mud mortar from Hamzalı Village: fiber, silt-clay (the binder), very fine sand, fine sand, middle size sand, coarse sand, very coarse sand and gravel ratios by weight.
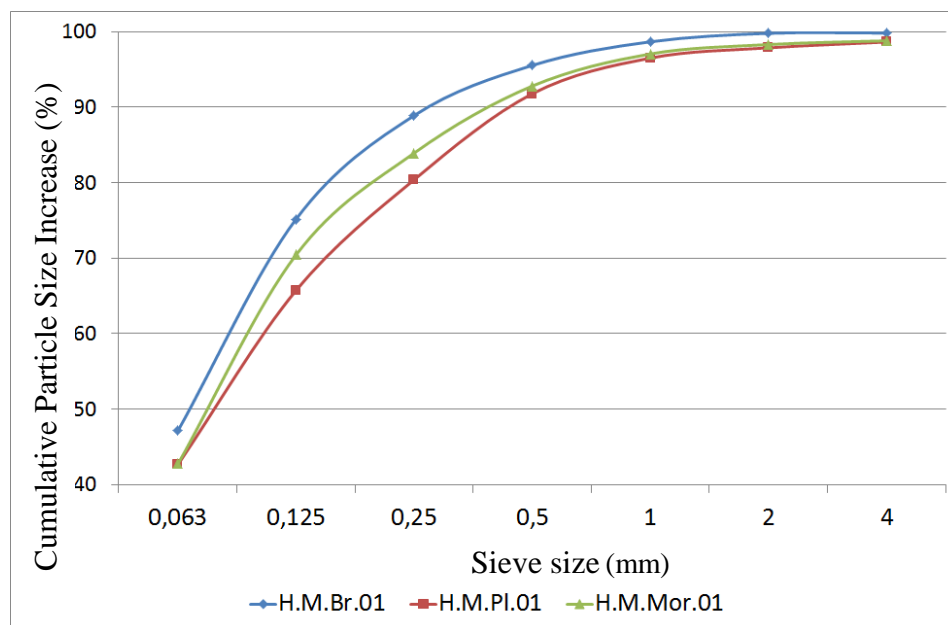
Figure 4.02. The graph which presents the cumulative increase of weight percentage from the finest particles to the largest, added on each other for the mud brick, mud plaster and mud mortar samples from Hamzalı Village, Kırıkkale.
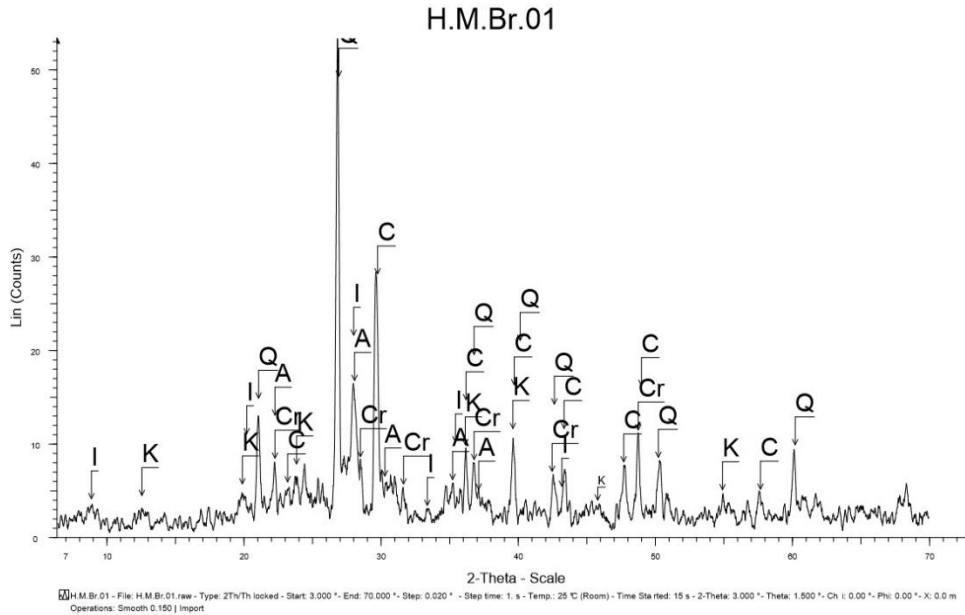
Figure 4.03. The XRD fingerprints of the oriented clay sample extracted from the mud brick with the code "H.M.Br.01" (Q: Quartz, C: Calcite, K: Kaolinite, I: Illite, A: Albite, Cr: Cristobalite).

4.2. Basic Physical, Physicomechanical and Mechanical Properties of Mud Brick

The data obtained from the analyses which are performed on mud brick and AAC samples in order to determine their physical and physicomechanical properties are presented on **Table 4.02**.

Table 4.02. The data obtained from the analyses performed in order to determine the density (ρ), porosity (ϕ), ultrasonic pulse velocity (UPV) and modulus of elasticity (MoE) of the mud brick and autoclave aerated concrete samples.

Sample Type	ρ (g.cm^{-3})	ϕ (%)	Ultrasonic Pulse Velocity (m.s^{-1})	MoE (GPa)
Mud brick	1.60 ± 0.03	42.37 ± 0.34	1321 ± 65	2.569 ± 0.242
G2 type AAC	0.42 ± 0.00	74.10 ± 1.23	1703 ± 20	1.109 ± 0.017
G4 type AAC	0.62 ± 0.02	67.67 ± 2.49	$1955 \pm 3\ 0$	2.168 ± 0.119

Uniaxial compressive strength (UCS) and point load stress index (I_s) of the mud brick and AAC samples are presented on **Table 4.03**.

Table 4.03. The indirectly calculated uniaxial compressive strength (UCS$_{indirect}$), point load stress index (I_s) of the samples.

Sample Type	UCS$_{indirect}$ (MPa)	Point Load Stress Index (I_s, MPa)
Mud brick	0.89 ± 0.40	0.17 ± 0.08
G2 type AAC	1.33 ± 0.11	0.25 ± 0.03
G4 type AAC	2.36 ± 0.18	0.51 ± 0.04

4.3. Water Vapor Permeability Characteristics

The results of water vapor permeability tests on mud samples are summarized on **Table 4.04** and **Table 4.05**. Water vapor resistance factor (μ) of the mud brick, plaster and mortar samples from Hamzalı Village are found to be between 3.3 and 3.8. The μ values for G2 and G4 types of AAC were found to be 2.13 and 3.34, respectively, while those values reducing to 1.34 and 2.34 after the same AAC samples exposed to high concentration of CO_2 in presence of moisture for one week.

Table 4.04. The water vapor resistance factors (μ) of AAC and mud brick, plaster and mortar.

Material Type	μ (unitless)
Mud brick (Hamzalı Village)	3.30 – 3.80
Mud mortar (Hamzalı Village)	3.60
Mud plaster (Hamzalı Village)	3.40
Unexposed G2 type AAC	2.13
Unexposed G4 type AAC	3.34
Exposed G2 type AAC	1.34
Exposed G4 type AAC	2.34

Table 4.05. Water vapor permeability equivalent air thickness (SD, m) and water vapor permeance (1/SD, m^{-1}) values for 18cm thick mud brick and AAC blocks.

Material Type	SD (m)	1/SD (m^{-1})
Mud brick (Hamzalı Köyü)	0.59 – 0.69	1.45 – 1.70
Unexposed G2 type AAC	0.38	2.60
Unexposed G4 type AAC	0.60	1.66
Exposed G2 type AAC	0.24	4.16
Exposed G4 type AAC	0.42	2.37
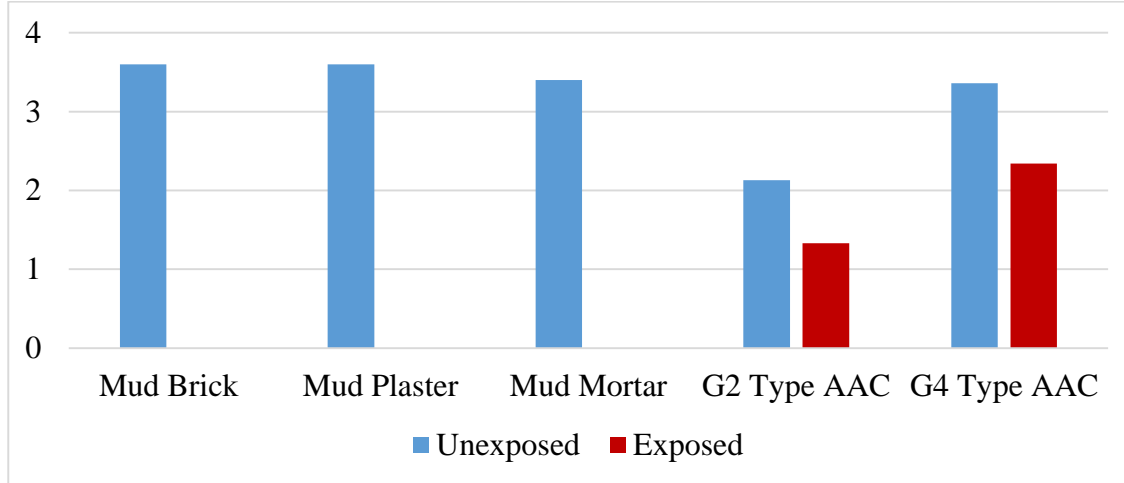
Figure 4.04. The μ values of the mud based materials from Hamzalı Village, exposed and unexposed AAC samples.

4.4. Carbon Dioxide Diffusion Characteristics

Calibration results, total CO_2 amounts released by the source and the results of the single and double-chamber CO_2 diffusion tests are presented in this part of the study under the related sub-headings.

4.4.1. Total CO_2 Amounts Released by the Source

The amount of the CO_2 generated by the sodium bicarbonate solution in acetic acid, to be used in the following experiments, and the duration of the reaction is monitored by a preliminary experimental set-up with a sealed airtight single chamber. The results are presented on **Table 4.06**. The reaction lasts for 5.5 hours and in the high concentration chamber 527 mg of CO_2 is generated, whereas the CO_2 amount in the low concentration chamber reaches to 61 mg.

Table 4.06. The results of the preliminary airtight single-chamber experiments performed for determination of the CO_2 amount and the duration of the reaction.

	C		**M$_{total}$**	**M$_{added}$**
	(ppm)	(mg.m^{-3})	(mg)	(mg)
High Concentration Chamber	18293	32927	527	513
Low Concentration Chamber	2116	3809	61	47

C: CO_2 concentration level reached in the airtight chamber (ppm, mg.m^{-3}), **M$_{total}$**: The total CO_2 amount in the airtight chamber at the end of the experiment (mg), **M$_{added}$**: The added CO_2 amount to the chamber (mg).

4.4.2. Single-Chamber CO_2 Diffusion Test Results

The data obtained from the single-chamber diffusion tests with low CO_2 concentration are presented in **Table 4.07** and **Figure 4.05**. The peak level of CO_2 concentration was determined as 1698ppm, which is lower than the initial level 2000ppm. Such a reduction in concentration level at the beginning of the test signaled high CO_2 diffusion characteristics of mudbrick. However, the duration needed for CO_2 concentration decay to the acceptable level of 1000ppm was 11.5 days. That period is a very long experiment duration. This experimental set up is far away from being a practical method for monitoring the diffusion behavior of a very breathable material in low pressure differences. Therefore, there is necessity to increase the initial CO_2 concentration to speed up the experiment and to achieve reliable and noticeable data.

Table 4.07. Results of the single-chamber CO_2 diffusion test with low CO_2 concentration.

Material Type	C_{MAX} (ppm)	(mg)	T_{DECAY} (h)
Mud brick	1698	3809	276 (11,5 days)

C_{MAX}: maximum CO_2 concentration reached in the single chamber (ppm), T_{DECAY}: CO_2 concentration decay time - down to 1000 ppm (h)
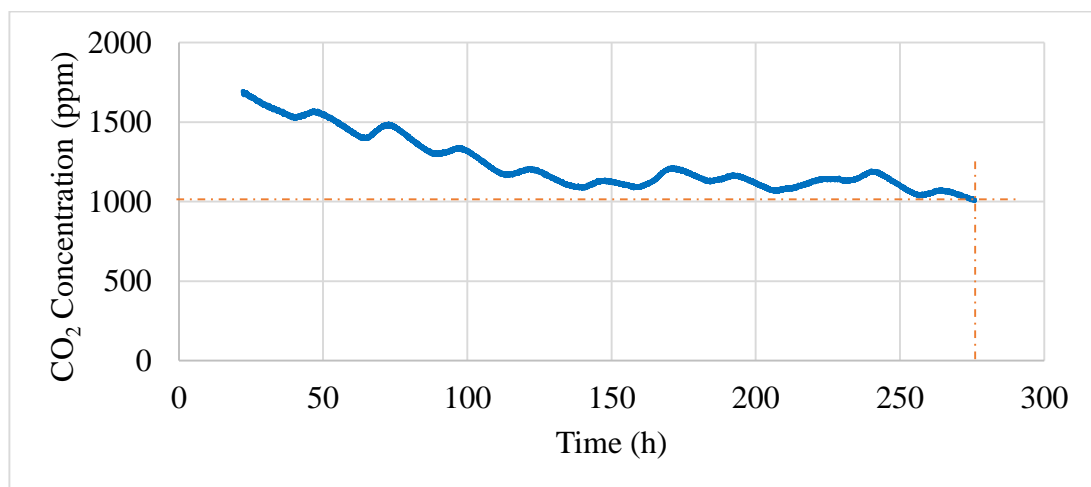
Figure 4.05. The CO_2 concentration decay curve of mudbrick sample versus time obtained by the single-chamber diffusion test (C_{MAX} = 1698ppm, 3809mg.m^{-3}), T_{DECAY} = 276 h, 11.5days).

For the mudbrick and unexposed AAC samples, the data obtained from the single-chamber diffusion test with high CO2 concentration are presented in **Table 4.08** and their CO$_2$ concentration decay curves are given **Figure 4.06**, **Figure 4.07**, and **Figure 4.08**. The data obtained for the G2 and G4 types of AAC samples after they have been exposed to high concentration of CO$_2$ are presented in **Table 4.08** and their decay curves are given in **Figure 4.09** and **Figure 4.10**, respectively.

The CO$_2$ concentration decay rate (**RD$_{SINGLE}$**) of mud brick is the highest by 0.47 mg.m^{-3} while it is 0.41 mg.m^{-3} for unexposed G2 type AAC, 0.35 mg.m^{-3} for unexposed G4, 0.26 mg.m^{-3} for exposed G2 and 0.23 mg.m^{-3} for exposed G4 type (**Table 4.08**).

The time passes until the concentration decay rate starts to slow down (**T$_{CRITICAL}$**) is the lowest for mud brick by 8.3h, while it is 10h for unexposed G2 type AAC, 9.8h for unexposed G4, 12.1h for exposed G2 and 11.1h for exposed G4 type (**Table 4.08**).

The CO$_2$ diffusion rate (**E**) of mud brick is the highest by 0.0075mg.s^{-1} while it is 0.0065mg.s^{-1} for unexposed G2 type AAC, 0.0055mg.s^{-1} for unexposed G4, 0.0041mg.s^{-1} for exposed G2 and 0.37mg.s^{-1} for exposed G4 type (**Table 4.08**).

The effective diffusion coefficient (**D$_{EFF}$**) of CO$_2$ in G2 type unexposed AAC is the highest by 0.014 cm^2.s^{-1} while it is 0.013 cm^2.s^{-1} for mud brick, 0.012 cm^2.s^{-1} for unexposed G4, 0.009 cm^2.s^{-1} for exposed G2 and 0.008 cm^2.s^{-1} for exposed G4 type (**Table 4.08**).

The diffusion index (**D$_i$**) of CO$_2$ in G2 type unexposed AAC is the highest by 3.02 d^{-1} while it is 2.92 d^{-1} for mud brick, 2.66 d^{-1} for unexposed G4 type, 1.91 d^{-1} for exposed G2, and 1.70 d^{-1} for exposed G4 type AAC (**Table 4.08**).

Table 4.08. The data on CO_2 diffusion properties of the mudbrick and AAC samples obtained from the single-chamber CO_2 diffusion tests with high CO_2 concentration conducted for 24 hours.

Material Type	RD_{SINGLE} (mg.m^{-3}s^{-1})	$T_{CRITICAL}$ (h)	E (mg.s^{-1})	D_{EFF} (cm^2.s^{-1})	D_i (1/d)	C_{MAX} (ppm)	(mg.m^{-3})
Mud brick	-0.4680	8.3	0.0075	0.0131	2.92	15349	27629
Unexposed G2	-0.4077	10.0	0.0065	0.0135	3.02	13181	23725
Unexposed G4	-0.3457	9.8	0.0055	0.0120	2.66	12646	22762
Exposed G2	-0.2572	12.1	0.0041	0.0086	1.91	13050	23490
Exposed G4	-0.2292	11.1	0.0037	0.0076	1.70	12933	23279

RD_{SINGLE}: CO_2 concentration decay rate in the chamber (mg.m^{-3}s^{-1}), **$T_{CRITICAL}$**: Critical time (h), **E**: Diffusion rate (mg.s^{-1}), **D_{EFF}**: Effective diffusion coefficient (cm^2.s^{-1}), **C_{MAX}**: CO_2 concentration peak level in the chamber (h).
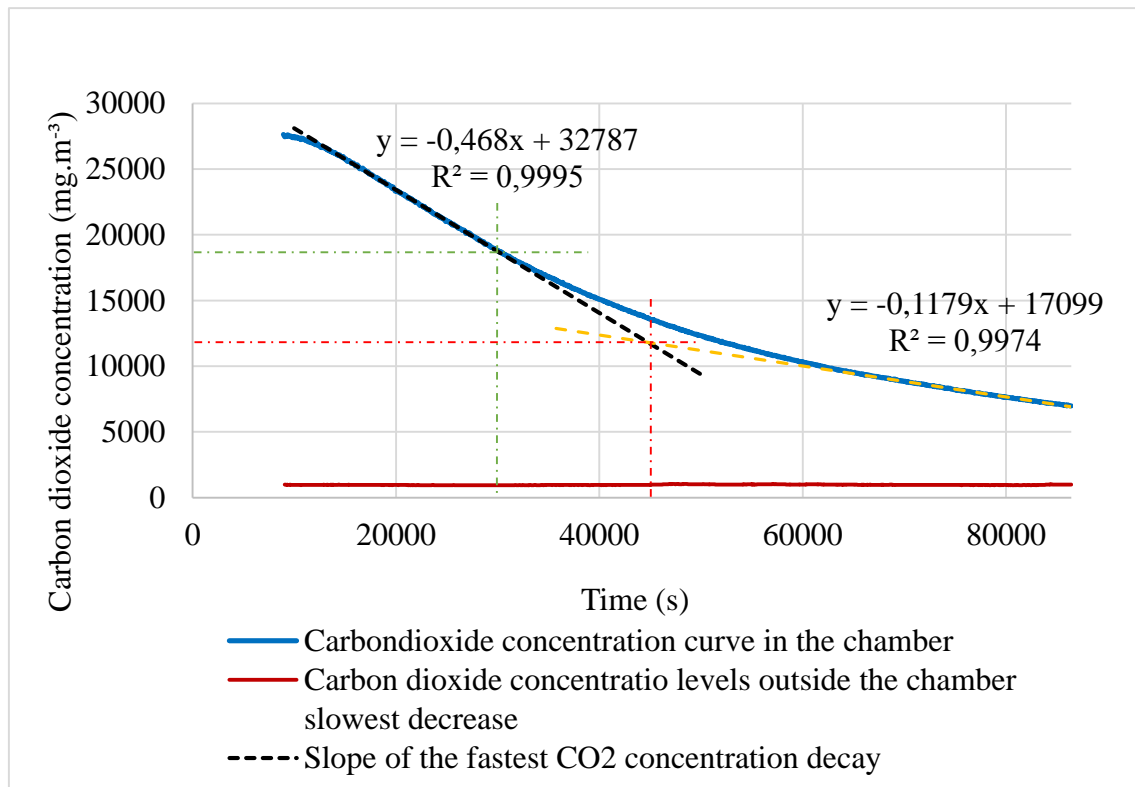
Figure 4.06. The CO_2 concentration decay curve of **mud brick** sample versus time obtained by the single-chamber diffusion test with high CO_2 concentration (**C_{MAX}** = 15349ppm,   27629mg.m^{-3}, **$T_{CRITICAL}$** = 30000s).
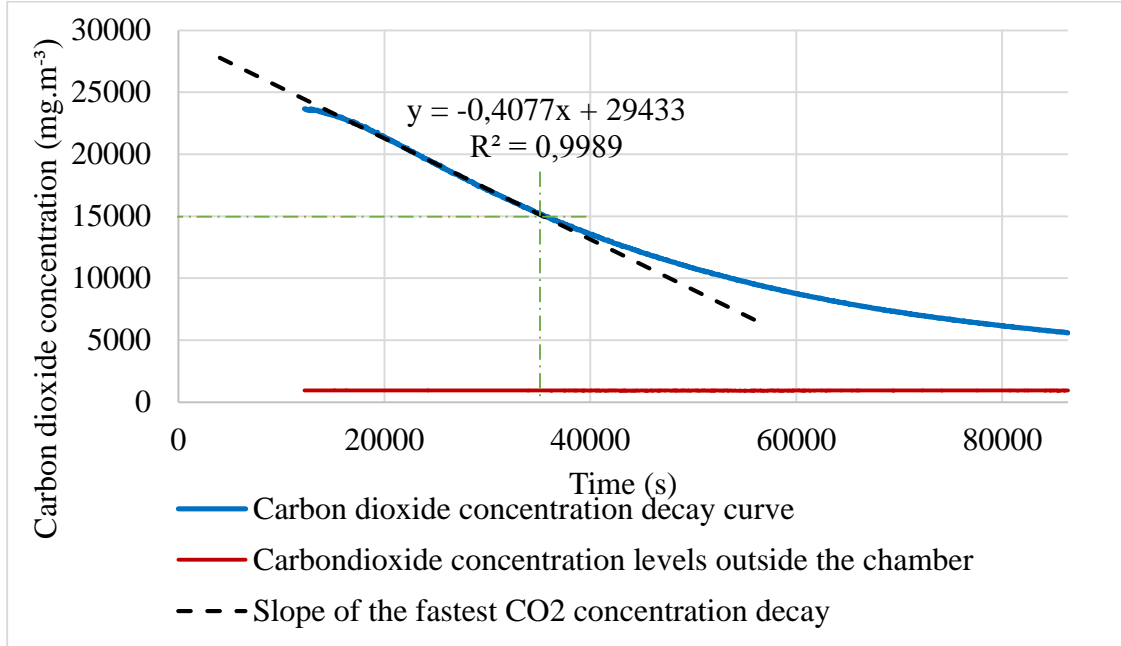
Figure 4.07. The CO_2 concentration decay curve of **unexposed G2** type AAC sample versus time obtained by the single-chamber diffusion test with high CO_2 concentration (C_{MAX} = 13181ppm, 23725mg.m^{-3}, $T_{CRITICAL}$ = 35940s).
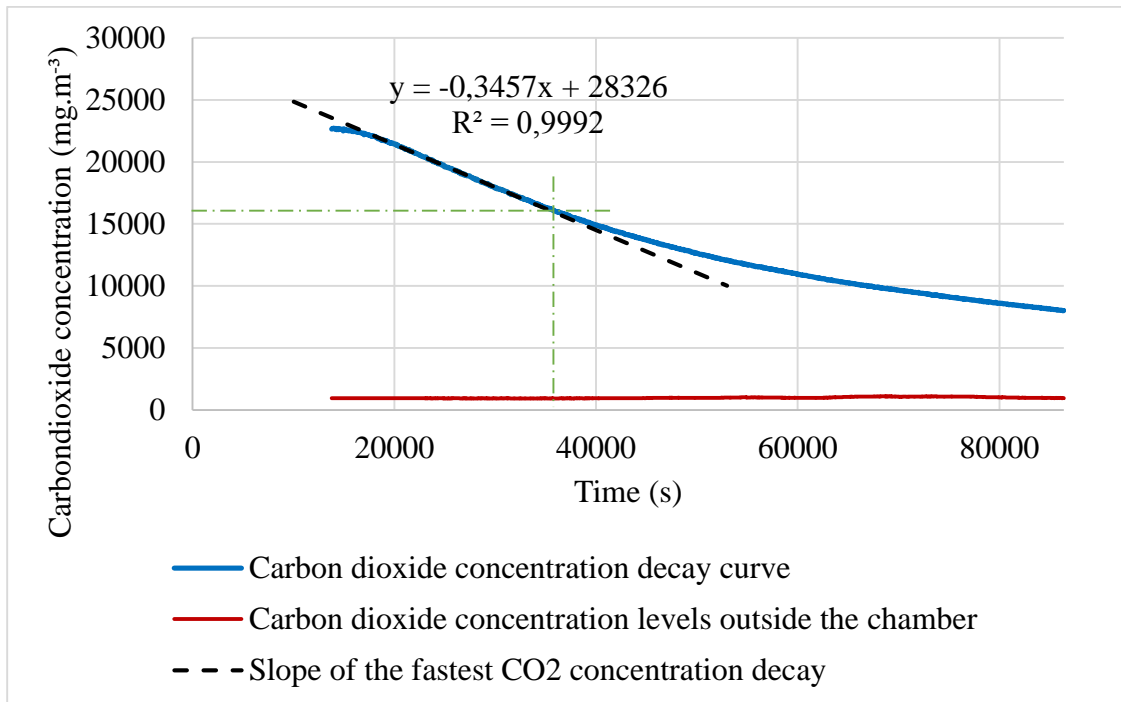
Figure 4.08. The CO_2 concentration decay curve of **unexposed G4** type AAC sample versus time obtained by the single-chamber diffusion test with high CO_2 concentration (C_{MAX} = 12646ppm, 22762mg.m^{-3}, $T_{CRITICAL}$ = 35220s).
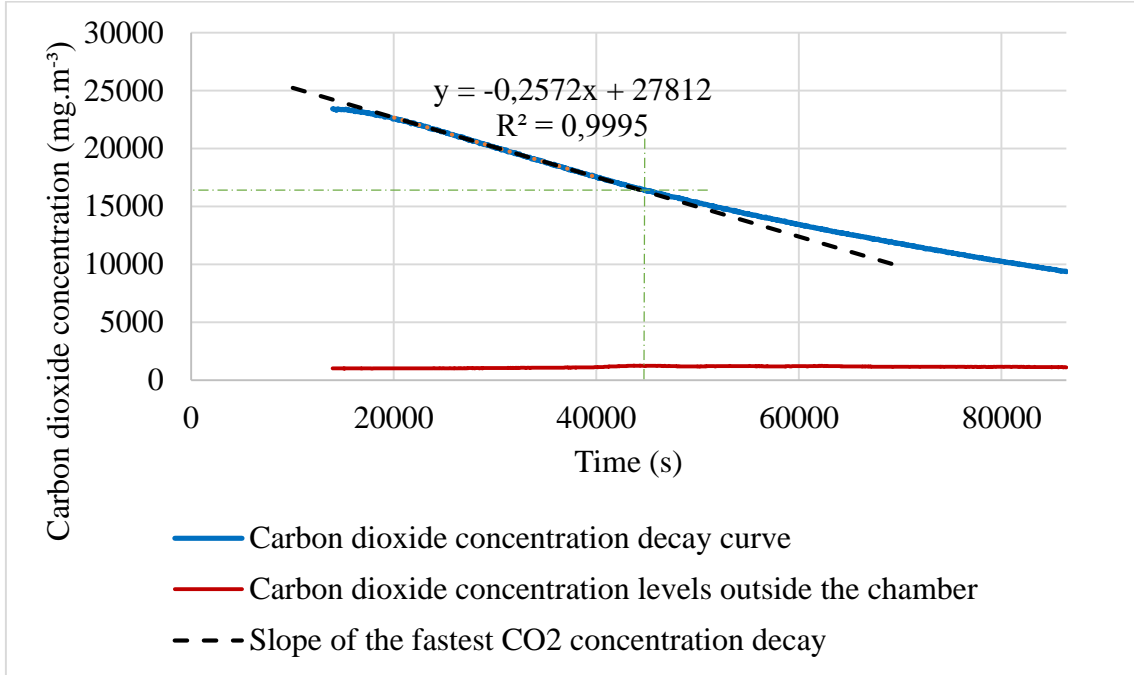
Figure 4.09. The CO_2 concentration decay curve of **exposed G2** type AAC sample versus time obtained by the single-chamber diffusion test with high CO_2 concentration (C_{MAX} = 13050ppm, 23490mg.m^{-3}, $T_{CRITICAL}$ = 43560s).
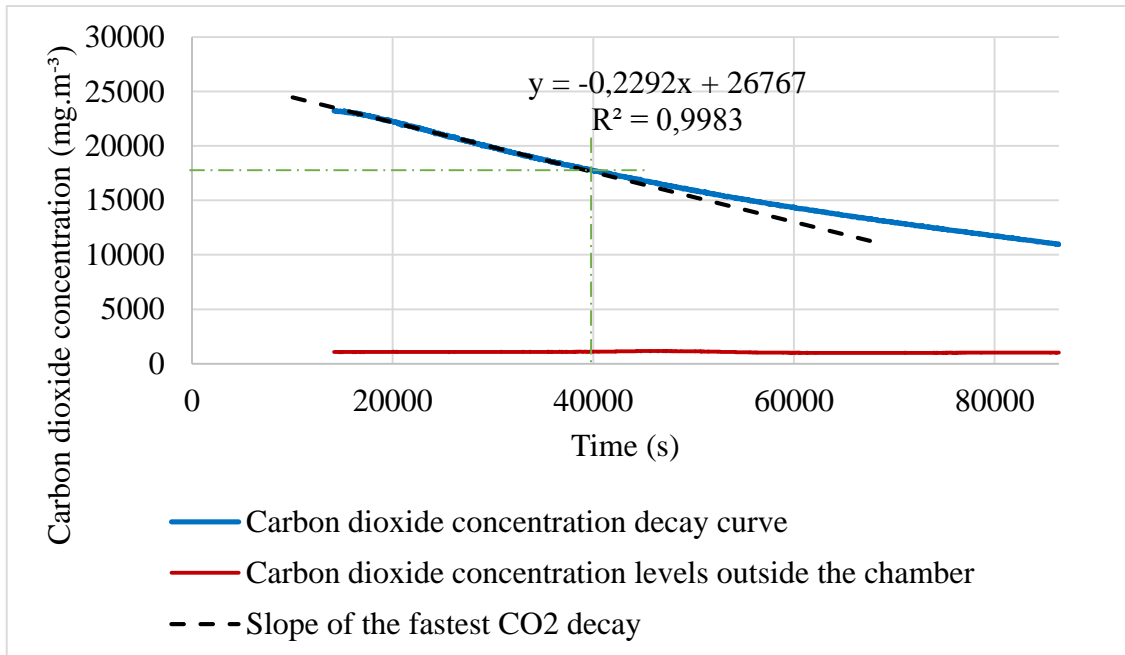
Figure 4.10. The CO_2 concentration decay curve of **exposed G4** type AAC sample versus time obtained by the single-chamber diffusion test with high CO_2 concentration (C_{MAX} = 12933ppm, 23279mg.m^{-3}, $T_{CRITICAL}$ = 40000s).

4.4.3. Double-Chamber CO_2 Diffusion Test Results

The data collected by the double-chamber tests are presented on the **Table 4.08**, **Figure 4.11**, **Figure 4.12**, **Figure 4.13**, **Figure 4.14**, **Figure 4.15**.

For the case of mud brick, the total amount of CO_2 was observed to be equally/evenly-distributed between two chambers. The results have shown that mud brick is not attracted to CO_2 and permits its transmission through its fabric with a high diffusion rate.

On the other hand, the CO_2 diffusion behavior of AAC is different from mud brick. It is observed that AAC blocks retain a considerable amount of CO_2. Unexposed G2 retained 53% of the total CO_2 and rest of distributed between the two chambers almost but not quite equally. After exposure to high CO_2 concentration and humid conditions, G2 retained less amount of CO_2 by 45% and the equal distribution of the rest of the CO_2 between the two chambers in 24 hours failed. This difference signals the changes in porosity characteristics and CO_2-philic behavior of G2 by exposure (Table 4.09).

Also the CO_2 permeability and retainment properties of G4 changes by exposure. The retained CO_2 amount by the G4 type AAC block decreases from 88% to 33% of the total CO_2 in the system after being exposed to high CO_2 concentration and humidity conditions. However, the amount of CO_2 passing to Chamber-2 from the Chamber-1 increases from 3% to 24% (Table 4.09).

Table 4.09. The amounts of CO_2 in the chambers, in the porous material block and their ratio to the total CO_2 amount in the system for mud brick and AAC samples at the end of double-chamber CO_2 diffusion tests conducted for 24 hours with high concentration.

Material type	RD$_{DOUBLE}$ (mg.m^{-3}.s^{-1})	RI$_{DOUBLE}$	M$_{CH-1}$ (mg)	(%)	M$_{CH-2}$ (mg)	(%)	M$_{RETAINED}$ (mg)	(%)
Mud Brick	-0.2865	0.5769	269	49.72	268	49.54	4	0.74
Unexposed G2	-0.4957	0.3569	132	24.40	121	22.37	288	53.23
Unexposed G4	-0.7589	0.0144	46	8.50	17	3.14	478	88.35
Exposed G2	-0.363	0.0767	287	53.05	79	14.60	175	44.92
Exposed G4	-0.351	0.1107	218	40.30	143	26.43	180	33.27

RD$_{DOUBLE}$: CO_2 concentration decay rate in the Chamber-1 (mg.m^{-3}s^{-1}),
RI$_{DOUBLE}$: CO_2 concentration increase rate in the Chamber-2 (mg.m^{-3}s^{-1}),
M$_{CH-1}$: The amount of CO_2 remained in Chamber-1 by the end of 24-hour double-chamber CO_2 diffusion tests (mg, %), **M$_{CH-2}$**: The amount of CO_2 transmitted to Chamber-2 by the end of 24-hour double-chamber CO_2 diffusion test (mg, %).
M$_{RETAINED}$: The amount of CO_2 retained by the material by the end of 24-hour double-chamber CO_2 diffusion test (mg, %).
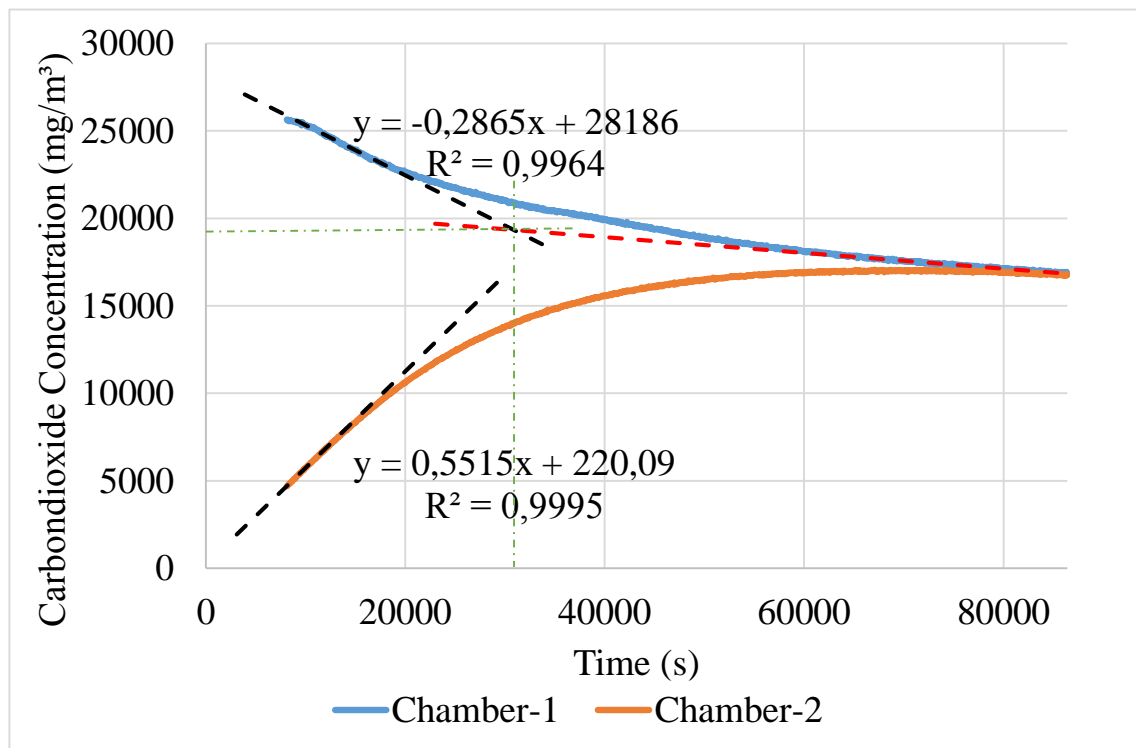
Figure 4.11. The regression analysis of the curves presenting the CO_2 concentration change by time in Chamber-1 and Chamber-2 during the double-chamber test with the **mud brick** sample.
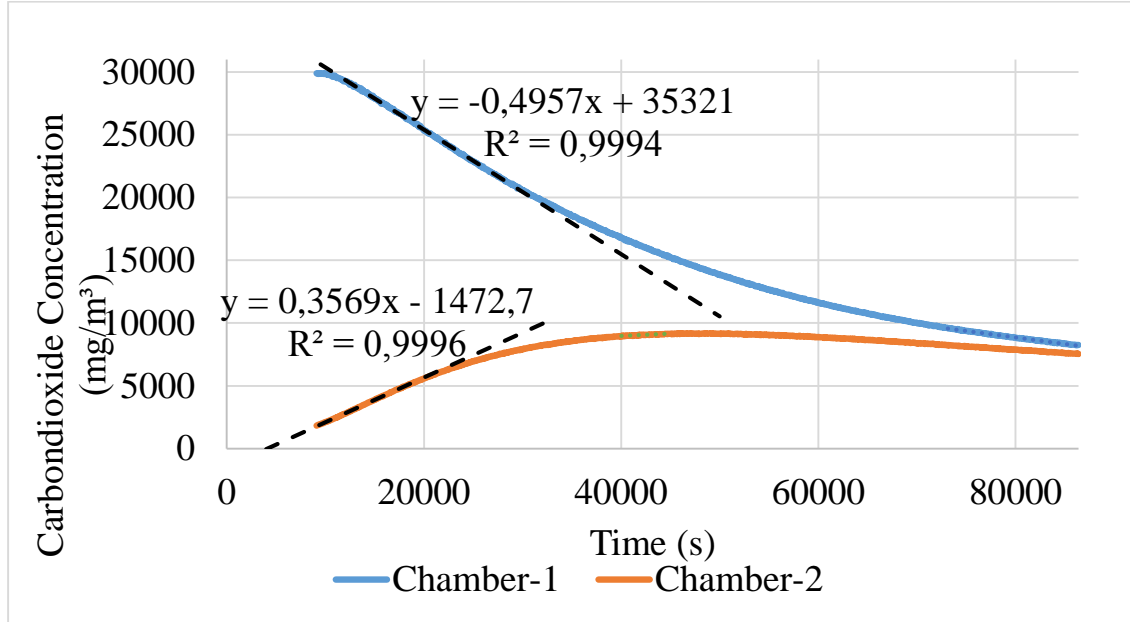
Figure 4.12. The regression analysis of the curves presenting the CO_2 concentration change by time in Chamber-1 and Chamber-2 during the double-chamber test with the **unexposed G2** type AAC sample.
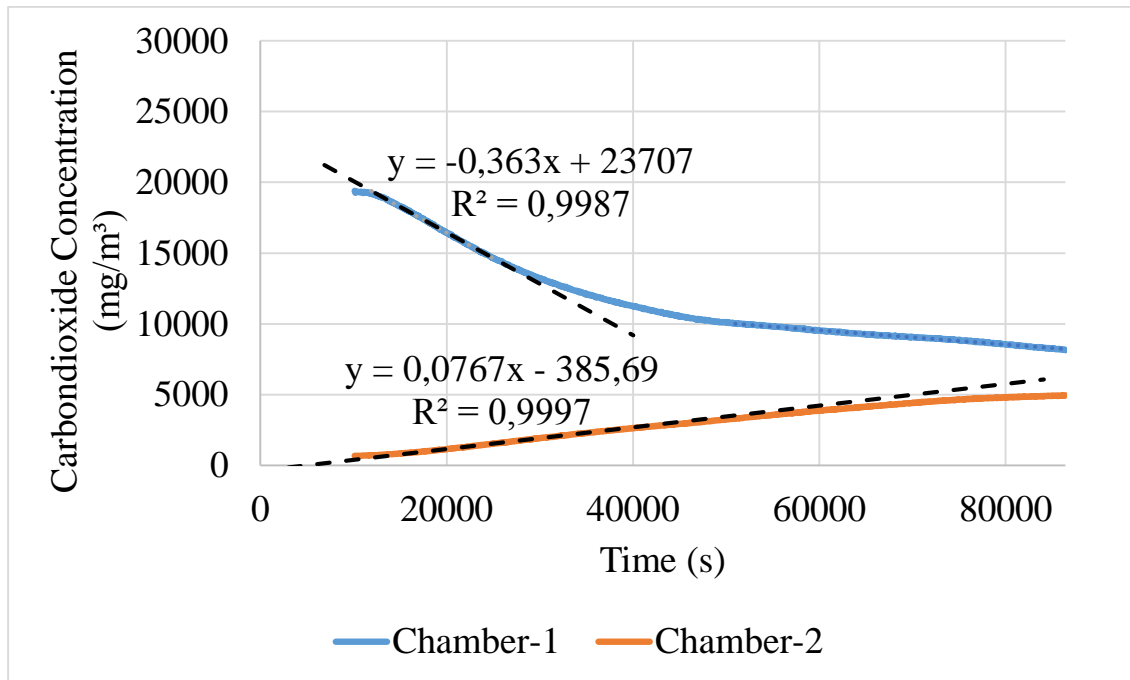
Figure 4.13. The regression analysis of the curves presenting the CO_2 concentration change by time in Chamber-1 and Chamber-2 during the double-chamber test with the **exposed G2** type AAC sample.

66
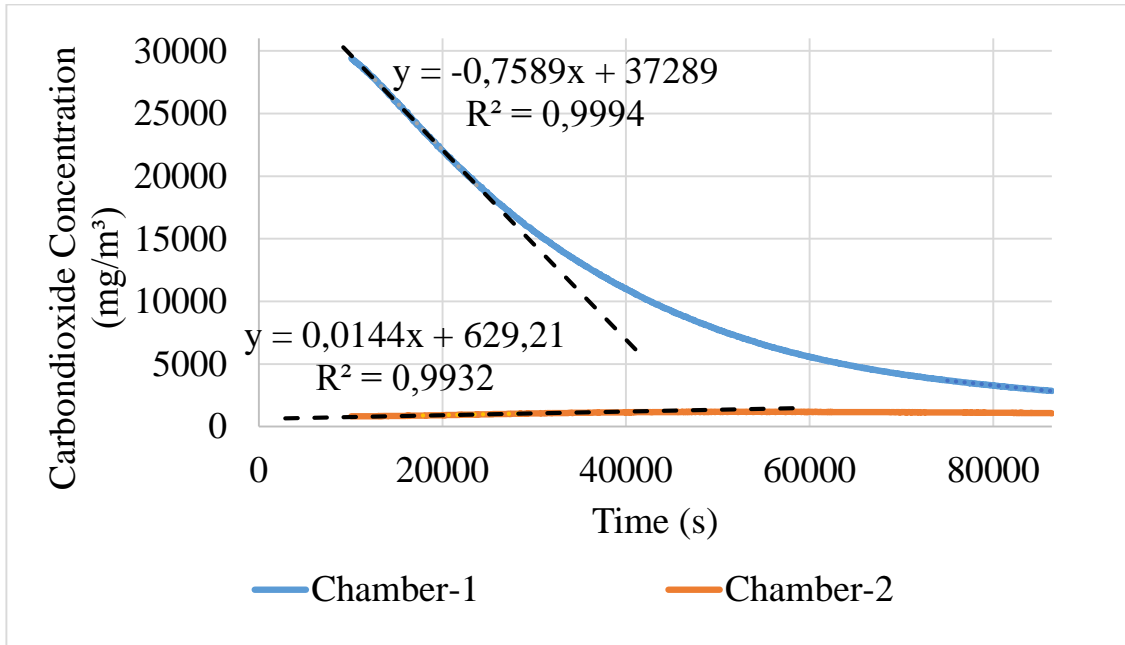
Figure 4.14. The regression analysis of the curves presenting the CO_2 concentration change by time in Chamber-1 and Chamber-2 during the double-chamber test with the **unexposed G4** type AAC sample.
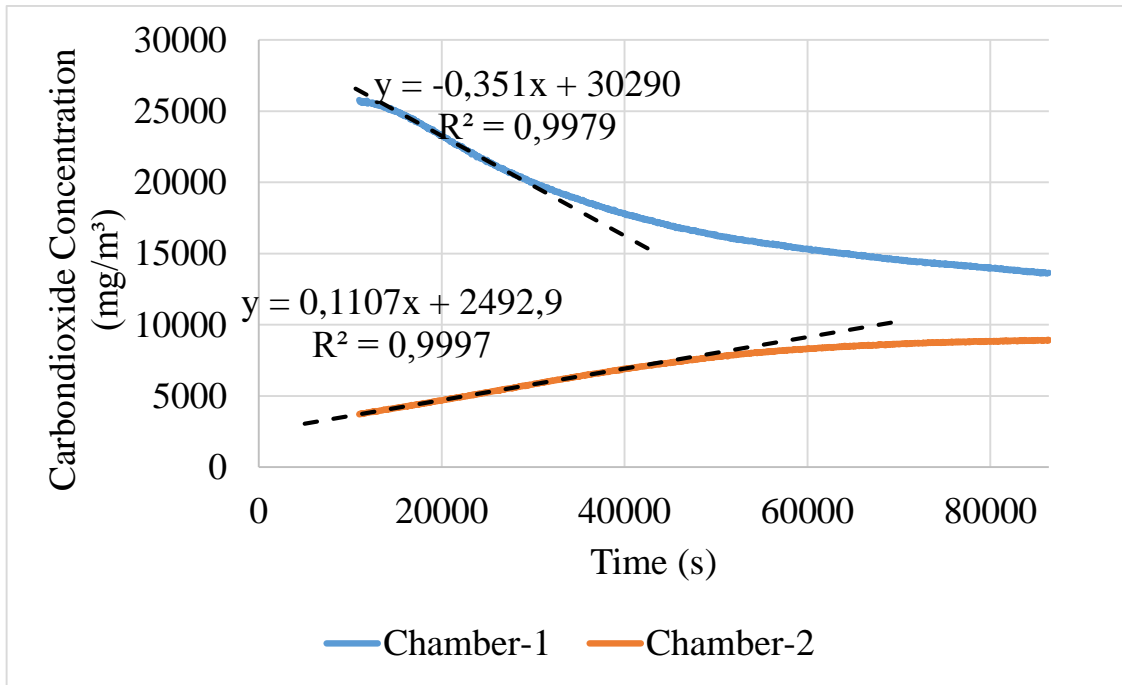
Figure 4.15. The regression analysis of the curves presenting the CO_2 concentration change by time in Chamber-1 and Chamber-2 during the double-chamber test with the **exposed G4** type AAC sample.

Double chamber test show that the amount of CO_2 retained by AAC blocks decrease when temperature increases and vice versa when the temperature is decreased back to lower degrees. This indicates the absorption/adsorption feature of AAC which can be reversed by rising temperature (**Table 4.10, Figure 4.16**).

Table 4.10. Ratios of retained CO_2 by AAC samples at different temperatures.

Sample Type	Temperature (°C)	Retained CO_2 Ratio (%)
Exposed G2 type AAC	23,5	67
	36	24
Exposed G4 type AAC	19	34
	38	23
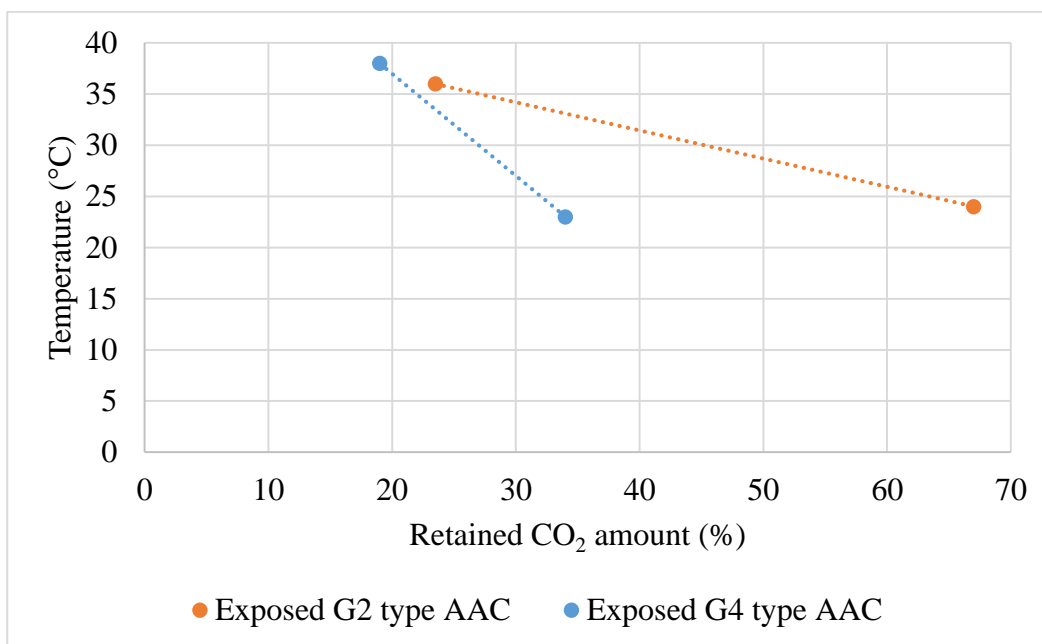
Figure 4.16. The lines showing the increase of retained CO_2 amount by temperature decrease.

4.5. Physical Physicomechanical and Mineralogical Properties of AAC after Exposure to High CO_2 Concentration

The data on physical, physicomechanical properties of AAC samples in terms of water vapor diffusion coefficient (μ), ultrasonic pulse velocity (UPV), and modulus of elasticity (MoE) before and after exposure of AAC samples to high CO_2 concentration were summarized in **Table 4.11.** The results are pointed out below:

− The dry weight of the G2 and G4 types of AAC samples increased by 12% and 13%, respectively after they were exposed to 20% CO_2 and 100% relative humidity for a week.

− The resistance to water vapor permeation decreases for G2 and G4 types of AAC samples with ratio of 37% and 30%, respectively after exposure. That meant that they were highly-breathable materials and became much more water vapour permeable getting close to 1, which is equivalent to the breathable feature of stable air.

− The ultrasonic velocity and modulus of elasticity values of the exposed G2 and G4 samples were noticeable decreased with an average percentage of 30% and 45%, respectively.

Table 4.11. The water vapor diffusion coefficient (μ, unitless), the ultrasonic pulse velocity (**UPV**, m.s^{-1}) and the modulus of elasticity (**MoE**, GPa) values of unexposed and exposed AAC samples and the percentage of the decrease in these values after exposure.

AAC Type	μ (unitless)		UPV (m.s^{-1})		MoE (GPa)	
	Before exposure	After exposure	Before exposure	After exposure	Before exposure	After exposure
G2	2.13	1.34	1703	1235	1.11	0.65
	37% decrease		28% decrease		42% decrease	
G4	3.34	2.34	1955	1293	2.17	1.05
	30% decrease		34% decrease		52% decrease	

In addition, the cracks parallel to diffusion direction were observed to occur in exposed G2 and G4 blocks indicating deterioration of the material after the intense CO_2 and humidity exposure. The horizontal and diagonal wide cracks reaching to 1mm in thick

were visible on the surface of the exposed G2 sample (**Figure 4.17**, **Figure 4.18**, **Figure 4.19**, **Figure 4.20**, **Figure 4.21**, **Figure 4.22**, **Figure 4.23**, **Figure 4.24**) whereas only horizontal and capillary cracks were observed on the exposed G4 sample (**Figure 4.25**, **Figure 4.26** and **Figure 4.27**).
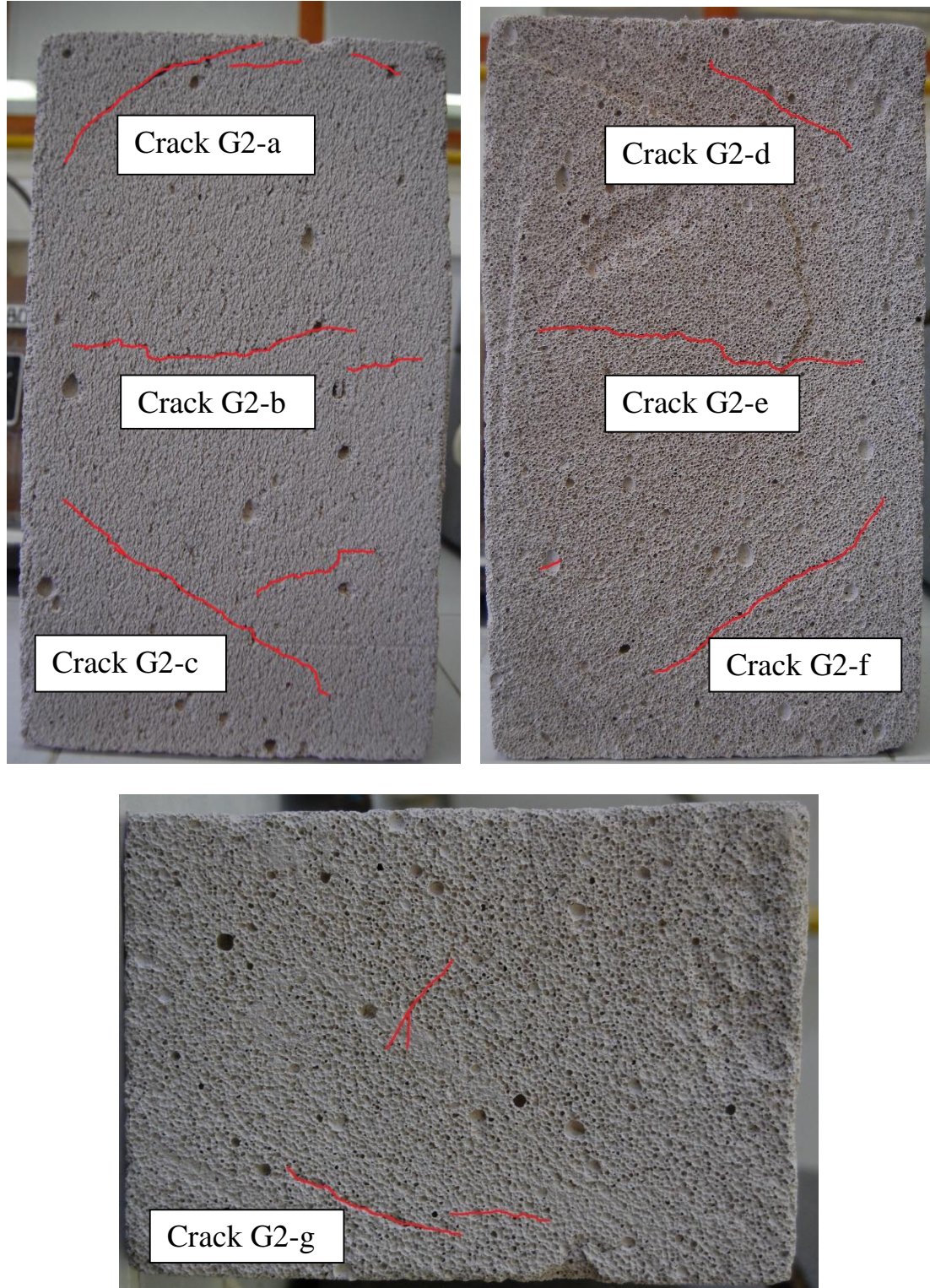
Figure 4.17. The diagonal and horizontal cracks occurred parallel to the diffusion direction and visible on the G4 type AAC block after exposed to 20% CO_2 and 100% relative humidity for a period of three weeks (highlighted in red).

Figure 4.18. The macro view of the crack G2-a on the exposed G4 type AAC block (See in reference to Figure 4.17).
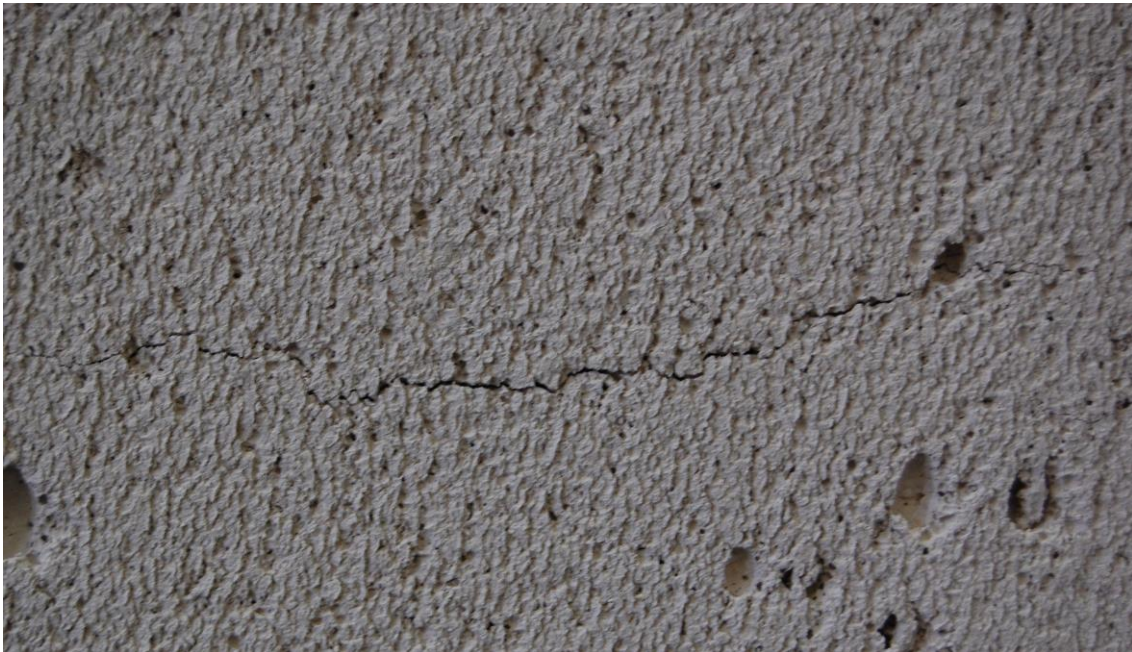
Figure 4.19. The macro view of the crack G2-b on the exposed G4 type AAC block (See in reference to Figure 4.17).

Figure 4.20. The macro view of the crack G2-c on the exposed G4 type AAC block (See in reference to Figure 4.17).

Figure 4.21. The macro view of the crack G2-d on the exposed G4 type AAC block (See in reference to Figure 4.17).

Figure 4.22. The macro view of the crack G2-e on the exposed G4 type AAC block (See in reference to Figure 4.17).

Figure 4.23. The macro view of the crack G2-f on the exposed G4 type AAC block (See in reference to Figure 4.17).

Figure 4.24. The macro view of the crack G2-g on the exposed G4 type AAC block
(See in reference to Figure 4.17).

Figure 4.25. The horizontal and capillary cracks occurred parallel to the diffusion direction and visible on the G4 type AAC block after exposed to 20% CO_2 and 100% relative humidity for a period of three weeks (highlighted in red).
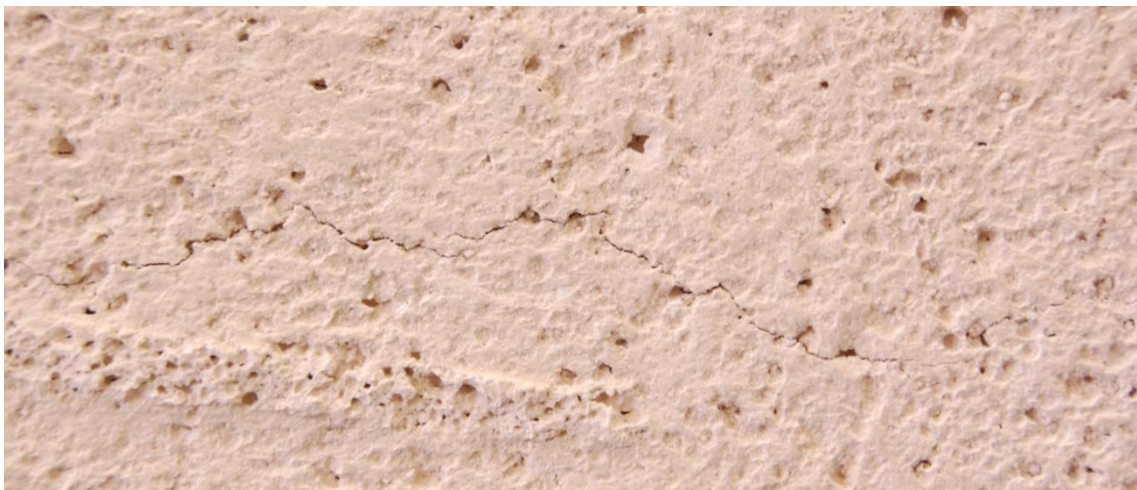
Figure 4.26. The macro view of Crack G4-a on the exposed G4 type AAC block (See in reference to Figure 4.25).

Figure 4.27. The macro view of the crack G4-b on the exposed G4 type AAC block
(See in reference to Figure 4.25).

The XRD analyses of the grinded powder obtained from the exposed surfaces of G2 and G4 samples have shown that the mineral composition of the AAC samples changes after exposure. The tobermorite 11A peaks vanish and the calcite peaks rise after being exposed to high CO_2 concentration and relative humidity levels (**Figure 4.28**).

AAC.G2.Unexposed Sample
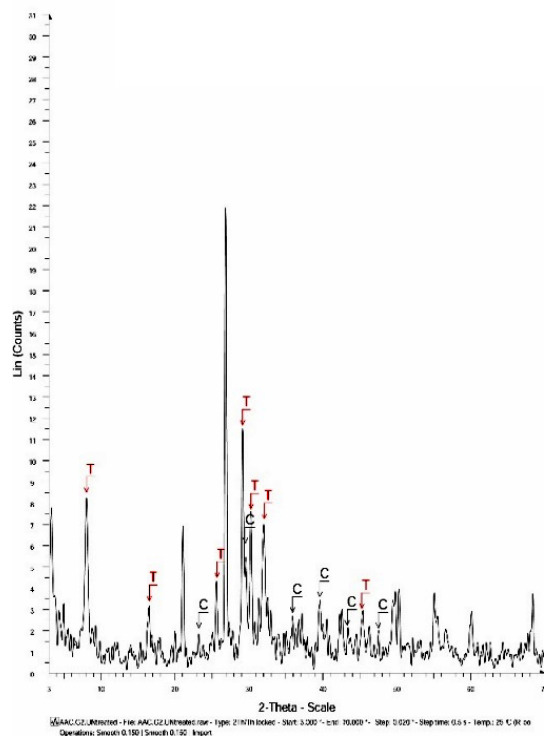
AAC.G2.Exposed Sample
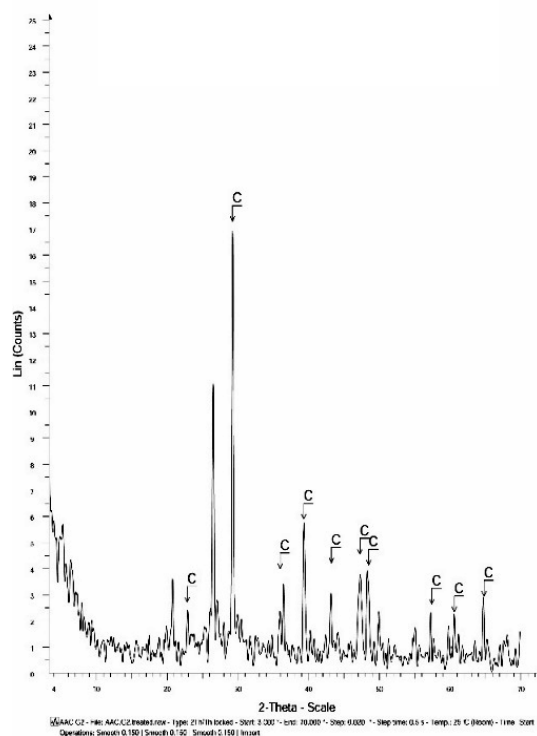
AAC.G4.Unexposed Sample
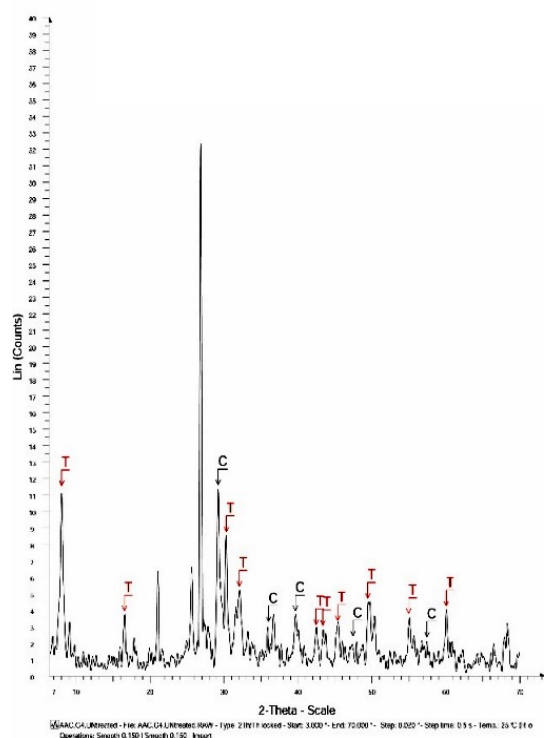
AAC.G4.Exposed Sample
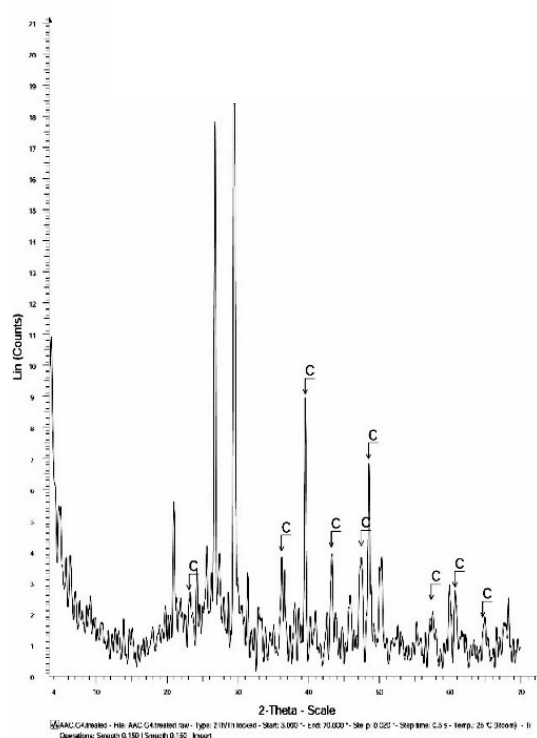
Figure 4.28. The XRD analysis of G2 and G4 type AAC samples before and after being exposed to high CO_2 concentration and humidity for a week. (T: tobermorite, C: calcite.)

78

CHAPTER 5

DISCUSSION

The results were evaluated together in order to compare mud brick and AAC units in terms of their basic physical and physicomechanical and mechanical properties, to assess their CO_2 diffusion characteristics in relation to their breathing features. In addition, CO_2 absorption and adsorption characteristics of AAC were discussed due to its inherent tendency to react with CO_2. Also, the fully-airtight building envelope and breathing walls are discussed in terms of sustaining good indoor air quality. The mud brick from Hamzalı Village were also defined in terms of its compositional and raw material characteristics.

5.1. Evaluation of Compositional and Raw Material Characteristics of Mud Brick from Hamzalı Village

Mudbrick load bearing units of Hamzalı Village traditional houses were determined to have particular features, specifically:

- High clay content with 49% by weight,
- Use of kaolin and illite types of clay minerals
- High portion of fine aggregate
- Enough mechanical strength provided by a highly porous microstructure.

Here, mud brick materials with high clay content are expected to suffer from cracking problems due to their inherent high water retaining characteristics and dimensional instability by excessive swelling and shrinkage movements during wetting-drying cycles (Clifton and Brown, 1978, Houben and Guillaud, 1989). However, a conscious selection of raw materials used in Hamzalı Village traditional houses, such as:

- presence of kaolin and illite types of qualified clay minerals that perform less swelling and shrinkage compared to smectite types of clay minerals,
- presence of coarse aggregate in small amount,

contribute to improve its dimensional stability and long term durability properties of that mudbrick material (Clifton and Brown, 1978; Stefanidou and Papayianni, 2005).

In short, Hamzalı Village mud brick was determined to be a high quality load bearing mud brick regarding to its raw material, compositional, basic physical, physicomechanical and mechanical characteristics.

5.2. Comparison of Mud Brick and AAC in Terms of Their Basic Physical, Physicomechanical and Mechanical Properties

The physical, physicomechanical and mechanical properties of Hamzalı village mudbrick, G2 and G4 types of AAC bocks have shown that those materials are highly-porous and breathable, lightweight and have enough mechanical strength while varieties in certain ranges signals differences in their porosity characteristics.

− The physical, physicomechanical and mechanical properties of Hamzalı Village mud brick, G2 and G4 type AAC have shown that those samples are highly porous, light weight water vapor permeable and have a certain material strength while signaling differences in their porosity characteristics.

− The data indicates that both mud brick and AAC samples have significantly low density and high porosity. Considering that the density of G4 type (load bearing) AAC is $0.62g.cm^{-3}$ and it is 68% porous, G4 type is significantly lighter and more porous compared to mud brick which has a density of $1.60g/cm^3$ and is 42% porous. On the other hand, G2 is the lightest and the most porous one among all by $0.42g.cm^{-3}$ density and 74% porosity (**Table 4.02**).

− Ultrasonic pulse velocity (UPV) of mud brick is much lower than both G2 and G4 type AAC samples. The UPV of mud brick is $1321m.s^{-1}$ and its modulus of elasticity (MoE) is 2.6GPa, whereas the UPV of G4 type AAC is $1955 m.s^{-1}$ and its MoE is 2.2GPa. In other words, even though the G4 type load bearing AAC has higher UPV, although it has MoE values close to mud brick, which indicates a similarity between them in physicomechanical characteristics (**Table 4.02**).

- Although the G2 type is the lightest and most porous of all, its UPV is still faster than mud brick which is the densest and the least porous among all the tested materials. (**Table 4.02**)

- According to the results, G4 type AAC, which is used as a load bearing structural material, has the highest uniaxial compressive strength by 2.36MPa. G2 type has the second high UCS value, 1.33MPa. The USC and MoE values of G4 and G2 type AAC materials have a similar hierarchy. On the other hand, mud brick, the material with highest MoE, has the lowest average UCS value, 0.89MPa. The UCS values for AAC obtained by direct measurement from related literature (Andolsun, 2006) are also present on **Table 5.01** for comparison.

Table 5.01. The indirectly calculated uniaxial compressive strength ($UCS_{indirect}$), point load stress index (I_s) of the samples and directly measured uniaxial compressive strength (UCS_{direct}) of the AAC from the literature.

Sample Type	$UCS_{indirect}$ (MPa)	Point Load Stress Index (I_s, MPa)	UCS_{direct} (MPa)
Mud brick	0.89 ± 0.40	0.17 ± 0.08	NA
G2 type AAC	1.33 ± 0.11	0.25 ± 0.03	1.88 [*]
G4 type AAC	2.36 ± 0.18	0.51 ± 0.04	2.76 [*]

* Direct measurement values of uniaxial compressive strength for AAC samples from related literature (Andolsun, 2006).

5.3. Assessment of CO₂ Diffusion Characteristics of Mud Brick and AAC

The highest CO_2 decay rate was observed at mud brick sample with $0.47 mg.m^{-3}s^{-1}$ followed by unexposed G2 type of AAC with RD_{SINGLE} of $0.41 mg.m^{-3}.s^{-1}$. The next RD value belongs to unexposed G4 type of AAC with RD_{SINGLE} value of $0.35 mg.m^{-3}.s^{-1}$. The CO_2 decay rate was determined to slow down for G2 and G4 type AAC samples with RD_{SINGLE} values of $0.26 mg.m^{-3}.s^{-1}$ and $0.23 mg.m^{-3}.s^{-1}$, respectively after they were exposed to high CO_2 concentration (**Figure 5.01**).
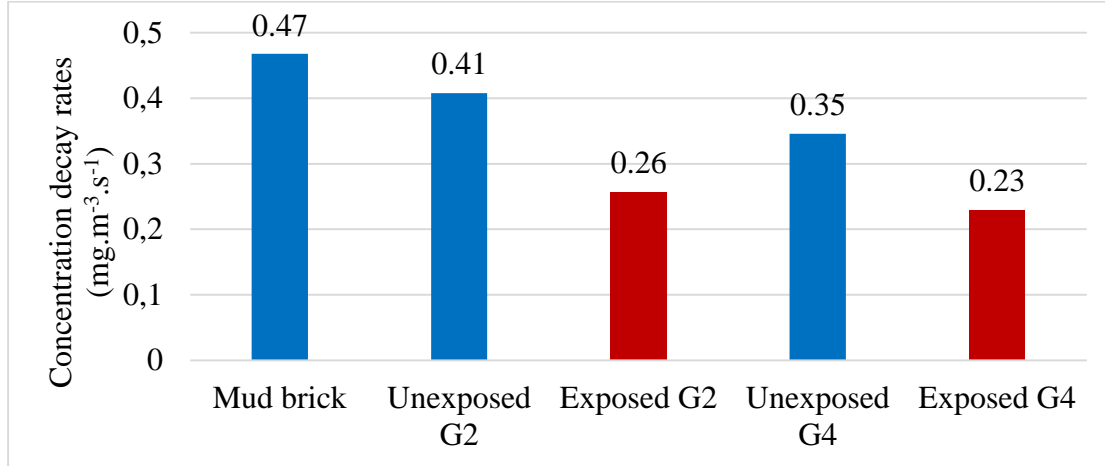
Figure 5.01. The CO_2 decay rates (RD_{SINGLE}, $mg.m^{-3}.s^{-1}$) obtained by the single-chamber test for mud brick and AAC samples.

On the other hand double-chamber diffusion tests have shown that AAC material is attracted to CO_2 while mud brick is not attracted to CO_2 and permits its transmission through its fabric with a high diffusion rate of $0.0075 mg.s^{-1}$. Owing to the fact that a significant portion of the CO_2 amount is absorbed/adsorbed by the AAC porous body, the CO_2 decay rate does not directly represent the CO_2 diffusion through the material. Therefore, the data on diffusion rate obtained for AAC samples are misleading and do not reflect the real diffusion characteristics of AAC material while the CO_2 concentration decay rate presents the reduction in CO_2 amount in the chamber due to the portion of CO_2 amount absorbed/adsorbed by the material itself and transmitted through.

For the analyses of diffusion characteristics of a material, a tracer gas which is not attracted to the material has to be selected for the diffusion tests.

The CO_2 diffusion behavior of AAC is different from mud brick. The results are presented in **Figure 5.02** and the evaluations were summarized below:

− For the case of mud brick, the total amount of CO_2 was observed to be equally/evenly-distributed between two chambers.

− AAC blocks, on the contrary, retain a considerable amount of CO_2 in their fabric while permitting less amount of CO_2 transmission from Chamber-1 to Chamber-2.

- The concentration decay rate (RD_{DOUBLE}) is inversely proportional with the CO_2 amount transmitted through the AAC material. This revealed that increase in concentration decay rate is related with the CO_2 amount kept by the AAC material (**Figure 5.03**).

- The unexposed G4 sample retains 88% of the total CO_2 amount while transmitting only 3% of the total CO_2 amount, which can be considered as a negligible range.

- In comparison to G4, the unexposed G2 sample transmits CO_2 more than G4 with the portion of 22% of the total CO_2 amount while still keeping 53% of the total CO_2 amount in its fabric.
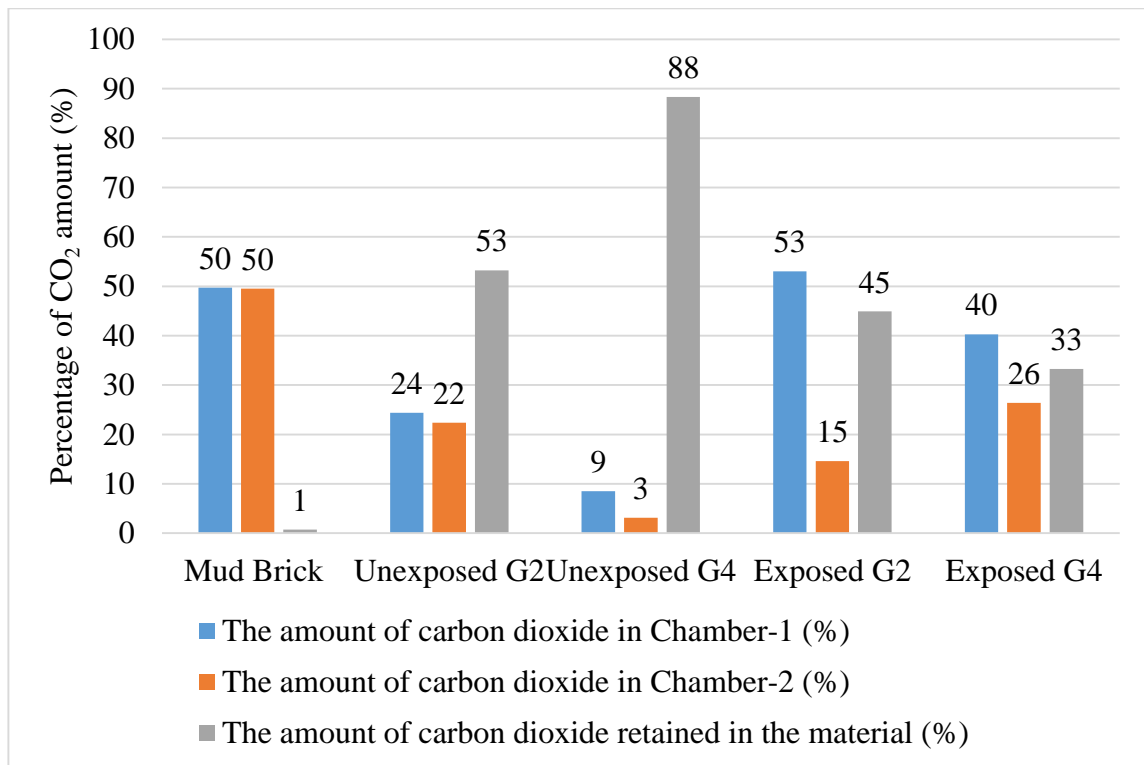
Figure 5.02. The CO_2 amounts remained in Chamber-1 (M_{CH-1}, %), in Chamber 2 (M_{CH-2}, %) and retained ($M_{RETAINED}$) by the mud brick and AAC block samples proportional to the total amount of CO_2 in the closed system of the double-chamber experimental setup at the end of 24-hours.
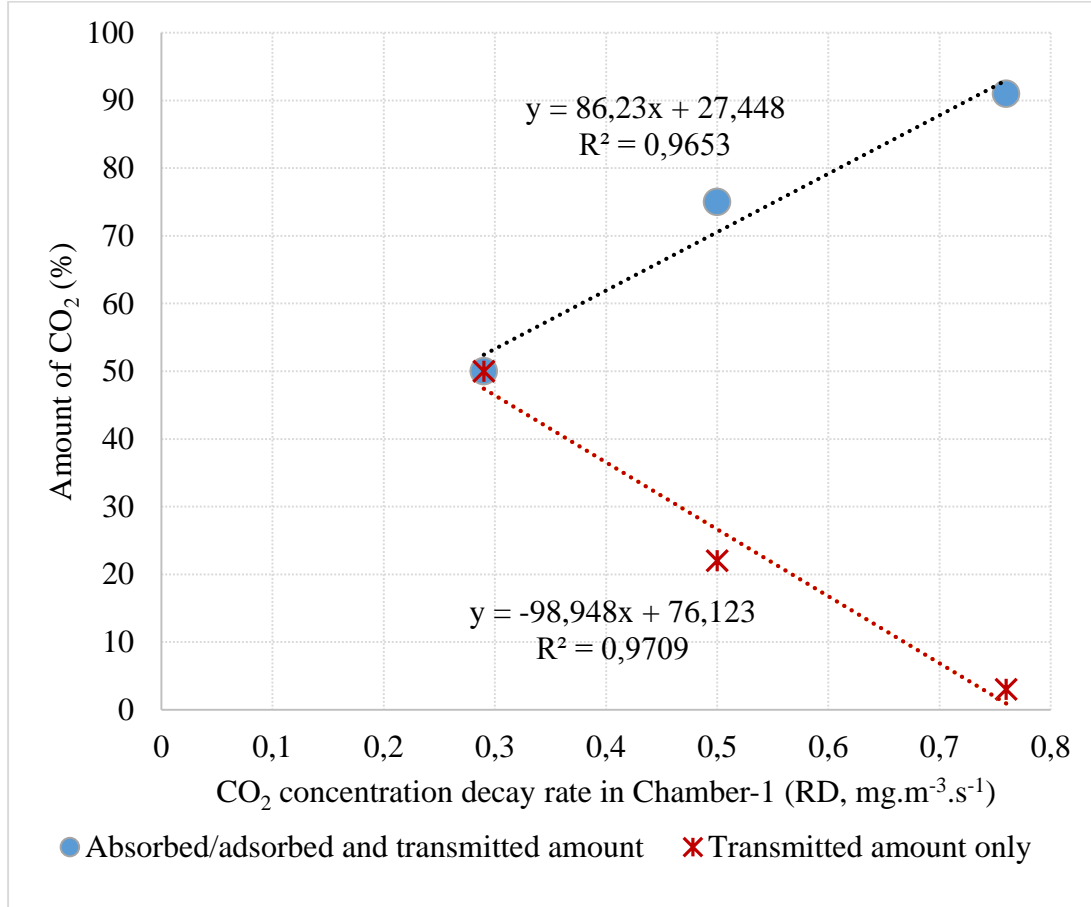
Figure 5.03. The trend line (in blue) showing the correlation between CO_2 concentration decay rate (RD_{DOUBLE}) and the CO_2 amount absorbed and transmitted by the material ($M_{CH-2} + M_{RETAINED}$) and the trend line (in red) showing the correlation between RD_{DOUBLE} and the CO_2 amount transmitted through the material only (M_{CH-2}).

The CO_2 diffusion behavior of the G2 and G4 samples changes after they have been exposed to high CO_2 concentration. The decay rates of G2 and G4 samples are determined to decrease after exposure, such as from $0.41 mg.m^{-3}s^{-1}$ to $0.26 mg.m^{-3}s^{-1}$ for G2 sample and from $0.35 mg.m^{-3}s^{-1}$ to $0.23 mg.m^{-3}.s^{-1}$. In short:

- The G2 sample retains less amount of CO_2 after exposure while still keeping 45% of the total CO_2 amount and that behavior results in decrease in CO_2 concentration decay rate.

- The G4 sample retains considerably-less amount of CO_2 after exposure with a decrease from 88% to 33% of the total CO_2 amount while transmitting more in comparison to

84

the unexposed G4 sample. In comparison to unexposed G4 sample, the exposed one presents a considerable increase in transmitted CO_2 amount from 3% to 26% of the total CO_2 amount remained in Chamber-2.

This is more visible in the graph shown in **Figure 5.04** in which the CO_2 amounts remained in Chamber-1 and transmitted to Chamber-2 are correlated. Here, the reference point is where a material allows CO_2 to diffuse through its body without retaining any of it and enables a balanced CO_2 distribution by 50% in Chamber-1 and Chamber-2 within 24 hours. The only material which provided a balance between two chambers with equal distribution of CO_2 concentration without retaining CO_2 in its fabric is the mudbrick (**Figure 5.02**, **Figure 5.03** and **Figure 5.04**). The G2 type AAC provided a balance between two chambers with approximately 25% CO_2 distribution while the remained portion of 50% CO_2 amount is kept by its fabric. The G4 type AAC sample on the hand, could not achieved a balance after 24 hours and presented very low transmission through its fabric while kept almost 88% of the total CO_2 amount in the closed system. The severe exposure of CO_2 resulted in more transmission of CO_2 through G4 while less transmission of CO_2 through G2. That difference might be due to the higher level of deterioration observed in G4 confirmed by 36% of reduction in their UPV and 52% reduction in its MoE **(Table 4.10)**.

Among the samples examined, only the data on concentration decay rate (RD_{SINGLE}) of mudbrick obtained by single-chamber CO_2 diffusion test with high CO_2 concentration is a valid data to calculate its CO_2 diffusion rate (E, mg.s^{-1}), the effective CO_2 diffusion coefficient in material (D_{EFF}, cm^2.s^{-1}) and the diffusion index (D_i, d^{-1}). Those are the determinative parameters to define the gas diffusion characteristics of a material and can be used for comparison purposes. Among those three, the diffusion index (D_i, d^{-1}) of a material is a gas diffusion parameter independent to its sizes, therefore can be used to compare diffusion performances of several materials even the samples are not available at the same sizes.

The results have shown that single chamber diffusion test method is suitable for the non-CO_2-philic materials such as mud brick from Hamzalı Village and that non-CO_2-philic nature of a material should be confirmed by the double chamber diffusion test method.
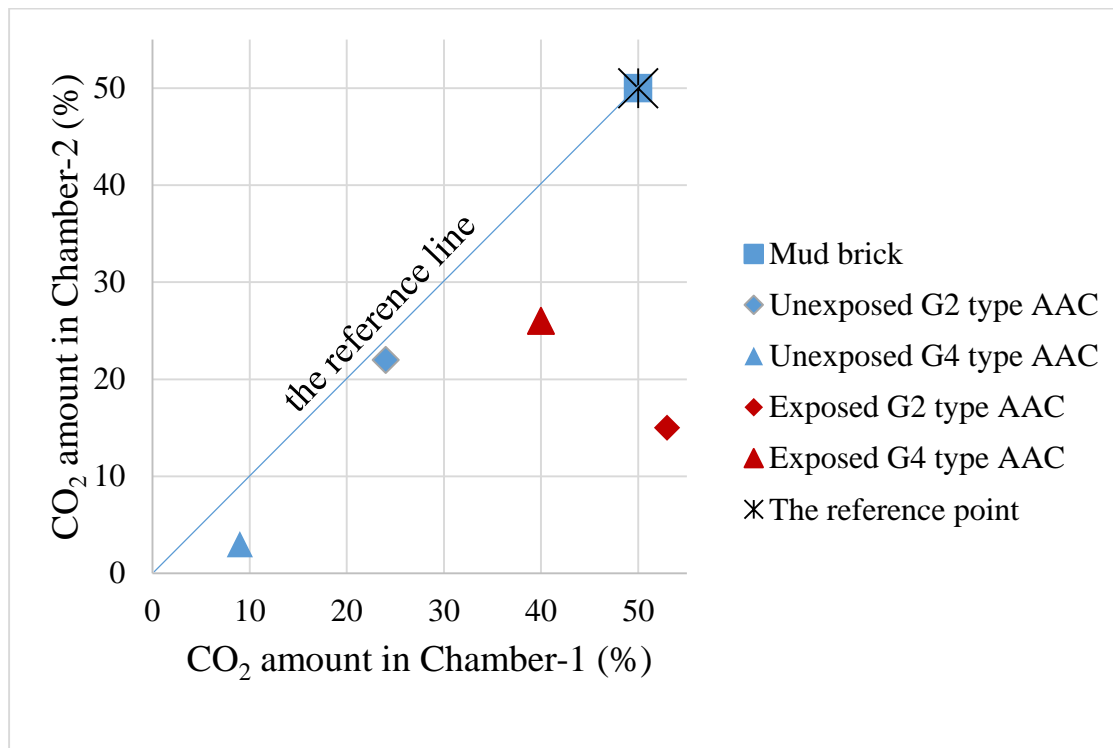
Figure 5.04. The reference point is where a material allows CO_2 diffusion through its body without retaining any of it and enables a balanced CO_2 distribution by 50% in Chamber-1 and Chamber-2 within 24h. The data below the reference point of 50% signals that a certain amount of CO_2 is retained in the material body. The data on the reference line and below the reference point means that the material retains a certain amount of CO_2 but allows the rest of the CO_2 to be distributed equally/evenly between the two chambers within 24h.

The double chamber diffusion tests have shown that the mudbrick has a capability to keep indoor air contamination in balance with neighboring both environments within 10 hours (**Figure 4.11**) without retaining a noticeable amount of CO_2 in its fabric. The single chamber diffusion tests have shown that at very high CO_2 concentration level, an 18cm-thick mudbrick block can transmit the large portion (2/3 two third) of indoor CO_2 amount to the outside within the first 13 hours (**Figure 4.06**) and the diffusion rate is the slowest and constant after 13 hours. However, the CO_2 diffusion rate of AAC material slows down but continues with a noticeable slope till the end of 24 hours.

86

5.4. Joint interpretation of CO_2 diffusion and water vapor permeability characteristics for Mud Brick and AAC

All samples both examined in the study and mentioned in the literature were compared with each other in terms of their SD values. The comparisons were based on an acceptance that all samples are prepared in 25mm thick in accordance with the standards ASTM E96/E96M (2015) and TS EN ISO 7783 (2012). Due to the SD values below 0.14, they are classified as highly permeable as shown in Table 5.02 (TSE, 2012).

The of water vapor permeability of mud brick and AAC samples examined in the study were found to be very high water vapor permeable (**Table 5.02** and **Figure 5.05**) and the relevant data obtained is consistent with the data given in literature (Andolsun, 2006; Andolsun et al., 2013, Meriç et al., 2014).

Table 5.02. The water vapor resistance factors (μ) of AAC and mud brick, plaster and mortar.

Sample Type	μ (unitless)	SD* (m)	Water vapor permeability class**
Mud brick (Hamzalı Village)	3,3 – 3,8	0.09	Highly permeable (<0.014)
Mud mortar (Hamzalı Village)	3,6	0.09	Highly permeable (<0.014)
Mud plaster (Hamzalı Village)	3,4	0.09	Highly permeable (<0.014)
Unexposed G2 type AAC	2,13 ±0.45	0.05	Highly permeable (<0.014)
Unexposed G4 type AAC	3,35 ±0.17	0.08	Highly permeable (<0.014)
Exposed G2 type AAC	1,34 ±1.03	0.03	Highly permeable (<0.014)
Exposed G4 type AAC	2,34 ±0.64	0.06	Highly permeable (<0.014)
Mud brick infill (Kavaközü Village, Güdül)***	1,4 – 1,6	0.04	Highly permeable (<0.014)
Unexposed G2 type AAC***	3,8 – 5,0	0.11	Highly permeable (<0.014)
Unexposed G4 type AAC***	3,2 – 6,4	0.12	Highly permeable (<0.014)

*The SD values are calculated for 25mm material thickness.
**Classification is done by SD values according to prEN ISO 7783-2,1999.
***The μ values of mud brick infill and AAC samples are taken from the literature (Andolsun, 2006; Erdil, 2015; Meriç *et al*., 2013, Meriç *et al*., 2014).
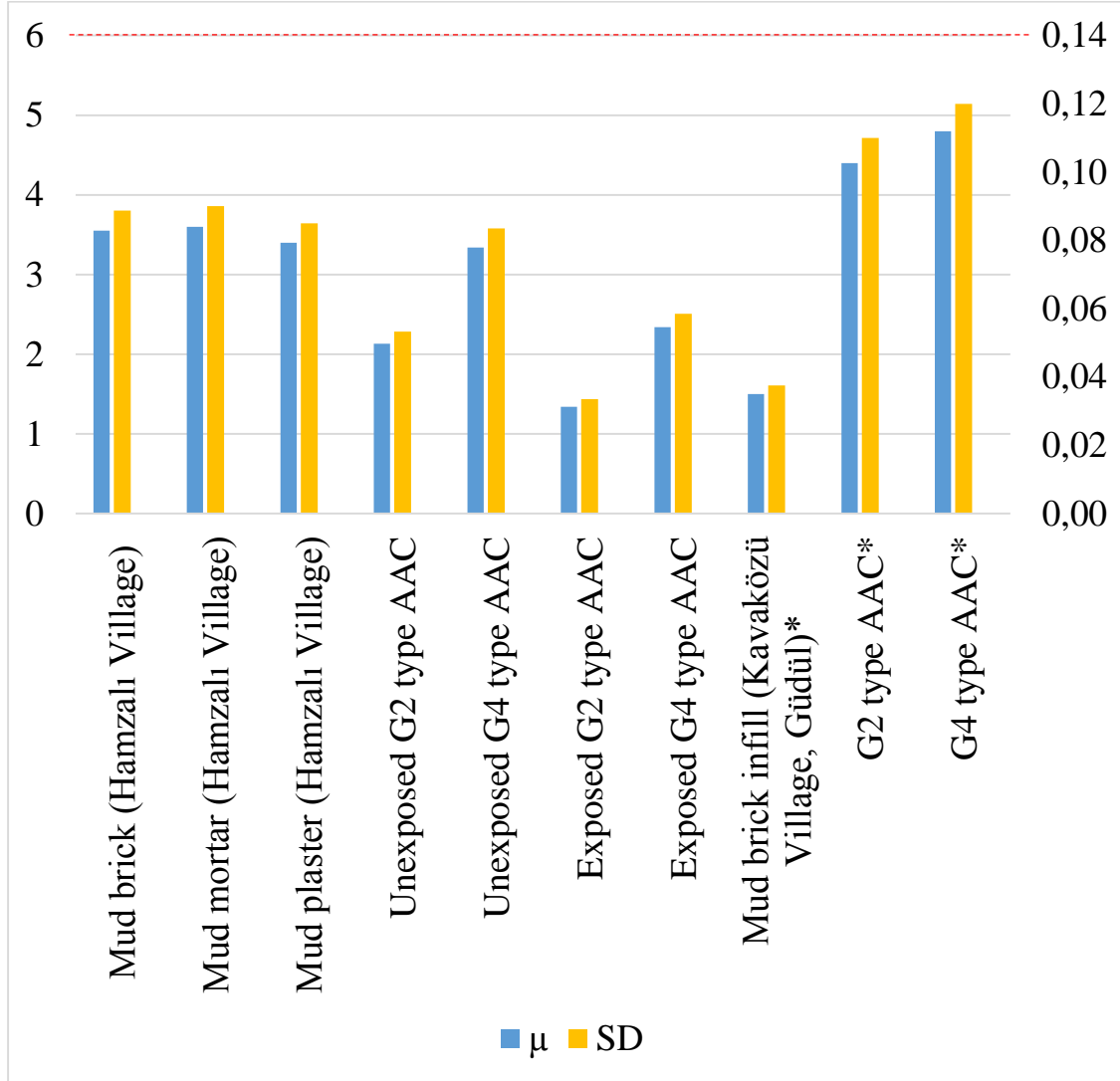
Figure 5.05. The comparison of μ and SD values of the mud based materials from Hamzalı Village and exposed and unexposed AAC samples of the study together with the data on similar materials given in literature(*) (Andolsun, 2006; Erdil, 2015; Meriç *et al.*, 2013, Meriç *et al.*, 2014)

Since both water vapor and CO_2 exists in air, water vapor and CO_2 permeability characteristics indicate their air permeability characteristics. The diffusion coefficient of H_2O molecules in air is higher than that of CO_2 due to the lower molecular volume and molar mass of H_2O. Therefore, differences between water vapor and CO_2 diffusion characteristics of materials are expected. That may result in various impacts of materials on indoor air quality.

Since water vapor permeability of G2 type of AAC is higher than mudbrick and G4 type of AAC, CO_2 diffusion has been expected to be at the highest level for G2 type of AAC sample, however, the data presented that mudbrick has the highest CO_2 diffusion level (**Figure 5.03**).
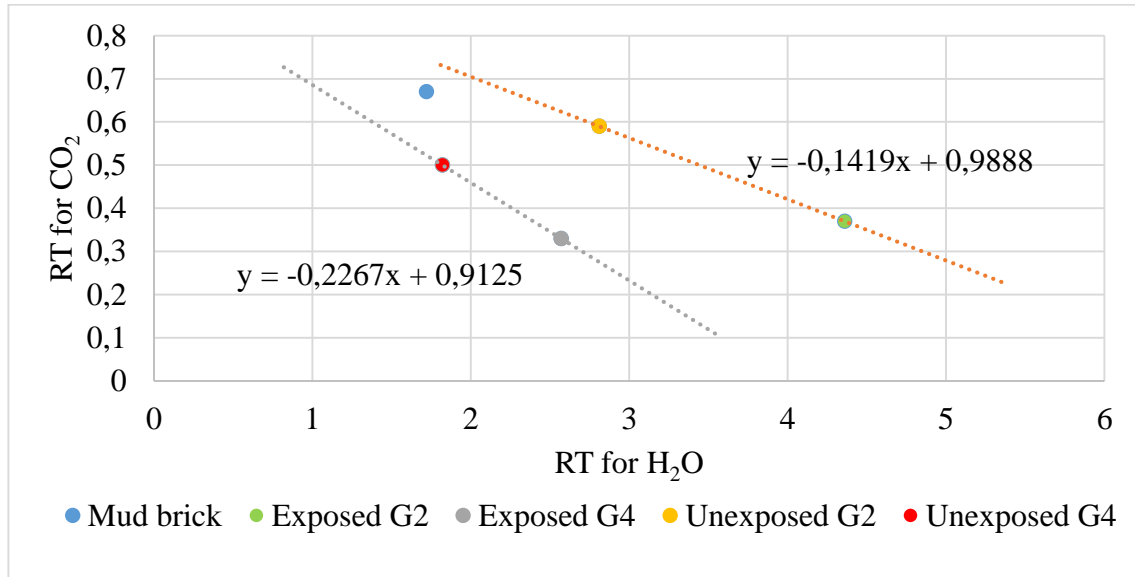
Figure 5.06. The scatter plot of transmission rate for CO_2 (RT_{CO2}) versus transmission rate for water vapor (RT_{H2O}), showing no correlation between water vapor and CO2 diffusion characteristics of mudbrick and AAC samples while inverse correlation between unexposed and exposed AAC samples.

As a result, mud brick and AAC samples examined in the study are highly-breathable materials while no correlation was determined between their water vapor and CO_2 diffusion characteristics (**Figure 5.06**). That result is consistent with the findings in literature as well that there is no evident correlation between water vapor permeability and air permeability (Mukhopadhyaya *et al.*, 2011).

The deterioration in AAC samples after they are exposed to high CO_2 concentration in presence of moisture increased their water vapor permeability, on the contrary, decreased their CO_2 diffusion rate. Such an unexpected behavior can be attributed to the attraction between AAC material and CO_2, therefore the CO_2 diffusion rate which represents a

phenomena occurred due to the CO_2 amount absorbed/adsorbed by and transmitted through the AAC material.

5.5. Discussion on the Degradation of AAC after Exposure to High CO_2 Concentration

The AAC material was observed to be severely-deteriorated when exposed to high concentration of CO2 in 100%RH conditions due to:

- the carbonation process in which tobermorite-11A° (5CaO_6SiO2_5H2O), the principal binding mineral of AAC, reacts with CO2 in the presence of moisture, and decomposes to silica gel and calcium carbonate (Matsushita et al., 2000; Matsushita et al. 2004; Kus and Carlsson, 2003),

- the carbonation process in which calcium hydroxide ($Ca(OH)_2$) existing in AAC reacts with CO_2 and converts to calcium carbonate (Matsushita et al., 2000; Matsushita et al. 2004; Kus and Carlsson, 2003), as well as,

- the degradation process accelerated with high concentrations of CO_2 in the presence of moisture which forms carbonic acid and reacts with $CaCO_3$, and thus produces calcium bicarbonate, which is soluble in water (Matsushita et al., 2000; Matsushita et al. 2004; Kus and Carlsson, 2003).

That deterioration in AAC samples after exposure is clearly observed with:

- the occurrence of visible cracks on the AAC material surface parallel to the diffusion direction (**Figure 4.17**, **Figure 4.18**, **Figure 4.19**, **Figure 4.20**, **Figure 4.21**, **Figure 4.22**, **Figure 4.23**, **Figure 4.24**, **Figure 4.25**, **Figure 4.26** and **Figure 4.27**),

- a certain increase in dry weight of AAC samples about 12%-13%, referring to the conversion of tobermorite to calcium carbonate ($CaCO_3$) and calcium hydroxide ($Ca(OH)_2$) to calcium carbonate (Table 5.03),

- an increase in intensity of calcite mineral peaks together with disappearance of tobermorite mineral peaks in XRD finger traces of AAC samples (**Figure 4.28**),

- a certain increase in water vapor permeability of AAC samples (**Table 4.11**, **Table 5.03**, **Figure 4.04**),

- a certain decrease in CO_2 diffusivity characteristics of AAC samples (**Table 5.03**)

90

- a significant decrease in ultrasonic pulse velocity and modulus of elasticity of G2 and G4 AAC types, reaching to 34% and 52%, respectively (**Table 4.11**, **Figure 5.09**).

The changes due to the reactions between AAC material and CO_2 in presence of moisture have shown that:

- AAC material is a CO_2-philic material while mudbrick is not.
- The G4 type AAC is more CO_2-philic material than G2 type AAC. After AAC blocks are exposed to high CO_2 concentration of CO_2, the G4's CO_2 attraction decreases.

Table 5.03. The water vapor resistance factors (μ), densities (ρ), effective diffusion coefficient (D_{EFF}) and diffusion index (D_i) values of the AAC samples before and after exposure to high CO_2 concentration and humid conditions.

Sample Type		ρ (g.cm^{-3})	μ (unitless)	D_{EFF} (cm^2.s^{-1})	D_i (1.d^{-1})
G2 type AAC	Unexposed	0.42	2.13	0,0135	0,0097
	Exposed	0.47	1.34	0,0086	0,0031
G4 type AAC	Unexposed	0.62	3.35	0,0119	0,0003
	Exposed	0.70	2.34	0,0076	0,0038

When AAC samples were exposed to 20% CO_2 concentration at 100%RH at 21˚C for 3 weeks, they presented a considerable reduction in their physicomechanical properties (**Figure 5.09**). The UPV values of G4 type AAC block exhibited 34% reduction that resulted in 52%decrease in its MoE. The G2 type of AAC exhibited a noticeable degradation as well while that degradation was not as much as G4 type of AAC suffered. G2 type of AAC exhibited 28% reduction that resulted in 42% decrease in its MoE. Such a decrease in their physicomechanical properties associated with the occurrence of horizontal and diagonal cracks parallel to the diffusion direction in G2 sample and with only horizontal tiny cracks parallel to the diffusion direction in G4 sample.
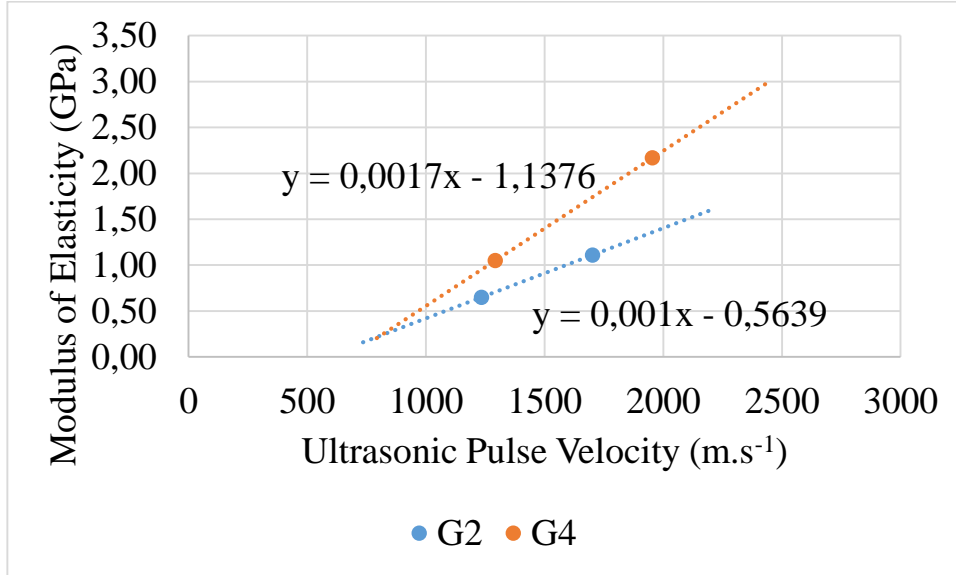
Figure 5.07. The ultrasonic pulse velocity and modulus of elasticity values of G2 and G4 types of AAC blocks before and after exposure to high CO_2 concentration showing the considerable reduction in their physicomechanical properties after exposure.

5.6. Discussion of the Fully-Airtight Building Envelope and Breathing Walls

The common trend in today's construction world is to establish airtight skins by introducing moisture and vapor proof layers to the multi-layered wall systems. The air leakages through the joints/interfaces where many building components or elements come together should be considered as defects that cause thermal bridges, moisture problems and further materials deterioration. Such failures may also adversely affect the thermal performance, physical comfort conditions at interiors and long-term durability of buildings. The airtightness of the building skins by eliminating the air leakages through any clearances is definitely an essential issue in buildings.

The establishing fully impermeable skins without permitting any air and/or vapor passage through the wall sections is the other common approach of today's constructions that is mentioned within the concept of airtightness. However, the occupants living in fully impermeable buildings suffer from unhealthy indoor conditions and sick building syndrome due to the lack of ventilation of airtight building envelopes and indoor air exchange efficiency. Those subjects are the research fields of the recent studies since such

troublesome healthy conditions sourced from the approach of fully-airtight building envelope have vital impacts adversely-effecting the health of occupants (EPA, 1991; Gochfeld, 2007; Kirch, 2008).

This study shows that breathing wall units like mud brick and AAC let air diffuse through their fabric and make a noticeable difference in indoor CO_2 concentrations without induced air flow. This indicates that breathing materials can have an effect on the indoor air quality and they can be used as passive indoor air cleaning systems in case that the outdoor air pollutants do not exceed the ranges of acceptable levels.

In short, instead of fully-airtight building envelope where unhealthy boundary conditions are occurred for occupants, self-breathing skins are needed to be designed. It is worthwhile to mention that there is necessity for building passive houses with breathing walls which encourages the indoor air exchange at a certain level. Therefore, further studies are needed on design criteria and requirements for breathing passive houses specifically to minimize the mechanical ventilation needs for fresh air intake. Advanced researches are necessitated on impacts of air diffusion characteristics of building materials on self-ventilation capacity of breathing wall systems. That is, in fact will be guiding for material selection starting from preliminary stages of building design and for enhancing its sustainable features.

CHAPTER 6

CONCLUSION

The study concerns the measuring water vapor and CO_2 diffusion characteristics of porous building materials, namely mud brick as a traditional building material and autoclaved aerated concrete (AAC) as a contemporary building material, in order to examine their breathing features adequacy for sustaining indoor air quality. In this regard, a practical experimental method composed of single and double chamber diffusion tests was developed in which the CO_2 diffusion/transmission from inside to outside was represented through a porous building wall.

The materials selected for the examinations are:
- the mudbrick load bearing units which are used in 70 years old traditional houses of Hamzalı Village, and
- the load bearing and infill AAC units manufactured by a Turkish company and commonly-used in contemporary houses.

It was determined that the mudbrick has particular features contributing its dimensional stability and long term durability properties due to a conscious selection of raw materials.

The physical, physicomechanical and mechanical properties of Hamzalı Village mud brick, G2 and G4 type AAC have shown that those samples are highly porous, light weight water vapor permeable and have a certain material strength while signaling differences in their porosity characteristics. Hamzalı Village mudbrick's density and porosity values are 1.60g/cm3 and 42%, respectively. In comparison to mudbrick, G2 and G4 types of AAC has lower density and higher porosity within the ranges of 0.4-0.5g/cm3 and 68%-74%, respectively. Among all, the mudbrick has the lowest UPV values while having the highest MoE with uniaxial compressive strength of 0.89MPa. The next highest MoE belongs to the G4 type AAC with the value of 2.2GPa while providing the highest uniaxial strength among all samples with the value of 2.36MPa. The lowest MoE and uniaxial compressive

strength values belong to the infill type of AAC, G2, with the values of 1.1GPa and 1.33MPa, respectively.

Their air permeability features of mudbrick and AAC materials were examined in terms of water vapor and carbon dioxide diffusion characteristics. All samples were found to be very water vapor permeable materials due to the μ values of 3.55, 2.13 and 3.34, respectively for the Hamzalı mudbrick, G2 and G4 types of AAC, as well as SD values below 0.14m for 25mm-thick samples.

The joint use of single chamber and double-chamber diffusion tests by using CO_2 at high concentration as the tracer gas are useful to assess the CO_2 diffusion characteristics of a porous material. Single chamber test is used to determine the CO_2 diffusion rate (E, mg.s^{-1}), effective diffusion coefficient (D_{EFF}, cm^2/s) and diffusion index (D_i, 1.d^{-1}) which are determinative parameters. The double chamber test is needed to examine whether the material is attracted to CO_2 gas or not by showing how much tracer gas is actually permeated through or retained in the material. In case that a porous material is attracted to CO2, the data on CO2 diffusion rate obtained from single chamber setup is misleading.

The CO_2 diffusion rate (E, mg.s^{-1}) through an 18cm-thick mudbrick was found to be 0.0075mg.s^{-1}. By using that value, the effective diffusion coefficient (D_{EFF}, cm^2/s) and diffusion index (D_i, 1.d^{-1}) of the mudbrick were determined to be 0.0131cm^2.s^{-1} and 2.92d^{-1}, respectively.

Double-chamber diffusion tests have shown that AAC material is attracted to CO_2 while mud brick is not a CO_2-philic material. Mud brick does not capture CO_2 within its body and the concentrations of two environments separated with a mud brick wall can easily come to an equilibrium without an induced air flow. AAC samples, on the other hand seemed to keep a considerable amount of CO_2 in their body reaching to 53% for G2 type and 88% for G4 type while transmitting a very small portion of CO_2, such as 22% for G2 type and 3% for G4 type. The analyses shows that a certain portion of that retainment is due to the reactions between the minerals in AAC and CO_2 in presence of moisture while some portion of that retainment is due to the absorption and/or adsorption of CO_2 within the pore structure of AAC. When temperature increases the CO_2 absorption/adsorption

capacity of AAC decreases or vice versa. In short, a considerable amount of CO_2 in the air can be kept by AAC but it doesn't mean that it filters the CO_2, since AAC releases CO_2 back to indoor in certain amounts when indoor temperature increases.

The study exhibits that both mud brick and AAC are highly water vapor permeable, therefore, breathing materials. In comparison to the mudbrick, AAC types are less CO_2 permeable although they are more water vapor permeable than mud brick. No correlation between CO_2 and water vapor diffusion characteristics was identified. The pore structure of mudbrick allows water vapor and CO_2 transmission from one side to the other side while the pore structure of AAC material allows water vapor transmission through its fabric while does not permit the transmission of CO_2 from one side to the other due to its attraction for CO_2.

The diffusion tests after exposure of AAC material to high concentration of CO_2 in case of moisture coexistence reveal that AAC material is a highly CO_2-philic material. The data on materials properties shows that being in contact with CO_2 and moisture results in a degradation process for both G2 and G4 type AAC blocks visible with:

- increase in density,
- decrease in μ value (unitless), MoE (GPa) and UPV ($m.s^{-1}$), and
- occurrence of visual cracks in the material.

The building enclosure if constructed as a breathable skin can contribute to create healthy indoor environments in case that the outdoor air is not polluted. This study proved that highly-breathable materials have a capability to level down the indoor air contamination at certain levels in order to achieve healthier indoor air conditions. For instance, the mudbrick has a capability to keep indoor air contamination in balance with neighboring both environments within 10 hours (**Figure 4.11**). In addition, at very high CO_2 concentration level, an 18cm-thick mudbrick block can transmit the large portion (two third) of indoor CO_2 amount to the outside within the first 13 hours (**Figure 4.06**).

In short, the experimental setups and the data achieved in the study are promising to measure and compare the gas diffusion/transmission properties of a porous building material in terms of measurable parameters as well as to calculate their potentials to reduce the indoor contamination to lower levels. However, further studies are needed to define gas diffusion characteristics of many porous materials as well as breathable wall compositions for comparisons. Due to the promising performance of breathing skins for healthier indoor air quality, comprehensive studies are necessitated to re-define design criteria and requirements for breathing passive houses in order to minimize the mechanical ventilation needs for fresh air intake.

Further researches related with the study can be suggested to conduct:

− on many types of breathing/porous building materials by using the measurable parameters introduced in this study,
− with CO_2 and other gasses as well as volatile organic compounds which are considered as indoor pollutants,
− with and without induced pressure differences,
− on measured-scale models and/or on building proper.

Thereby, a library of breathing materials and adequate data can be generated by using single and double chamber experimental set-ups in order to correlate the "parameters of breathing characteristics" with "indoor air exchange efficiency" of buildings. These correlations can be benefitted as inputs to improve computer-based modelling and simulation analyses for design and assessment purposes, therefore can contribute to maintain indoor air quality in the range of acceptable levels. The inclusion/integration of the knowledge on indoor air exchange efficiency of breathable materials is expected to improve effectiveness of contemporary passive house and its design criteria.

REFERENCES

AKG Gazbeton, (2013). Kapsamlı Broşür, Retrieved from http://www.akg-gazbeton.com. (Last accessed on 15.04.2016)

Akkuzugil, E. (1997). A study in historical plasters, Unpublished Master Thesis, Ankara: METU.

Akyazı, M. (1998). A proposal for the repair and conservation of Haraçoğlu Konak in Bursa, Unpublished Master Thesis, Ankara: METU.

Andolsun, S., Tavukçuoğlu, A., and Caner-Saltık, E. N. (2005). Evaluation of autoclaved aerated concrete (AAC) as repair material for timber framed historical structures. Proceedings of Postgraduate Researchers of the Built and Natural Environment (PROBE) 2005 Conference, pp. 505-519, 16-17 November 2005, Glasgow, Scotland.

Andolsun, S. (2006). A study on material properties of autoclaved aerated concrete and ist complementary wall elements. Their compatibility and historical wall sections. *Unpublished Master Thesis*. Graduate Program in Building Science, Department of Architecture, Middle East Technical University, Ankara, Turkey.

ASHRAE 62.1-2004 (2006). *Ventilation for Acceptable Indoor Air Quality.* American Society of Heating, Refrigerating and Air Conditioning Engineers.

ASTM E96-93 - *Water Vapor Transmission of Materials*. (1993). American Society for Testing and Materials, Philadelphia.

ASTM E 741-11 – *Standard Test Method for Determining Air Change in a Single Zone by Means of a Tracer Gas Dilution* (2011). American Society for Testing and Materials, Philadelphia.

ASTM D 2845-08 – *Standard Test Method for Laboratory Determination of Pulse Velocities and Ultrasonic Constants of Rock* (2008). American Society for Testing and Materials, Philadelphia.

Beruz, N. E. (2012). Assessment of indoor air quality in crowded educational spaces, Unpublished Thesis, Ankara: METU.

Bray, D.E. and McBride, D. (1992). Nondestructive Testing Techniques. Canada: John Wiley & Sons Inc.

Binici, H., Aksoğan, O., Bakbak, D., Kaplan, H., Işık, B. (2009). Sound Insulation of Fibre Reinforced Mud Brick Walls, *Construction and Building Materials*, 23(2) February 2009, 1035-1041.

Bulut, H. (2011). Havalandırma ve İç Hava Kalitesi Açısından CO_2 Miktarının Analizi, X. Ulusal Tesisat Mühendisliği Kongresi, İzmir, Türkiye.

Caner, E. (2003). Archaeometrical investigation of some Seljuk plasters, Unpublished Master Thesis. Ankara: METU.

Chang, R., Thoman, J.W. (2014). *Physical chemistry for physical sciences*. Canada: University Science Books.

Clifton, J.R. and Brown, P.W. (1978). "Adobe I: The properties of Adobe", Studies in Conservation, 23:139-146.

Corsi R.L., Torres V.M., Sanders M., Kinney K.L. (2002). Carbon dioxide levels and dynamics in elementary schools: results of the TESIAS Study. In: *Indoor Air '02: Proceedings of the 9th International Conference on Indoor Air Quality and Climate*, June 30-July 5 2002 2002, Monterey, CA:Indoor Air, 74-79.

Di Giulio, M. Grande, R., Di Campli, E., Di Bartolomeo, S., Cellini, L. (2009). Indoor air quality in university environments, *Environmental Monitoring and Assessment*, 170, 509-517.

DIN 52615 – Determination of Water Vapor (Moisture) Permeability of Construction and Insulating Materials (1987). Berlin, Deutsches Institut für Normung.

Esen, S., Tunç, N., Telatar, S., Tavukçuoğlu, A., Caner-Saltık, E.N., Demirci, Ş. (2004). Manisa Çukur Hamam'ın Onarımına Yönelik Malzeme Çalışmaları, Proceedings of '. Ulusal Yapı Malzemesi Kongresi ve Sergisi, pp. 494-505, 6-8 Ekim, 2004, Istanbul: TMMOB Mimarlar Odası.

Erdil, M. 2015. Assessment of sound transmission characteristics of traditional timber framed dwellings in Ankara, Turkey; *Unpublished Master thesis*, Graduate Program in Building Science, Middle East Technical University. Ankara, Turkey.

Fennell, H.C. and Haehnel, J. (2005). Setting Airtightness Standards, *ASHRAE Journal*, 47(9), 26-30.

Fisk W.J., Sullivan D.P., Faulkner D, Eliseeva E. (2010). CO_2 Monitoring for Demand Controlled Ventilation in Commercial Buildings. LBNL-3279E. Berkeley, CA: Lawrence Berkeley National Laboratory.

Gochfeld, M. (2007). *Toxicology, Chemicals in the environment*, Public and Health Preventive Medicine, Fifteenth Edition, pp.508-509.

Güdücü, G. (2003). Archaeometrical Investigation of Mud Plasters on Hittite Buildings in Sapinuwa-Çorum, Unpublished Master Thesis. Ankara: METU.

Hansen, K. K. (1989). Equipment for and results of water vapour transmission tests using cup methods, Proceedings of ICHMT Symposium on Heat and Mass Transfer in Building Materials and structures, Dubrovnik, Yugoslavia, pp. 267-271.

Hess-Kosa, K. (2011). Indoor Air Quality - The Latest Sampling and Analytical Methods, Boca Rota, Florida, USA:CRC Press,.

Hodgson, M. (1992). Field Studies on the Sick Building Syndrome, *Annals of the New York Academy of Science*, 641(1), 21-36.

Houben, H., and Guillaud, H. (1989). Earth construction. London, UK: Intermediate Technology Publications.

ISO 4638 (1984). *Polymeric Materials Cellular Flexible – Determination of Air Flow Permeability*. International Organization for Standardization.

ISO 9053 (2011). *Materials for Acoustical Applications - Determination of Air Flow Resistivity*. International Organization for Standardization.

ISRM, Point Load Test, 1985, Suggested Method for Determining Point Load Strength, *Int. J. Rock Mech. Min. Sci. & Geomech. Abstr.*, 22(2):51-70.

Jacobs, F. and Mayer, G. (1992). Porosity and permeability of autoclaved aerated concrete, *Proceedings of the Third RILEM International Symposium on Autoclaved Aerated Concrete* (p.71-75). 14-16 October, 1992. Advances in Autoclaved Aerated Concrete, F.H. Wittmann, ed. A.A. Balkema, Rotterdam, Brookfield.

Jacobs, M.H. (1967). Diffusion process. Berlin: Julius Springer.

Jimenez Delgado, M.C. and Guerrero, I.C. (2007). The selection of soils for unstabilized earth building-A normative review. *Construction and Building Materials*. 21, pp.237-251.

Kajtar L, Herczeg L, Lang E. (2003). Examination of influence of CO_2 concentration by scientific methods in the laboratory. In: *Proceedings of Healthy Buildings 2003*, 7-11 December 2003, Singapore:Stallion Press, 176-181.

Kajtar L, Herczeg L, Lang E, Hrustinszky T, Banhidi L. 2006. Influence of carbon-dioxide pollutant on human well-being and work intensity. In: *Proceedings of Healthy Buildings 2006*, 4-8 June 2006, Lisbon, Portugal:Universidade do Porto, Porto, Portugal, 85- 90.

Katunsky, D., Nemec, M. and Kamensky, M. (2013). Airtightness of buildings, Advanced Materials Research, 649, 3-6.

Keefe, L. (2005). Earth Building - Methods and materials, repair and conservation, pp.153-154, New York, USA: Taylor & Francis.

Kirch, W. (2008a). Sick Building Syndrome, Encyclopedia of Public Health, v.2, pp.1303, New York, USA: Springer Science+Business Media, LLC.

Kirch, W. (2008b). Chemical Sensitivity Syndromes, Encyclopedia of Public Health, v.1, pp.107, New York, USA: Springer Science+Business Media, LLC.

Kömürcüoğlu, E. A. (1962). Yapı Malzemesi Olarak Kerpiç ve Kerpiç İnşaat Sistemleri. İstanbul: İTÜ Matbaası.

Kus, H., Carlsson, T. (2003). Microstructural investigations of naturally and artificially weathered autoclaved aerated concrete. *Cement and Concrete Research,* 33(2003), 1423-1432.

Lange, N. A. and Forker, G.M. (1967). *Handbook of Chemistry*. USA: McGraw-Hill, Inc.

Langer, S. and Bekö, G. (2013). Indoor air quality in the Swedih housing stock and its dependence on building characteristics, *Building and Environment*, 69, 44-54.

Liley, P.E., Gambill, W.R. (1973). Physical and chemical data. Perry, R.H., Chilton, C.H. (Eds.). *Chemical engineer's handbook.* (p.222-233) USA: R.R. Donnelley & Sons.

Matsushita, F., Aono, Y. and Shibata, S. (2000). Carbonation Degree of Autoclaved Aerated Concrete, in: *Cement and Concrete Research* (p.1741- 1745, v.30).

Matsushita, F., Aono, Y., and Shibata, S.. Calcium silicate structure and carbonation shrinkage of a tobermorite-based material. *Cement and Concrete Research, 34* (2004), 1251-1257.

Meriç, I., Erdil, M., Madani, N., Alam, B. A., Tavukcuoglu, A., Caner Saltik, E. (2013). Technological Properties of Earthen Building Materials in Traditional Timber Frame Structures. In: *Kerpic'13 3rd International Conference – New Generation Earthern Architecture: Learning from Heritage*, 11-15 September 2013 (pp.465-473),. Istanbul, Turkey: Istanbul Aydın University

Meriç, I., Erdil, M., Madani, N., Alam, B. A, Tavukçuoğlu, A., Caner Saltık, E.N. (unpublished). Material characterization of mudbrick and neighbouring plasters in traditional timber framed structures. *9th International Symposium on Conservation of Monuments in Mediterranean Basin*, Ankara, Turkey, 2-5 June 2014. Ankara, Turkey: Middle East Technical University.

Miller C., Rupperta K. and Kucharski T. (2010). Home Energy Analysis: Highlighting the Blower Door Test. *The Carbon Challenge Series for the Florida Energy Systems Consortium*. Retrieved from: http://www.floridaenergy.ufl.edu/wp-content/uploads. (Last accessed on 15.05.2016)

FESC_Home_Energy_Analysis_final_7-27-10.pdf. Last accessed on 10th December 2015.

Morton, T. (2008). Earth masonry design and construction guidelines, Berkshire: IHS BRE Press.

Mukhopadhyaya, P., Batcheller, D., Kumaran, K., Lackey, J., Van Reenen, D., Normandin, N. (2011). Correlation between water vapor and air permeability of building materials: experimental observations. *Journal of ASTM International*. 8(3): 1-6. Retrieved from http://compass.astm.org/download/JAI102924.19410.pdf

Narayanan, N., and Ramamurthy, K. (2000). Structure and properties of aerated autoclaved concrete: a review. *Cement and Concrete Composites*. 22, 321-329.

Ng, L. C., Musser, A., Persily, A. K., Emmerich, S. J. (2012). Indoor air quality analyses of commercial buildings. *Building and Environment*. 58, 179-187.

Örs, K. (2006). An investigation on compatibility properties of exterior finish coats for insulated walls in terms of water vapor permeability and modulus of elasticity, Unpublished Master Thesis, Ankara: METU.

Persily, A.K. (2007) ASHRAE Transactions, 103(2).

Phillips, M., Herrera, J., Krishnan, S., Zain, M., Greenberg, J, Cataneo, R.N. (1999), Variation in volatile organic compounds in the breath of normal humans, *Journal of Chromatography*, 729, 75-88.

RILEM. (1980). Tentative Recommendations, Comission-25-PEM. Recommended test to measure the deterioration of stone and to access the effectiveness of treatment methods. *Materiaux and Construction. 13(73)*:173-253.

Šadauskiene, J., Stankeviciıs, V., Bliudzius, R., Gailius, A. (2009). The impact of the exterior painted thin-layer render's water vapour and liquid water permeability on the wall insulating system, *Construction and Building Materials*, 23(8), 2788-2794.

Sherman, M.H. and Chan, Z. (2004). Building Airtightness: Research and Practice. Lawrence Berkeley National Laboratory Report No. LBNL-53356.

Schiavi, A., Guglielmone, C., Miglietta, P. (2011) Effect and importance of static-load on airflow resistivity determination and its consequences on dynamic stiffness, *Applied Acoustics*, 72:705-710.

Shin, D. M., Kim, C.N., Park, C., Kim, D. and Nam, Y. (2013). On the determination of VOCs emission factors in dry building materials, *Heat Mass Transfer*, 49, 1625-1635.

Silberberg, M.S. (2013). *Chemistry. The molecular nature of matter and change*. USA: McGraw-Hill Companies, Inc.

Stefanidou M. and Papayianni, I. (2005). The role of aggregates on the structure and properties of lime mortars, *Cement and Concrete Composite,* 27: 914-919.

Swift, J.M., Lawrence, T.,and Pavlik, A. (2010). Indoor Environmental Quality, *ASHRAE GreenGuide The Design, Construction and Operation of Sustainable Buildings*, Third Edition, USA: American Society of Heating, Refrigerating and Air-Conditioning Engineers Incorporated.

Tavukçuoğlu, A., Örs, K., Düzgüneş, A., Demirci, Ş. (2013) Compatibility Assessment of Exterior Finish Coats for Insulated Walls, *METU Journal of the Faculty of Architecture*, 30(1), 79-97.

Taşdemir, C. and Ertokat, N. (2002). Gazbetonun Fiziksel ve Mekanik Özellikleri Üzerine Bir Değerlendirme, Proceedings of 1. Ulusal Yapı Malzemesi Kongresi ve Sergisi, pp.425-437, İstanbul: TMMOB Mimarlar Odası.

Toracca, G. (2009). Earth as a building material, *Lectures on Materials Science for Architectural Conservation*, pp.38-41, Los Angeles, USA: The Getty Conservation Institute.

Tro, N. (2013). *Principles of chemistry. A molecular Approach.* USA: Pearson Education Inc.

TS EN 1015-19 (2000). *Methods of Tests for Mortar for Masonry-Part 19: Determination of Water Vapor Permeability of Hardened Rendering and Plastering Mortars*. Ankara, Institute of Turkish Standards.

TS EN 29053 (1996). *Acoustics-Materials for Acoustical Applications-Determination of Air Flow Resistance*. Ankara, Institute of Turkish Standards.

TS EN ISO 12572 (2001). *Hygrothermal performance of building materials and products - Determination of water vapor transmission properties.* Ankara, Institute of Turkish Standards.

TS EN 12602 (2011). *Prefabricated Reinforced Components of Autoclaved Aerated Concrete*. Ankara, Institute of Turkish Standards.

TS EN 771-4:2011+A1 (2015). *Specification for Masonry Units – Part 4: Autoclaved Aerated Concrete Masonry Units.* Ankara, Institute of Turkish Standards.

TS EN ISO 7783 (2012). *Paint and Varnishes - Determination of Water Vapour Transmission Properties - Cup Method.* Ankara, Institute of Turkish Standards.

United States Environmental Protection Agency (1991). Indoor Air Facts No.4 (revised), Sick Building Syndrome, Fact Sheets. US EPA. Retrieved from www.epa.gov/iaq/pdfs/sick_building_factsheet.pdf . (Last accessed on 15.05.2016)

Wang, J., and Zhang, X. (2010). Recommended concentration levels of indoor air pollution indicators for requirement of acceptable indoor air quality, *International Journal of Energy and Environment* Yang, X., and Cheng, Q. (2001). A coupled airflow and source/sink model for simulating indoor VOC exposures, Indoor Air, 11(4), 257-269.

Wang, L., Emmerich, S. J., Persily, A.K., Lin, C. (2012). Carbon monoxide generation, dispersion and exposure from indoor operation of gasoline-powered electric generators under actual weather conditions, *Building and Environment*, 56, 283-290.

Whitmore C.A., Clayton A, Akland A. (2003). California Portable Classrooms Study, Phase II: Main Study, Final Report, Volume II. Research Triangle Park, NC: RTI International.

Wilson, S., Card, G., Haines, S. (2009). *Ground gas handbook*. Latvia: InPrint.

Wolkoff, P. (1998). Impact of Air Velocity, Temperature, Humidity and Air on Long-term VOC Emissions from Building Products, *Atmospheric Environment*, 32 (14/15), 2659-2668.

Wolkoff, P. (1999). How to measure and evaluate volatile organic compound emissions from building products - A perspective, *The Science of Total Environment*, 227, 197-213.

World Health Organization (2010), Guidelines for indoor air quality: Selected pollutants, Copenhagen, Denmark: WHO Regional Office of Europe.

Yates, J.T., Johnson, J.K. (2007). *Molecular chemistry for engineers.* USA: University Science Books.

Yates, W.D. (2015). Safety Professional's Reference & Study Guide. Boca Raton, FL: CRC Press.

Yoon, S, and Hoyano, A (1998). Passive ventilation systems that incorporates a pitch roof constructed of breathing walls for use in a passive solar house, *Solar Energy*, 64 (4-6), pp.189-195., 1(4), 697-704.

APPENDIX A

Density, Porosity, Ultrasonic Pulse Velocity, Modulus of Elasticity, Point Load Stress Index, Indirect Uniaxial Compressive Strength, Water Vapor Transmission Coefficient, Water Vapor Transmission Rate, Equivalent Air Thickness of Water Vapor Permeability and Water Vapor Permeability Values of Mud Brick and AAC

Material Type	ρ (g.cm⁻³)	ϕ (%)	UPV (m.s⁻¹)	MoE (GPa)	I_s (MPa)	$UCS_{indirect}$ (MPa)	μ (unitless)	RT* (g.h⁻¹.m⁻²)	SD* (m)	SD** (m)	1/SD* (m⁻¹)
Mud brick from Hamzalı Village, Kırıkkale	1.60	42.37	1321	2.60	0.17	0.89	3.55	1.72	0.64	0.09	1.58
G2 type AAC (unexposed)	0.42	74.10	1703	1.11	0.25	1.33	2.13	2.81	0.38	0.05	2.60
G4 type AAC (unexposed)	0.62	67.67	1955	2.17	0.51	2.36	3.34	1.82	0.60	0.08	1.66
G2 type AAC (exposed)	0.46	-	1235	0.65	-	-	1.34	4.36	0.24	0.03	4.16
G4 type AAC (exposed)	0.68	-	1293	1.05	-	-	2.34	2.57	0.42	0.06	2.37
G2 type AAC***	0.40	78	1965	1.4	-	-	3.8-5.0	-	0.11	-	-
G4 type AAC***	0.60	68	1962	2.1	-	-	3.2-6.4	-	0.12	-	-
Mud brick infill from Kavaközü Village, Güdül****	-	-	-	-	-	-	1.4-1.6	-	0.04	-	-

*The RT, SD and 1/SD values calculated for 180mm thick material blocks

**SD values calculated for 25mm thick materials

*** The values for G2 and G4 type AAC materials taken from the literature (Andolsun, 2006)

****The values for the mud brick from the literature (Erdil, 2015; Meriç et.al.,2013; Meriç et.al.,2014)

CO$_2$ Concentration Decay Rate for Single Chamber, Critical Time, CO$_2$ Concentration Peak Level, CO$_2$ Diffusion Rate, Effective CO$_2$ Diffusion Coefficient, CO$_2$ Diffusion Index, CO$_2$ Concentration Decay Rate for Double Chamber and CO$_2$ Concentration Increase Rate for Double Chamber

Material Type	RD$_{SINGLE}$ (mg.m^{-3}.s^{-1})	T$_{CRITICAL}$		C$_{MAX}$		E (mg.s^{-1})	D$_{EFF}$ (cm^2.s^{-1})	D$_i$ (d^{-1})	RD$_{DOUBLE}$ (mg.m^{-3}.s^{-1})	RI$_{DOUBLE}$ (mg.m^{-3}.s^{-1})
		(s)	(h)	(ppm)	(mg.m^{-3})					
Mud brick from Hamzalı Village, Kırıkkale	-0.4680	30000	8.3	15349	27629	0.0075	0.0131	2.92	-0.2865	0.5769
G2 type AAC (unexposed)	-0.4077	35940	10.0	13181	23725	0.0065	0.0135	3.02	-0.4957	0.3569
G4 type AAC (unexposed)	-0.3457	35220	9.8	12646	22762	0.0055	0.0120	2.66	-0.7589	0.0144
G2 type AAC (exposed)	-0.2572	43560	12.1	13050	23490	0.0041	0.0086	1.91	-0.3630	0.0767
G4 type AAC (exposed)	-0.2292	40000	11.1	12933	23279	0.0037	0.0076	1.70	-0.3510	0.1107